SHEAR STRENGTH BEHAVIOUR
OF
SAND - CLAY MIXTURES

A THESIS SUBMITTED TO
THE GRADUATE SCHOOL OF NATURAL AND APPLIED SCIENCES
OF
MIDDLE EAST TECHNICAL UNIVERSITY

BY

MEHMET SALİH ÖLMEZ

IN PARTIAL FULFILMENT OF THE REQUIREMENTS
FOR
THE DEGREE OF MASTER OF SCIENCE
IN
CIVIL ENGINEERING

MAY 2008

Approval of the thesis:

SHEAR STRENGTH BEHAVIOUR OF SAND - CLAY MIXTURES

submitted by **MEHMET SALİH ÖLMEZ** in partial fulfillment of the requirements for the degree of **Master of Science in Civil Engineering Department, Middle East Technical University** by,

Prof. Dr. Canan Özgen _____
Dean, Graduate School of **Natural and Applied Sciences**

Prof. Dr. Güney Özcebe _____
Head of Department, **Civil Engineering**

Prof. Dr. M. Ufuk Ergun
Supervisor, **Civil Engineering Dept., METU** _____

Examining Committee Members:

Prof. Dr. Orhan Erol _____
Civil Engineering Dept., METU

Prof. Dr. M. Ufuk Ergun _____
Civil Engineering Dept., METU

Prof. Dr. Yıldız Wasti _____
Civil Engineering Dept., METU

Assoc. Prof. Dr. B. Sadık Bakır _____
Civil Engineering Dept., METU

Mengüç Ünver (M.S.) _____
General Manager, ARGEM

Date: 22/05/2008

I hereby declare that all the information in this document has been obtained and presented in accordance with academic rules and ethical conduct. I also declare that, as required by these rules and conduct, I have fully citied and referenced all material and results that are not original to this work.

Name, Last Name : Mehmet Salih ÖLMEZ

Signature :

ABSTRACT

SHEAR STRENGTH BEHAVIOUR OF SAND - CLAY MIXTURES

ÖLMEZ, Mehmet Salih
M.S., Department of Civil Engineering
Supervisor: Prof. Dr. Mehmet Ufuk ERGUN

May 2008, 106 pages

A clean sand having about 5 % fines has been mixed with 5 to 40 % commercial kaolin to form different sand-clay soil mixtures. The purpose of making this study is to observe the effects of fraction of fine materials in the soil mixture on the behavior of shear strength. Three series of experiments have been performed throughout the study. Undrained triaxial compression tests (series 1) are performed on specimens taken out from homogeneously mixed soil mixtures at specified kaolin contents consolidated in a box without keeping the mixture under water.

In series 2 experiments specimens are taken from a box where soil mixtures are consolidated under water and undrained triaxial compression tests are performed on the samples. Drained direct shear tests are performed on samples prepared without performing initial consolidation in large boxes but directly prepared in the direct shear boxes and consolidated prior to shear (series 3).

It has been found that about 20 % kaolin - 80 % sand mixture seems to be a threshold composition and changes in both undrained and drained shear stress-strength behaviour occur afterwards with increasing fine material content.

Key Words: Shear Strength, Clay-Sand Mixture, Undrained Shear Strength, Clayey-Sand, Drained Shear Strength Parameters.

ÖZ

KUM - KİL KARIŞIMLARININ KAYMA DAYANIMI ÖZELLİKLERİ

ÖLMEZ, Mehmet Salih
Yüksek Lisans, İnşaat Mühendisliği Bölümü
Tez Yöneticisi: Prof. Dr. Mehmet Ufuk ERGUN

Mayıs 2008, 106 sayfa

Farklı oranlarda kum-kil karışımları oluşturmak amacıyla içinde ince malzeme muhtevası yaklaşık % 5 olan temiz bir kum numunesi, muhtevası % 5' ten % 40' a kadar değişen kaolin kili ile karıştırılmıştır. Bu çalışmada amaç zemin karışımı içinde değişen ince malzeme miktarının, kayma dayanımı üzerindeki etkilerini incelenmektir. Çalışma süresince üç seri deney yapılmıştır. İlk serideki deneylerde drenajsız üç eksenli basınç deneyleri yapılmıştır. Bu serideki karışımlar, muhtevası önceden belirlenmiş kaolin ile kumun homojen bir şekilde karıştırılması sonucunda oluşturulmuştur. Deneylerde kullanılan numuneler, daha önceden hazırlanmış homojen zemin karışımının bir kutu içinde ve kutunun su altına bırakılmadan konsolide edilmesi sonucunda elde edilmiştir.

İkinci seri deneylerde drenajsız üç eksenli basınç deneyleri yapılmıştır. Bu serideki deney numuneleri, yine önceden hazırlanmış homojen zemin karışımının bir kutu içinde ve kutunun su altına bırakılarak konsolide edilmesi sonucunda elde edilmiştir. Üçüncü seri deneylerde ise drenajlı direk kesme deneyleri yapılmıştır. Buradaki deney numuneleri başlangıçta konsolide edilmeden doğrudan direk kesme kutusu

içinde hazırlanmıştır. Kesme kutusu içine yerleştirilen numuneler, kesme deneyi başlatılmadan önce konsolide edilmişlerdir.

İçerisinde % 20 kaolin - % 80 kum bulunduran karışımın bir eşik noktası olduğu görülmüştür çünkü ince malzeme miktarı bu eşik noktasını geçecek düzeyde arttırıldıkça drenajlı ve drenajsız kayma gerilmesi-dayanımı davranışlarında değişmeler olmaktadır.

Anahtar Kelimeler : Kayma Dayanımı, Kil-Kum Karışımı, Drenajsız Kayma Dayanımı, Killi-Kum, Drenajlı Kayma Dayanımı Parametreleri.

To My Family

ACKNOWLEDGEMENTS

I would like to thank my supervisor Prof. Dr. M. Ufuk Ergun, who exhibited sincere supervision, guidance, advice, criticism, patience and encouragement at every stage of this study.

To my family, for their support whenever I needed.

Special thanks to METU Soil Mechnanics Laboratory Technician Mr. Ali Bal and Geological Engineer Mr. Ulaş Nacar for their continuous help in the experiments. Their contributions were valuable

I would like to extend my appreciation to Özgür Lütfi Ertuğrul, Selman Sağlam, and other Assistants of Geotechnics Division of the Civil Engineering Department, METU, for their support and encouragement.

TABLE OF CONTENTS

LIST OF TABLES

TABLE

LIST OF FIGURES

FIGURE

LIST OF SYMBOLS

A	Cross-sectional area of specimen in shear box test
A_c	Corrected area of the sheared specimen
A_o	Initial cross-sectional area of specimen
a	Length of square box in shear box test
a'	Modified shear strength parameter
$\overline{A}$	Skempton's pore pressure parameter
B	Skempton's pore pressure parameter
c	Cohesion intercept in terms of total stresses
c'	Cohesion intercept in terms of effective stresses
CD	Consolidated drained test
C_f	Clay fraction
CL	Low plasticity clay
C_p	Proving ring constant in shear box test
C_{pt}	Proving ring constant in triaxial test
c_u	Undrained shear strength
D	Internal diameter of circular box in shear box test
E_{sec}	Secant modulus
e	Overall void ratio of soil
e_f	Interfine void ratio
e_{max}	Maximum void ratio
$e_{max,HS}$	Maximum void ratio of host sand
e_o	Initial void ratio
e_s	Intergranular void ratio
e_{sk}	Skeleton void ratio

f	Ratio of weight of fines to total weight of solids
f_c	Silt content
Gs	Specific gravity
H_o	Initial height of the sample in shear box test
K_o	Coefficient of earth pressure at rest
LL	Liquid limit
N	Normal load on the soil sample in shear box test
NC	Normally consolidated soil
OC	Overconsolidated soil
OCR	Over consolidation ratio
PL	Plastic limit
PI	Plasticity index
SC	Clayey sand
SM	Silty sand
SP	Poorly graded sand
S_{us}	Undrained shear strength
T	Shear force acting on the soil sample in shear box test
t_f	The minimum time required for failure
t_{90}	Time for reaching 90% of the primary consolidation
u	Total pore-water pressure
u_c	Pore-water pressure in soil specimen after applying chamber pressure
UU	Unconsolidated undrained shear test
v	Unit change in volume in triaxial test
V_{max}	Maximum rate of shearing
V_0	Initial volume of specimen
w_f	Final water content
w_i	Initial water content
α'	Modified shear strength parameter
δ_f	Lateral displacement required to reach the soil peak strength
ΔL	Change in height of specimen

δ_p	Proving ring deflection
ΔV	Change in volume of the specimen
$\Delta\sigma_d$	Deviator stress (principal stress difference)
ε_a	Axial strain
ε_h	Shear strain
ε_v	Vertical strain
ϕ	Friction angle in terms of total stresses
ϕ'	Friction angle in terms of effective stresses
ϕ_{cv}	Ultimate friction angle in shear box test
ϕ'_r	Drained residual friction angle
ρ_{bulk}	Initial bulk density
ρ_{dry}	Dry density
σ	Normal stress in shear box test
σ_f	Total normal stress on failure plane
σ_f'	Effective normal stress at failure plane
σ_v , σ_n	Vertical pressure (normal stress)
σ_1	Major principal stress in triaxial test
σ_3	Minor principal stress in triaxial test
σ_1'	Effective major principal stress in triaxial test
σ_2'	Effective intermediate principal stress
σ_3'	Effective minor principal stress in triaxial test
$\overline{\sigma}$	Effective intergranular stress
θ	Theoretical angle between the major and failure planes in triaxial test
τ	Shear stress in shear box test and drained shear strength
τ_{cv}	Ultimate shear stress in shear box test
τ_f	Shear stress on the failure plane
τ_m	Maximum shear stress in shear box test

CHAPTER 1

INTRODUCTION

In this thesis, it was aimed to observe shear strength behavior of sand - clay mixtures. Three series of experiments were performed. In all series, behavior of shear strength under different testing conditions was investigated against increasing fine materials in the mixtures. Kaolin clay is used as fine material. Shear strength parameters, failure strains, secant moduli of mixtures, stress - strain behaviors were studied. Changes in basic characteristics such as void ratios, particle size distributions, consistency limits and soil index properties were also studied. These properties were then correlated with shear strength.

The present thesis is composed of six Chapters. The theoretical background of the present study and a review of the literature about subject are given in Chapter 2. In Chapter 3, the experimental methods are explained by presenting the procedures of samples preparation and by describing the testing program followed. In the 1st series of experiments, soil mixtures having 5, 10, 15, 20, 25 percent kaolin based on dry weight of soil mixture, were consolidated under 50 kPa vertical pressure without keeping them under water and they are tested under cell pressure of 35, 60, and 85 kPa in the unconsolidated undrained triaxial compression test for obtaining shear strength in terms of total stresses. In the 2nd series, soil mixtures having 10, 20, 30, and 40 percent kaolin were consolidated under 100 kPa vertical pressure keeping them under water and they were tested under cell pressure of 50 and 100 kPa, and they were repeated two times at each cell pressure in the unconsolidated undrained triaxial compression test. In the 3rd series, soil mixtures having 0, 10, 20, 30, and 40 percent kaolin were prepared and initial consolidation stage was not applied on these mixtures. Soil specimens were tested under vertical loads of 50, 100, and 150 kPa and they were repeated two times at each pressure in consolidated drained shear box test in order to measure effective shear strength parameters. The test results obtained

in each experimental series are given in Chapter 4. In Chapter 5, the interpretation and discussion of test results are presented. Finally the conclusions obtained from the present investigation are given in Chapter 6.

CHAPTER 2

BACKGROUND TO THE STUDY

2.1 General Review of Shear Strength of Soils

The shear strength of soils is an important aspect in many foundation engineering problems such as the bearing capacity of shallow foundations and piles, the stability of the slopes of dams and embankments, and lateral earth pressure on retaining walls. In this chapter, the shear strength characteristics of granular and cohesive soils and the factors that control them will be discussed (Das, 1983).

In 1910, Mohr presented a theory for rupture in materials. According to this theory, failure along a plane in a material occurs by a critical combination of normal and shear stresses, and not by normal or shear stress alone. The functional relation between normal and shear stress on the failure plane can be given by

$$\tau_f = f(\sigma_f) \tag{2.1}$$

where τ_f is the shear stress at failure and σ_f is the normal stress on the failure plane. The failure envelope defined by Eq. 2.1 is a curved line, as shown in Figure 2.1.

In 1776, Coulomb defined the function f(σ) as

$$\tau_f = c + \sigma_f . \tan\phi \tag{2.2}$$

where c is cohesion and ϕ is the angle of friction of the soil. Eq. 2.2 is generally referred to as the Mohr-Coulomb failure criteria. The significance of the failure

envelope can be explained using Figure 2.1. If the normal and shear stresses on a plane in a soil mass are such that they plot as point A, shear failure will not occur along that plane. Shear failure along a plane will occur if the stresses plot as point B, which falls on the failure envelope. A state of stress plotting as point C cannot exist, since this falls above the failure envelope; shear failure would have occurred before this condition was reached (Das, 2005).

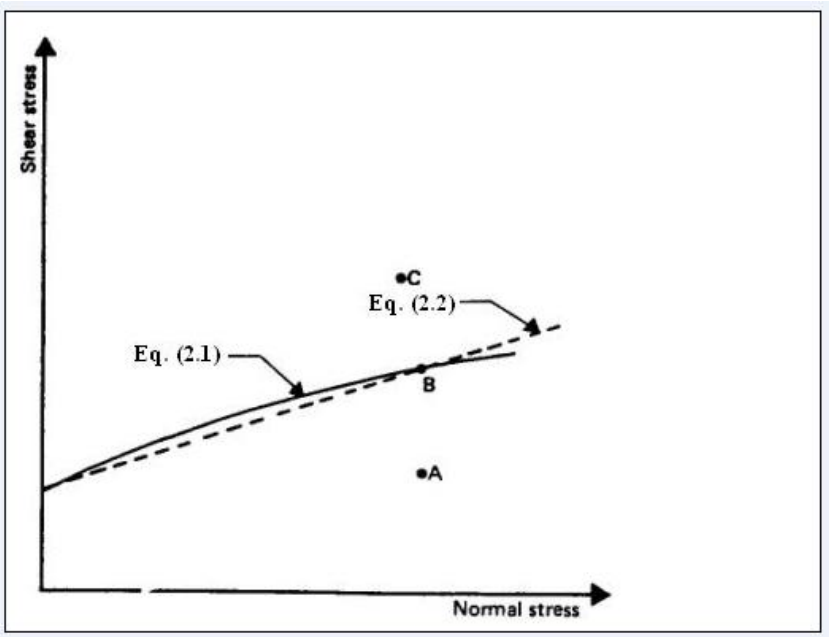

Figure 2.1 Mohr-Coulomb failure criteria (Das, 1983)

$$\tau_f = c' + \sigma_f'.\tan\phi' \qquad (2.3)$$

where,

τ_f : shear stress at failure plane

c : cohesion intercept in terms of total stresses

c' : cohesion intercept in terms of effective stresses

σ_f : total normal stress at failure plane

σ_f' : effective normal stress at failure plane

ϕ : friction angle in terms of total stresses

ϕ' : friction angle in terms of effective stresses

Equation (2.2) is applicable for σ_f defined as total normal stress and c and ϕ are termed as total stress parameters. Equation (2.3) applies for σ_f' defined as effective normal stress and c' and ϕ' are effective stress parameters. Effective stress affecting the frictional resistance between soil particles is accepted as the basic factor influencing strength. Effective parameters are generally used under conditions where effects of the drained conditions on the shear strength are more critical than that of undrained conditions such as the stability problems of the slopes. However total parameters are generally taken into consideration for undrained conditions if they are more critical in shear strength problems such as the bearing capacity problems of shallow foundations (Head, 1982).

As a matter of fact that shear strength of a soil depends on many factors which are,

- stress history,
- soil composition,
- water content,
- degree of saturation,
- soil structure,
- void ratio,
- drainage conditions,
- isotropic media in the soil,
- rate of loading.

All of the factors may be effective on the shear strength and values of c and ϕ can be depended on these factors. Consequently, a variety of types of friction angle and cohesion parameters can be defined for total and effective stresses.

2.1.1 Shear Strength of Cohesionless Soils

The shear strength of a cohesionless soil may be represented by Eq. 2.4. This is a special case of Eq. 2.3, where c = 0.

$$\tau_f = \sigma_f . \tan\phi \tag{2.4}$$

Generally, the value of ϕ is influenced by,

- The state of compaction and the void ratio of the soil. The friction angle increases with decreasing void ratio (increasing density), but not linearly.
- Coarseness, shape and angularity of the grains. Angular grains interlock more effectively than rounded ones, thereby creating a larger friction angle.
- Mineralogical content. Hard gravel particles result in higher friction angles than soft grains, which may crush more easily, thereby reducing the interlocking or bridging effects. For sand, however, the mineralogical content seems to make little difference except if the sand contains mica. In that case the void ratio is usually larger, thereby resulting in loose interlocking sand lower friction angle.
- Grain size distribution. A dense, well-graded sand usually displays a higher friction angle than a dense uniform-sized sand (Cernica, 1995).

The characteristics of dry and saturated sands are the same provided there is zero excess pore water pressure in the case of saturated sands. However, the shear strength might be altered significantly by a change in the pore pressures. Hence, the shear strength of a saturated cohesionless soil might be given by Eq. 2.5.

$$\tau_f = (\sigma - u).\tan\phi = \bar{\sigma}.\tan\phi \tag{2.5}$$

where $\bar{\sigma}$ = effective (intergranular) stress

u = pore-water pressure

When the pore-water pressure approaches σ, the shear strength approaches zero. When that happens, we may approach impending instability or perhaps motion (e.g., slope failures, boiling). Fluctuation in the water table is a common cause of significant variations in the pore stress and, thereby, in the shear strength of the soil.

The determination of the friction angle ϕ is commonly accomplished by one of two methods; the direct shear test or the triaxial test. A brief theoretical background for direct shear test is explained in the following.

Direct Shear Test

Direct shear test is used to determine the shear strength of soils on predetermined failure surfaces. The principle of the direct shear test is illustrated in Figure 2.2. The soil sample confined inside the upper and lower rigid boxes, is subjected to the normal load N and is sheared by the shear force T. If A is the area of surface CD, the shear stress τ acting on surface CD is equal to T/A, and the normal stress σ is equal to N/A.

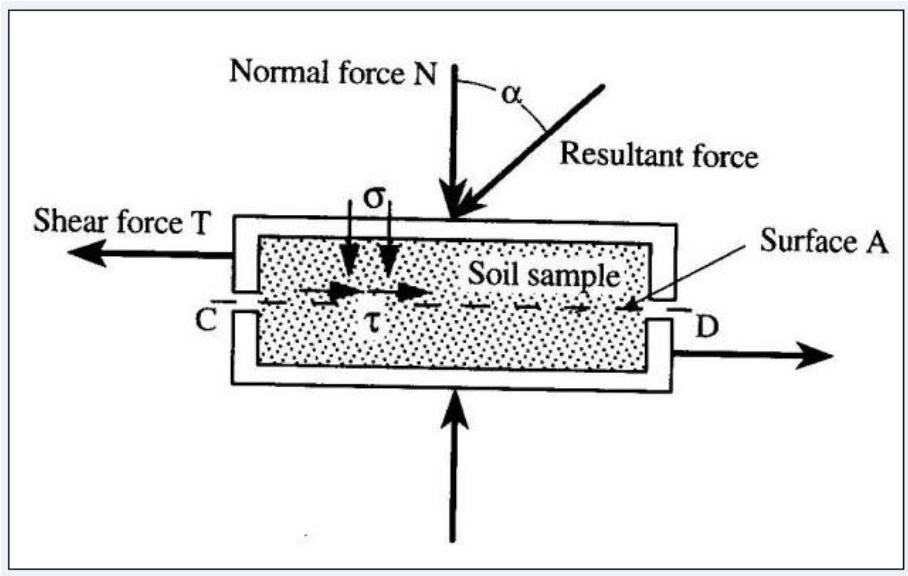

Figure 2.2 Soil sample in the direct shear box

The soil shear strength is the shear stress τ that causes the soil to slip on surface CD. It can be defined by Mohr-Coulomb theory (in Eq. 2.2).

The nature of the results of typical direct shear tests in loose, medium, and dense sands are shown in Figure 2.3. Based on Figure 2.3, the following observations can be made:

- In dense and medium sands, shear stress increases with shear displacement to a maximum or peak value τ_m and then decreases to an approximately constant value τ_{cv} at large shear displacements. This constant stress τ_{cv} is the ultimate shear stress.
- For loose sands, the shear stress increases with shear displacement to a maximum value and then remains constant.

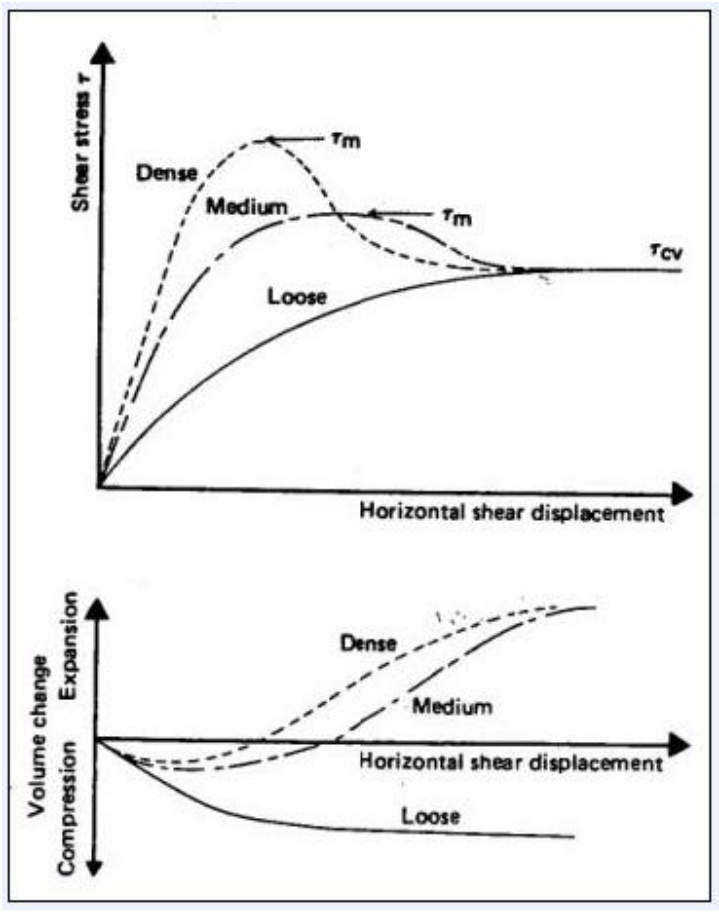

Figure 2.3 Direct shear test result in loose, medium, and dense sands (Das, 1983)

- For dense and medium sands, the volume of the specimen initially decreases and then increases with the shear displacement. At large values of shear displacement, the volume of the specimen remains approximately constant.
- For loose sands, the volume of the specimen gradually decreases to a certain value and remains approximately constant thereafter.

The angle of friction ϕ for the sand can be determined by plotting a graph of the maximum or peak shear stresses vs. the corresponding normal stresses, as shown in Figure 2.4. The Mohr-Coulomb failure envelope can be determined by drawing a straight line through the origin and the points representing the experimental results. The slope of this line will give the peak friction angle ϕ of the soil.

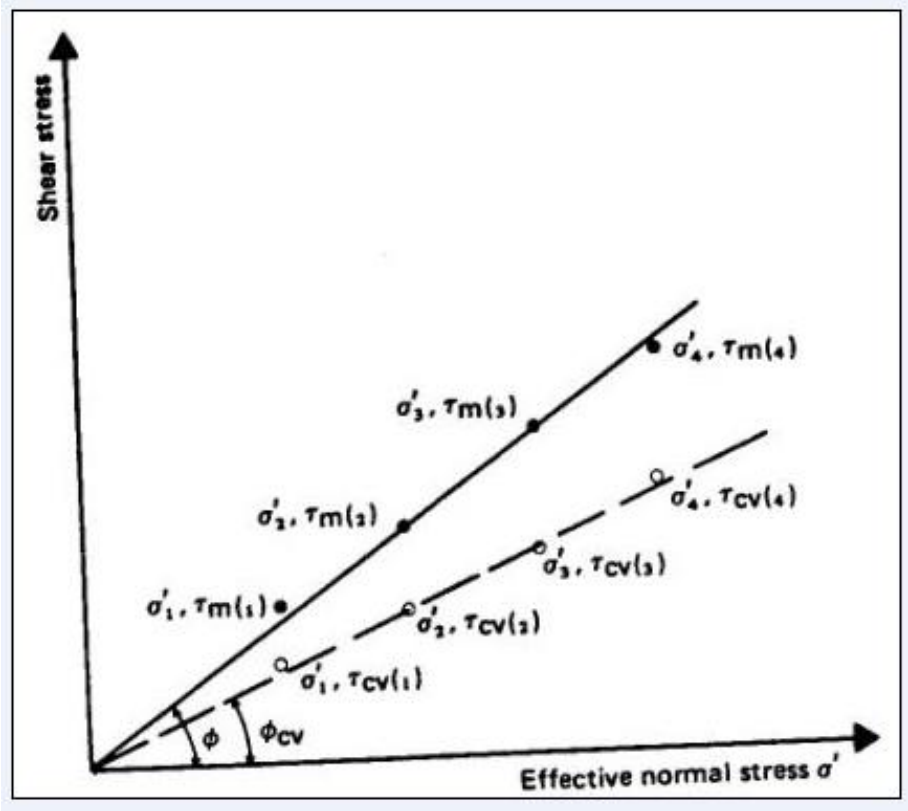

Figure 2.4 Determination of peak and ultimate friction angles from the direct shear test (Das, 1983)

Similarly, the ultimate friction angle ϕ_{cv} can be determined by plotting the ultimate shear stresses τ_{cv} vs. the corresponding normal stresses, as shown in Figure 2.4. The ultimate friction angle ϕ_{cv} represents a condition of shearing at constant volume of the specimen. For loose sands, the peak friction angle is approximately equal to the ultimate friction angle.

Calculations

Shear stresses on the horizontal surface are computed for every gauge reading intervals as follows:

$$\tau = \frac{C_P . \delta_p}{A_C} \tag{2.6}$$

where, τ : shear stress,

A_C : the corrected area of the sheared specimen,

C_p : proving ring constant

δ_p : proving ring deflection.

The normal stress σ (in kN / m^2) on the horizontal surface is calculated from:

$$\sigma = \frac{N}{A_c} \tag{2.7}$$

Boxes in square and cylindrical shape are practicable in practice. The corrected area A_C of the sheared specimen is for the square box of length a (in m.),

$$A_c = a.(a - \delta) \tag{2.8}$$

and for the circular box of internal diameter D (in m.),

$$A_c = \frac{D^2}{2}.\left(\theta - \frac{\delta}{D}.\sin\theta\right) \tag{2.9}$$

where, $\theta = \cos^{-1}\left(\frac{\delta}{D}\right)$ in radians.

The contact area between the two specimen halves varies with the relative shear displacement δ between the lower and upper boxes are shown in Figure 2.5. (Bardet, 1997).

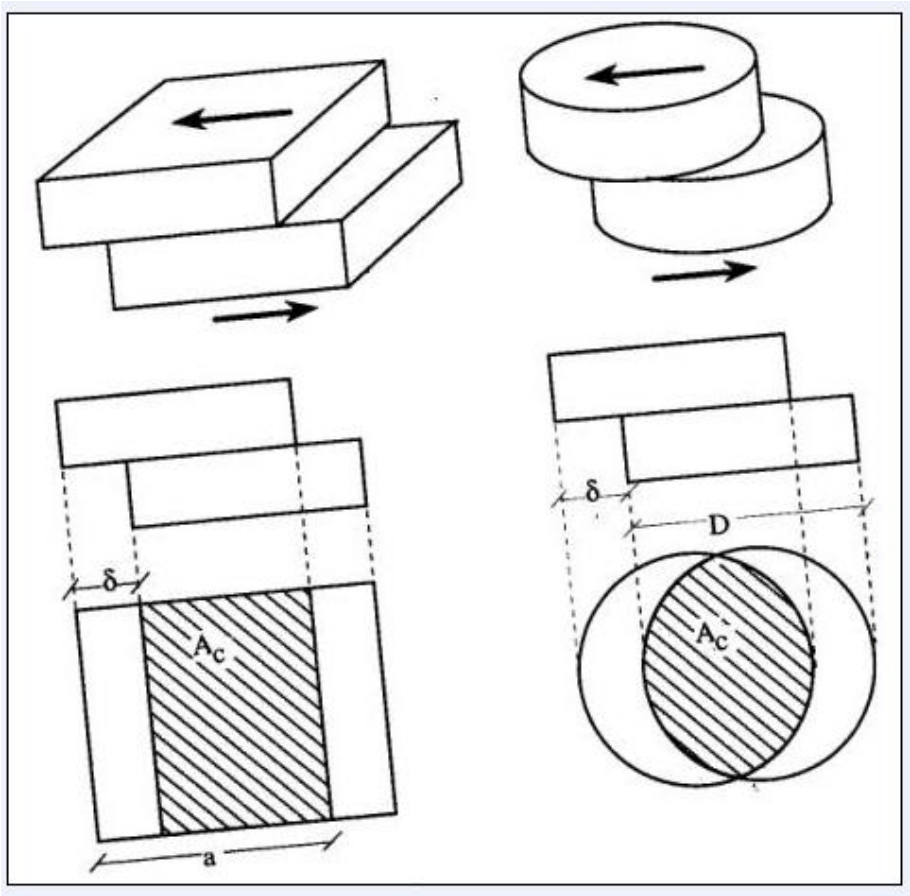

Figure 2.5 Corrected area for the calculation of shear and normal stresses (Bardet, 1997)

Shear strain ε_h (%) on the specimen in the square box is computed from,

$$\varepsilon_h = \frac{\delta}{a}.100 \qquad (2.10)$$

and for the cylindrical box,

$$\varepsilon_h = \frac{\delta}{D}.100 \qquad (2.11)$$

Vertical strain ε_v (%) on the specimen is calculated from,

$$\varepsilon_v = \frac{\delta_v}{H_o}.100 \qquad (2.12)$$

where, δ_v : vertical displacement

H_o : initial height of the sample.

The test procedures and technical information about the direct shear box test will be explained in detail in Chapter 3.

2.1.2 Shear Strength of Cohesive Soils

The shear strength of cohesive soils can, generally, be determined in the laboratory by either direct shear test equipment or triaxial shear test equipment; however, the triaxial test is more commonly used. Only the shear strength of saturated cohesive soils will be treated here. The shear strength based on the effective stress can be given by Eq. 2.3. For normally consolidated (NC) clays, $c' \cong 0$; and, for overconsolidated (OC) clays, $c' > 0$.

A number of considerable differences exist between cohesive and noncohesive soils:

- The frictional resistance of cohesive soils is less than that of granular soils.
- The cohesion of clay is appreciably larger than that of granular soils.
- Clay is much less permeable than a sandy soil, and the water drainage is, therefore, significantly slower. Hence, the pore pressure induced by an increase in load is dissipated very slowly, and the transfer of stress and the corresponding increase in intergranular pressure are likewise much slower.
- The time-related changes of volume in clays are slower than that of granular material (e.g., consolidation).

Of the number of factors that are recognized to have a direct effect on the shear strength of cohesive soils, most are recognized as individually quite complex. Also, it is recognized that most are significantly interrelated, thereby further increasing the complexity of the problem. Generally, the degree of consolidation, the drainage, effective stress, and pore pressures are relevant factors to be considered in the strength evaluation of cohesive soils (Cernica, 1995).

The shear strength of a soil can also be expressed in terms of effective major and minor principal stresses σ_1' and σ_3' at failure at the point in question. At failure the straight line represented by Eq. 2.3 will be tangential to the Mohr circle representing the state of stress, as shown in Figure 2.6, compressive stress being taken as positive. The coordinates of the tangent point are τ_f and σ'_f, where:

$$\tau_f = \frac{1}{2}.\left(\sigma'_1 - \sigma'_3\right).\sin 2\theta \qquad (2.13)$$

and θ is the theoretical angle between the major principal plane and the plane of failure. It is apparent that in Figure 2.7.

$$\theta = 45^o + \frac{\phi'}{2} \qquad (2.14)$$

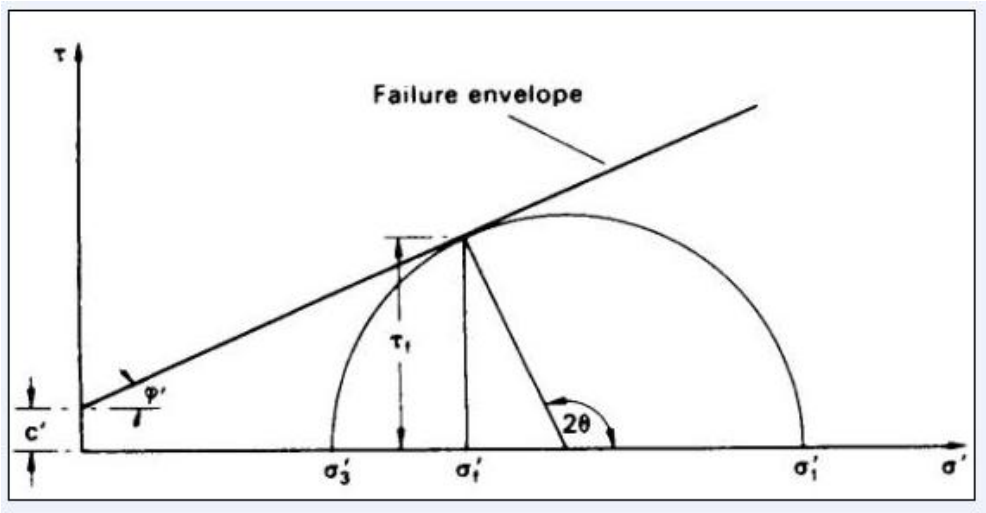

Figure 2.6 Stress conditions at failure (Craig, 1997)

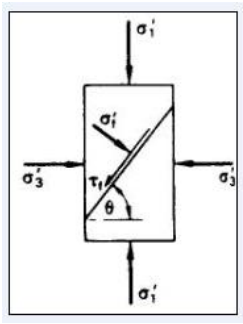

Figure 2.7 Stresses on the failure plane (Craig, 1997)

From Figure 2.6 the relationship between the effective principal stresses at failure and the shear strength parameters can also be obtained. Now:

$$\sin\phi' = \frac{\frac{1}{2}.\left(\sigma'_1 - \sigma'_3\right)}{c'.\cot\phi' + \frac{1}{2}.\left(\sigma'_1 + \sigma'_3\right)} \tag{2.15}$$

Therefore

$$(\sigma'_1 - \sigma'_3) = (\sigma'_1 + \sigma'_3).\sin\phi' + 2.c'.\cos\phi' \tag{2.16}$$

or

$$\sigma'_1 = \sigma'_3 . \tan^2(45^o + \frac{\phi'}{2}) + 2.c' . \tan(45^o + \frac{\phi'}{2}) \quad (2.17)$$

Equations 2.15, 2.16, and 2.17 are referred to as the Mohr-Coulomb failure criterion. If a number of states of stress are known, each producing shear failure in the soil, the criterion assumes that a common tangent, represented by Eq. 2.3, can be drawn to the Mohr circles representing the states of stress. The criterion implies that the effective intermediate principal stress σ_2' has no influence on the shear strength of the soil.

By plotting $\frac{1}{2}.(\sigma'_1 - \sigma'_3)$ against $\frac{1}{2}.(\sigma'_1 + \sigma'_3)$ any state of stress can be represented by a stress point rather than by a Mohr circle, as shown in Figure 2.8, and on this plot a modified failure envelope is obtained, represented by the equation:

$$\frac{1}{2}.(\sigma'_1 - \sigma'_3) = a' + \frac{1}{2}(\sigma'_1 + \sigma'_3).\tan\alpha' \quad (2.18)$$

where a' and α' are the modified shear strength parameters. The parameters c' and ϕ' are then given by:

$$\phi' = \sin^{-1}(\tan\alpha') \quad (2.19)$$

$$c' = \frac{a'}{\cos\phi'} \quad (2.20)$$

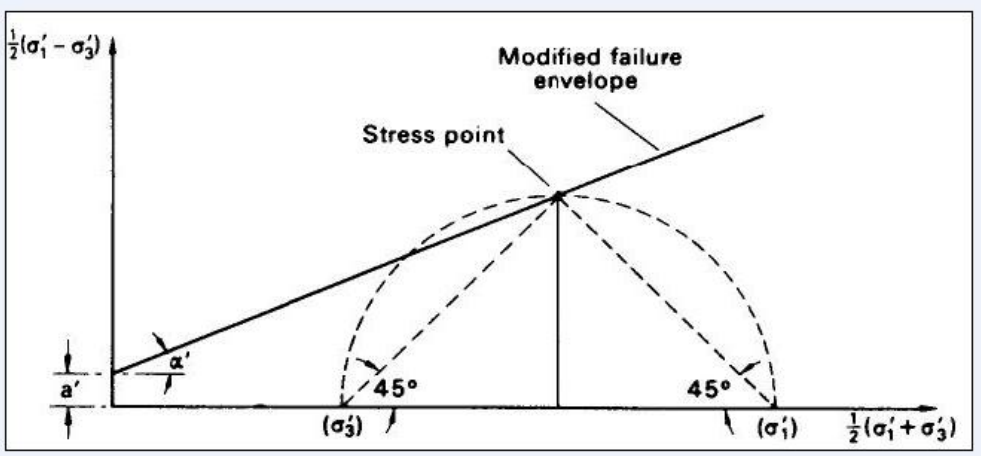

Figure 2.8 Alternative representation of stress conditions (Craig, 1997)

Triaxial Test

The triaxial shear test is one of the most reliable methods available for determining the shear strength parameters. It is widely used for both research and conventional testing. The test is considered reliable for the following reasons:

- It provides information on the stress-strain behavior of the soil that direct shear test does not.
- It provides more uniform stress conditions than the direct shear test does with its stress concentration along the failure plane.
- It provides more flexibility in terms of loading path.

Many variations of test procedure are possible with the triaxial apparatus but three principal types of the test are as follows:

1) Unconsolidated-Undrained. The specimen is subjected to a specified all-round pressure and then the principal stress difference is applied immediately with no drainage being permitted at any stage of the test.
2) Consolidated-Undrained. Drainage of the specimen is permitted under a specified all-round pressure until consolidation is complete: the principal stress difference is then applied with no drainage being

permitted. Pore water pressure measurements may be made during the undrained part of the test.

3) Consolidated-Drained. Drainage of the specimen is permitted under a specified all-round pressure until consolidation is complete: with drainage still being permitted, the principal stress difference is then applied at a rate slow enough to ensure that the excess pore water pressure is maintained at zero (Craig, 1997).

The unconsolidated-undrained test is usually conducted on clay specimens. The added axial stress at failure $(\delta\sigma_d)_f$ (deviator stress at failure) is practically the same regardless of the chamber confining pressure. This result is shown in Figure 2.9. The failure envelope for the total stress Mohr's circles becomes a horizontal line and hence is called a $\phi = 0$ condition, and

$$\tau_f = c_u \tag{2.21}$$

where c_u is the undrained shear strength and is equal to the radius of the Mohr's circles (Das, 2005).

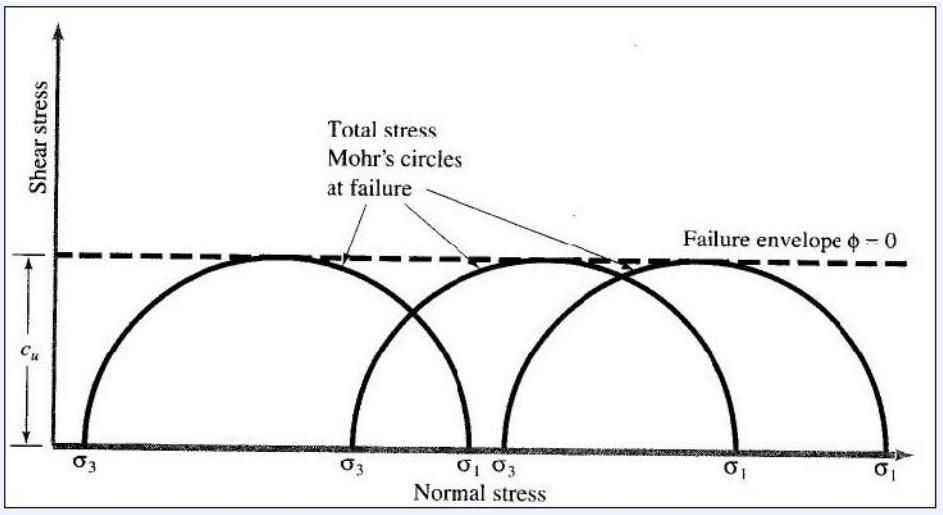

Figure 2.9 Total stress Mohr's circle and failure envelope ($\phi = 0$) obtained from triaxial UU tests (Das, 2005)

The general patterns of variation of $\delta\sigma_d$ and δu_d (pore water pressure) with axial strain for NC clays are represented in Figures 2.10 and 2.11, respectively. For OC clays, they are shown in Figures 2.12 and 2.13, as respectively.

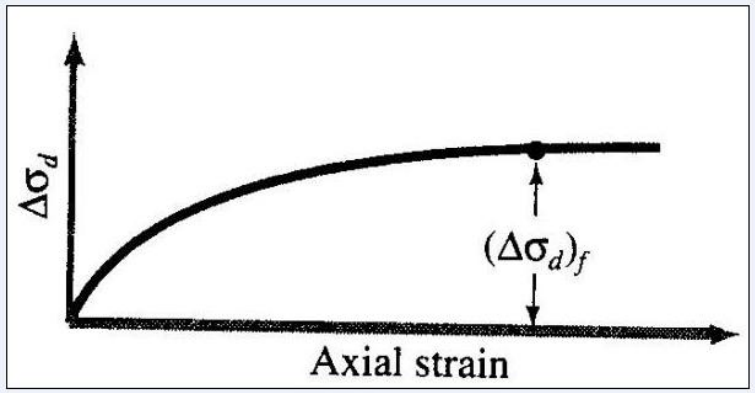

Figure 2.10 Deviator stress against axial strain for NC clays (Das, 2005)

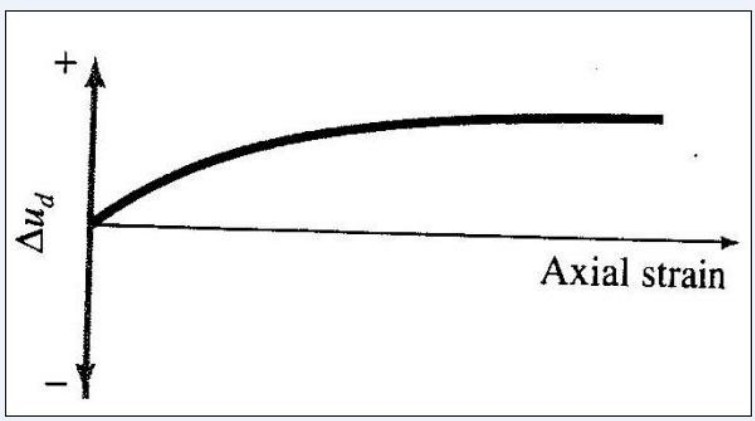

Figure 2.11 Variation of pore water pressure with axial strain for NC clay (Das, 2005)

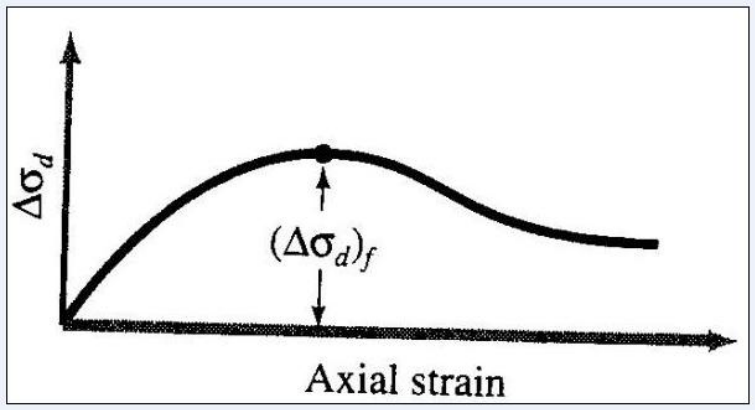

Figure 2.12 Deviator stress against axial strain for OC clays (Das, 2005)

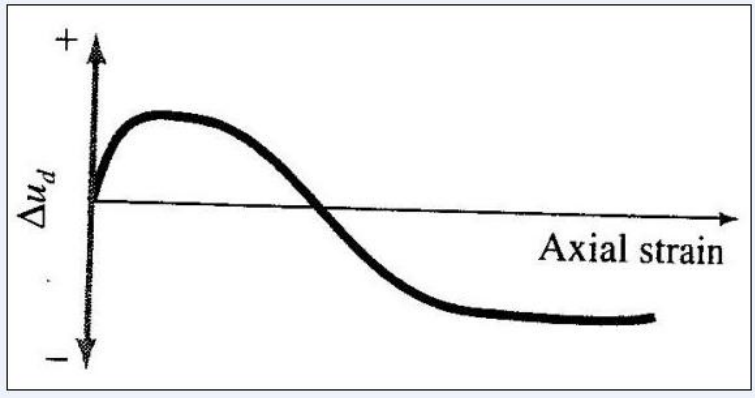

Figure 2.13 Variation of pore water pressure with axial strain for OC clay (Das, 2005)

Calculations

Using the proving ring deflection readings, the deviator loads (F) on the specimens were calculated by converting the deflections to the force applied using the proving ring constant. This load was calculated for each stage of the test. And then the forces were converted into stresses dividing each by corrected area of the specimen.

The vertical strain (ε_v) was obtained by dividing longitudinal compression measured by the dial gauge, by initial height of the specimen.

$$\varepsilon_v = \frac{\delta L}{H_o} \tag{2.22}$$

where ε_v = vertical strain,

δL = change in height of specimen,

H_o = initial height of specimen.

The average cross-sectional area which changes depending on the increase in strain was obtained for each stage of the test from the following formula.

$$A_c = \frac{A_o}{(1-\varepsilon_v)}.(1+v) \tag{2.23}$$

where A_c = corrected cross-sectional area of the specimen,

ε_v = vertical strain,

A_o = initial cross-sectional area of specimen,

v = unit change in volume = $\delta V / V_o$ = 0 because no volume change is assumed in undrained tests of saturated specimens,

δV = change in volume of the specimen,

V_o = initial volume of the specimen.

So the equation simplifies to:

$$A_c = \frac{A_o}{(1-\varepsilon_v)} \tag{2.24}$$

This formula is true for the calculation of average cross-sectional area of the saturated specimen

$$\sigma_1 - \sigma_3 = \frac{F}{A_c} \tag{2.25}$$

where σ_1 = major principal stress,

σ_3 = minor principal stress,

A_c = corrected cross-sectional area,

F = applied force = $\delta.C_{pt}$

δ = proving ring deflection

C_{pt} = proving ring constant (0.000995 kN/division)

The test procedures and technical information about the triaxial compression UU test will be explained in detail in Chapter 3.

2.2 Literature Survey

Wasti and Alyanak (1968) have worked on sand-clay mixtures and stated that when clay content is just enough to fill the voids of the granular portion at its maximum porosity, the structure of the mixture changes and the linear relationship between the Atterberg limits (plastic and liquid limits) and the clay content is no more valid and soil changed its behavior from sand to clay. For mixture including kaolin clay at its liquid limit, they showed out that this threshold value exists about 25 % kaolin content.

Novais and Ferreira (1971) performed consolidated-drained direct shear tests on artificial mixtures with increasing proportions of clay, including two types of sand (fine and coarse) and a montmorillonitic clay. They found that maximum and limiting shear stresses showed a tendency to decrease as the clay content increased. They also described the existence of three zones of behavior of the mixtures as a function of clay content (C_f): 1) Incoherent behavior ($C_f \leq 28$ %) where the cohesion is null and the angle of friction is high (above 30^o) the effects of

fluctuations in soil grain size variations are not significant. 2) ($28 < C_f < 41$) where the soil is sensitive to grain size fluctuations. 3) Coherent behavior ($C_f \geq 41$) where the cohesion is high and the angle of friction is low.

Georgiannou, V.N. (1988), made an investigation on the behavior of clayey sands under monotonic and cyclic loading. He concluded that the fines content has a remarkable influence on the stress-strain response of the soil mass. As the fines content increases, the dilatant behavior of the soils is suppressed, and the response gradually becomes controlled by the fine matrix at about % 40 fines content.

Georgiannou, Burland & Hight (1990) performed an experimental study about stress-strain behavior of anisotropically consolidated clayey sands using computer controlled triaxial cells. The specimens were prepared by sedimenting Ham River sand into a kaolin suspension. They observed the effects of variations in clay content and initial granular void ratio. They concluded that this method creates a material which is markedly less stable, which has a higher granular void ratio and exhibits a higher undrained brittleness behaviour, which is the engineering characteristic like ductile behaviour and it is determined by stress history, formative history, microstructure, rate of shearing and composition and fabric of clays, if compared with the same sand that is sedimented through clean water (i.e. contains no clay). Moreover they showed that a sand that has 30 % clay fraction the normally consolidated material is no longer dilatant and exhibits the response that would be expected in a sedimented clay. They also stated that for clay fractions up to 20 %, the clay does not significantly reduce the angle of shearing resistance of the granular component.

Georgiannou, Burland & Hight (1991) have described the undrained behavior of natural clayey sand from the site of the Gulfoks C oil production platform in the North Sea. The behavior of a model soil formed from Ham River sand and kaolin was observed. This model soil was selected in order to display relatively closer response of the soil at the field. These reconstituted specimens have been subjected

to Ko consolidation and undrained shear in the triaxial compression test under displacement control. They concluded that undrained brittleness in compression increases as the clay content increases from 4.5 % to 11.5 %, but reduces as the overconsolidation ratio, OCR, increases. They also showed that the clayey sand reaches its peak resistance at small axial strains: ε_a in compression increases from 0.1 % to 0.3 % as OCR increases from 1 to 2.

Pitman, Robertson & Sego (1994) have carried out a study to investigate the influence of fines and gradation on the behavior of loosely prepared sand samples. Loose sand samples, formed by moist tamping and consolidated to the same effective stress level, were prepared with varying percentages of both plastic and nonplastic fines. Samples were isotropically consolidated and subjected to monotonic undrained triaxial compression. They stated that undrained brittleness decreased as the fines content, for both plastic and nonplastic type, increased. They also concluded that the undrained brittleness may not be controlled by the plasticity of the fines but more by the amount of fines (<74μm), at least for percentages greater than 10 %.

Bayoğlu, Esra (1995), made an experimental study. In this study, effects of the fine particles (diameter < 0.074 mm.) on the shear strength and compressibility properties of the soil mixtures were investigated. Soil mixtures having wide range of grain size from sand to silt-clay mixtures were studied. Drained shear box and consolidated-undrained triaxial tests were performed on normally consolidated clay-sand mixtures to obtain strength and compressibility parameters. According to the results of drained direct shear tests which are shown in Figures 2.14 and 2.15, on mixtures containing 5 %, 15 %, 35 %, 50 %, 75 %, and 100 % fines, the internal friction angles varied between 30-38 degrees until 50 % fines and a slight decrease existed in the friction angle with increasing fine content. At fine contents higher than 50%, the reduction in the friction angle was significant and decreased to about 10 degrees

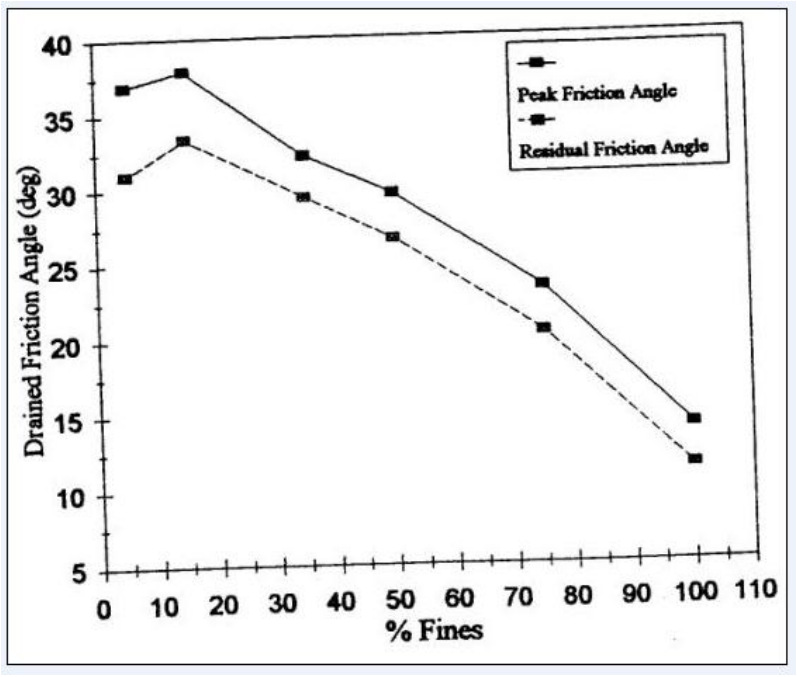

Figure 2.14 Drained friction angle - % fines relation (After Bayoğlu, 1995)

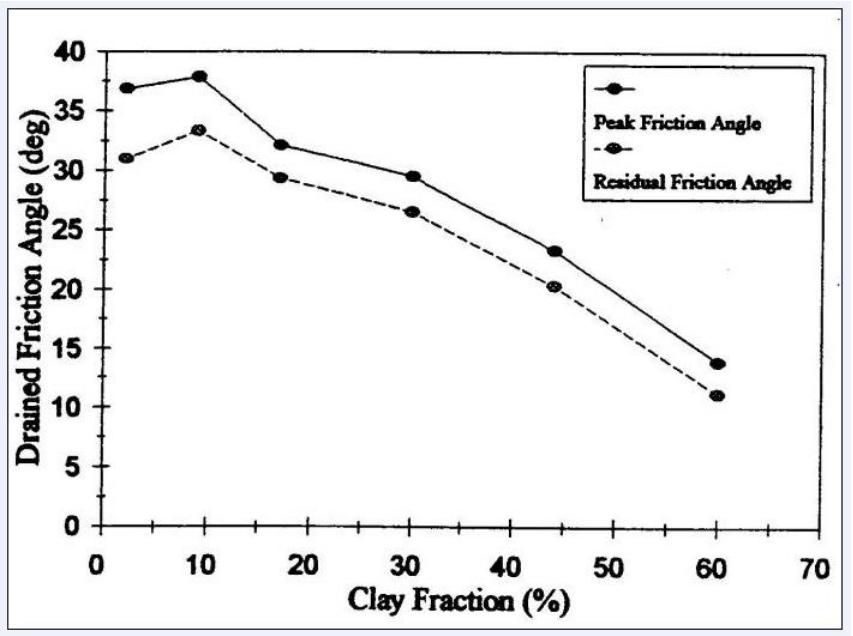

Figure 2.15 Drained friction angle - % clay fraction relation (After Bayoğlu, 1995)

The relation between drained friction angle and plasticity index and liquid limit is given in Figures 2.16 and 2.17. The behavior, which is about the same for the two properties, is more likely a linear reduction of the angles with increasing PI and LL.

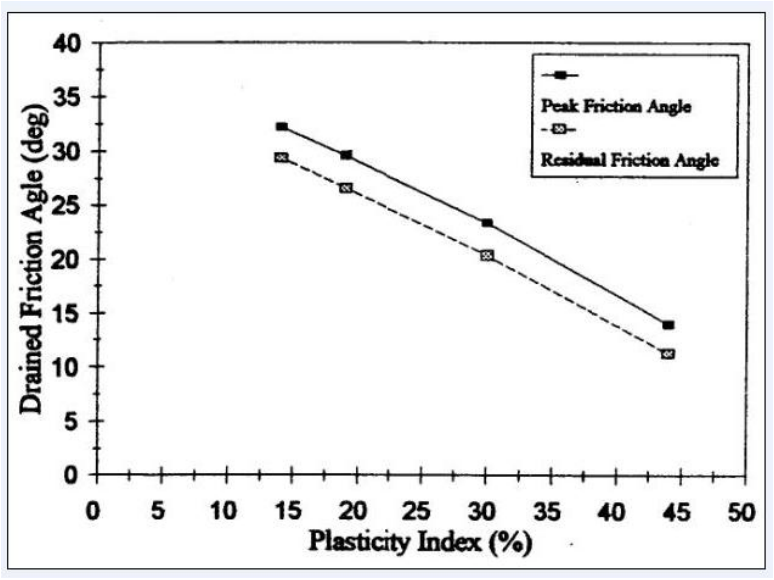

Figure 2.16 Drained friction angle plotted against plasticity index (After Bayoğlu, 1995)

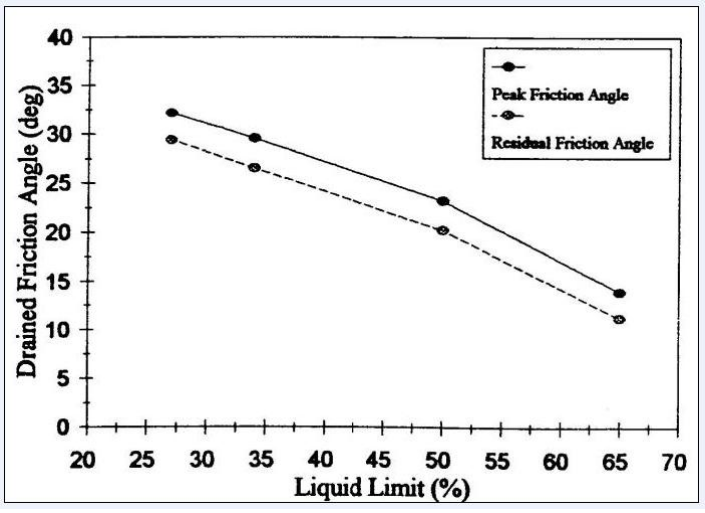

Figure 2.17 Drained friction angle plotted against liquid limit (After Bayoğlu, 1995)

According to the results of consolidated-undrained triaxial tests which are presented in Figure 2.18, on 35%, 50%, 75%, and 100% fines, there was no a current relation between undrained friction angle and percentage of fines and the measured angle of shearing resistances were in the same order of magnitude irrespective of percent fines.

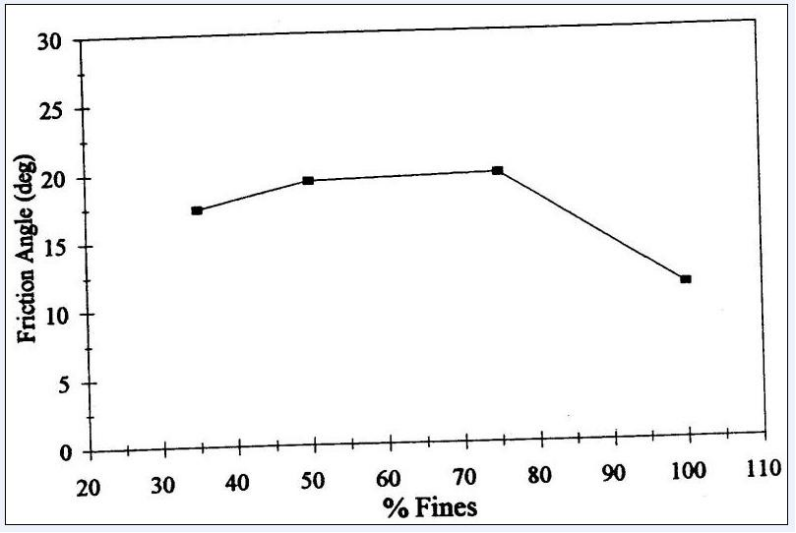

Figure 2.18 Undrained friction angle plotted against % fines (After Bayoğlu, 1995)

S. Thevanayagam (1998), carried out a series of experiments to obtain large strain undrained shear strength (s_{us}) in triaxial compression for a particular host sand mixed with different amounts of nonplastic fines. Results indicate that the intergranular void ratio, e_s, which is the void of the sand-grain-matrix (given by $((e+f_c)/(1-f_c)$, where f_c is the silt content fraction by weight) plays an important role on s_{us} of silty sands. At the same void ratio, e, a silty sand shows low s_{us} compared to that of the host sand. However, when compared at the same e_s, provided that it is less than the maximum void ratio of the host sand, $e_{max,HS}$, both the silty sand and the host sand show similar s_{us} that is fairly independent of the initial confining stress. When e_s of the silty sand is in the vicinity of or exceeds $e_{max,HS}$ the

s_{us} depends on the initial effective confining stress. At such "loose" states, initial consolidation stress is very low, s_{us} decreases with a further increase in e_s. At a fine content greater than about 30 %, a silty sand is expected to behave as a silt at an interfine void ratio, e_f, defined as the void ratio of the silt-matrix (given by e/f_c), unless the silty sand or sandy silt is very dense.

R. Salgado (2000) made an experimental investigation about the effects of nonplastic fines on the shear strength of sands. A series of laboratory tests was performed on samples of Ottawa sand with fines content in the range of 5-20 % by weight. They used triaxial tests that were conducted to axial strains in excess of 30 %. They used the concept of the skeleton void ratio e_{sk} (Kuerbis et al. 1988), which is the void ratio of the silty sand calculated as if the fines were voids.

$$e_{sk} = \frac{1+e}{1-f} - 1 \tag{2.26}$$

where, e = overall void ratio of soil,

f = ratio of weight of fines to total weight of solids.

Whenever e_{sk} is greater than the maximum void ratio $(e_{max})_{f=0}$ of clean sand, the sand particles are not in contact and mechanical behavior is no longer controlled by the sand matrix. They suggested that silty sand with nonfloating fabric in the 5-20 % silt content range is more dilatant than clean sands; dilatancy appears to peak around 5 % silt content, but even at 20 % silt content it remains above that of clean sand.

CHAPTER 3

EXPERIMENTAL WORK

3.1 Testing Program

The test series are briefly summarized below. Details are given section 3.4.

In series 1 experiments, soil mixtures at specified kaolin contents are consolidated under 50 kPa vertical pressure in a cubical box without keeping them under water. Undrained triaxial compression tests are performed in this series.

In series 2 experiments, soil mixtures are consolidated under 100 kPa vertical pressures in the cubical box with keeping them under water. Undrained triaxial compression tests are performed in this series.

In series 3 experiments, samples are directly prepared in the direct shear boxes and consolidated before shearing in a drained way.

3.2 Experimental Set-Up

The laboratory model testing system consists of:

1. Plexiglas Boxes with 20x20x20 cm inside dimensions (Figure 3.1 .a)
2. Geotextiles for drainage and prevention of drying (Figure 3.1 .b)
3. Loading jack for the application of constant (consolidation) pressure (Figure 3.2)
4. Commercial kaolin type of clay (Figure 3.3)
5. Water tank used at initial consolidation stage (Figure 3.4)

6. Displacement dials (Figure 3.4)
7. Steel sampling molds (Figures 3.5 .a and .b)
8. Direct Shear Box Test machine (Figures 3.6, 3.7, and 3.8)
9. Triaxial Test machine (Figure 3.9- Figure 3.13).

3.2.1 Testing Box Assembly

A Plexiglas testing box system was used for achieving initial consolidation stage. The box has the inside dimensions of 20x20x20 cm and 1 cm wall thickness. Two steel clusters were attached in order to strengthen the box for lateral straining.

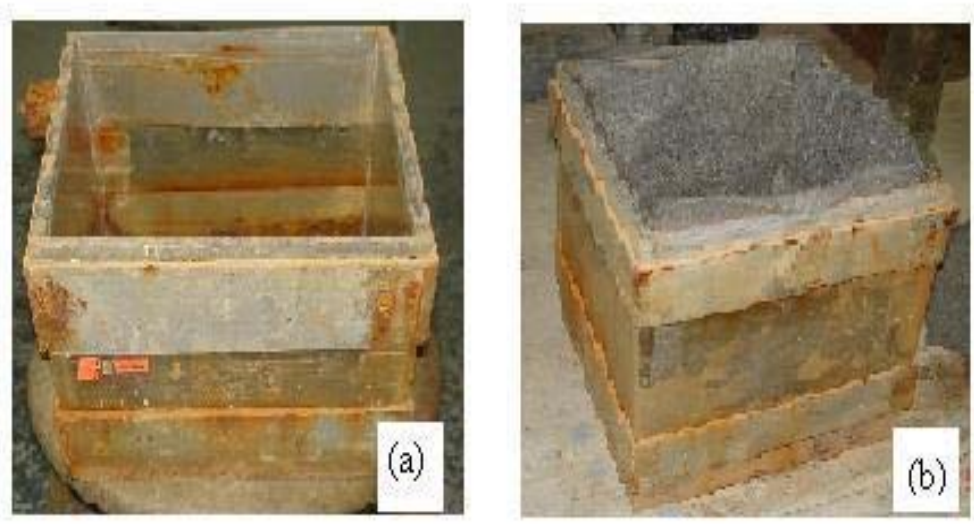

Figure 3.1 (a) Plexiglas box empty, (b) After geotextile sheets placed

3.2.2 Loading Frame and Loading Jack

Jacks with loading capacities of 375 kgf (3.75 kN), was connected to the loading frames consisting of four steel rods and U steel plates. The piston rod of the loading jacks pressed the test specimens as seen in Figure 3.2. Desired amount of consolidation pressure was applied by means of the jack.

Figure 3.2 Loading frame and jack system

3.2.3 Commercial Type of Kaolin Clay

In these experiments commercial type of kaolin clay, which has low plasticity and low activity, was used. This type of clay seen in Figure 3.3 is usually preferred in model testing in avoidance of potential complications in behavior due to swelling, shrinkage...etc.

Kaolin powder was obtained by grinding the oven-dried kaolin samples. Soil specimens used in the tests were prepared by mixing the kaolin powder and sand with water in desired consistencies.

Figure 3.3 Commercial type of kaolin clay

3.2.4 Water Tank

A water tank system was used for immersing the Plexiglas testing box under water in order to get full saturation. This tank was only used in series 2 experiments and it is shown in Figure 3.4.

Figure 3.4 Water tank

3.2.5 Displacement Dials

Displacement dials are used for monitoring the settlements at initial consolidation stage. It is shown in Figure 3.4.

3.2.6 Steel Sampling Molds

Steel sampling molds are used to place samples in testing machines. To do this cylindrical molds are used in both 1st and 2nd series of experiments. They are shown in Figure 3.5.a and Figure 3.5.b. The cylindrical mold has the inside diameter of 36 mm and 71 mm height.

(a) Steel sampling mold before taking sample

(b) Steel sampling mold after taking sample

Figure 3.5

3.2.7 Direct Shear Box Test Machine

The shear box test is often referred to as the direct shear test because an attempt is made to relate shear stress at failure directly to normal stress, thus directly defining the Mohr-Coulomb failure envelope.

Essentially, a sample of soil is subject to a fixed normal stress and a shear stress is induced along a predetermined plane until shear failure of the soil takes place. The apparatus is shown diagrammatically in Figure 3.6. The soil sample is usually square in plan and rectangular in cross-section. The sample can either be remolded or undisturbed and the box is capable of accepting coarse-grained soils. Obviously, when testing remolded or coarse-grained samples care must be taken to ensure that the tested samples are prepared at bulk unit weight and moisture content values relevant to the problem under consideration. This can be difficult to achieve.

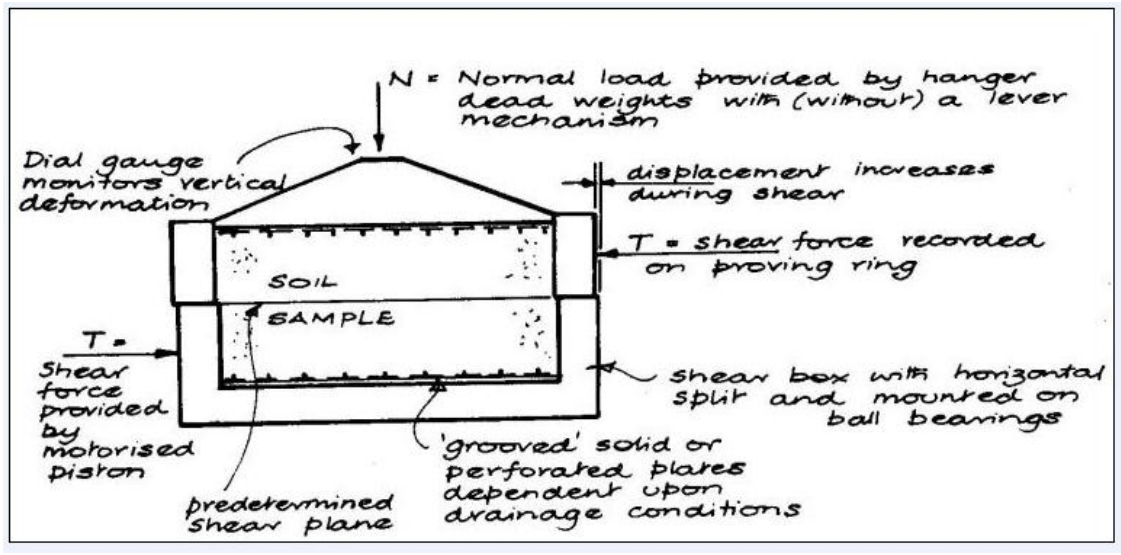

Figure 3.6 Shear box test (Vickers, 1984)

The box is of rigid metal construction, open at the top, and is immersed in a water container. The box is manufactured in two halves so that the upper half is able to

move horizontally relative to the lower half; the sample can thus be sheared on a horizontal plane.

The normal load is applied vertically to the sample, usually through a loading platen by means of hanger weights. For higher normal stresses a 5:1 or 10:1 lever mechanism can be used.

The shear force is applied horizontally to the sample by a motor-driven push rod. The motor drive is usually multi-geared so that a variety of shear loading rates can be applied. To facilitate free movement of the lower and upper halves of the shear box, the box is mounted on ball-bearing slides.

The shear load applied to the sample is recorded by means of a proving mounted in a horizontal plane. Deformation of the proving-ring, monitored by a dial gauge, is related to the shear load applied by means of a calibration graph.

In addition, it is usual to monitor vertical deformation of the sample by a dial gauge fixed to the top loading platen.

Tests can be performed under either undrained or drained conditions by the insertion of either solid metal or perforated metal plates adjacent to the soil sample's upper and lower faces and they are shown in Figure 3.7. Usually these metal plates are grooved to facilitate grip on the faces of the sample. A typical set-up is shown in Figure 3.8. (Vickers, 1984).

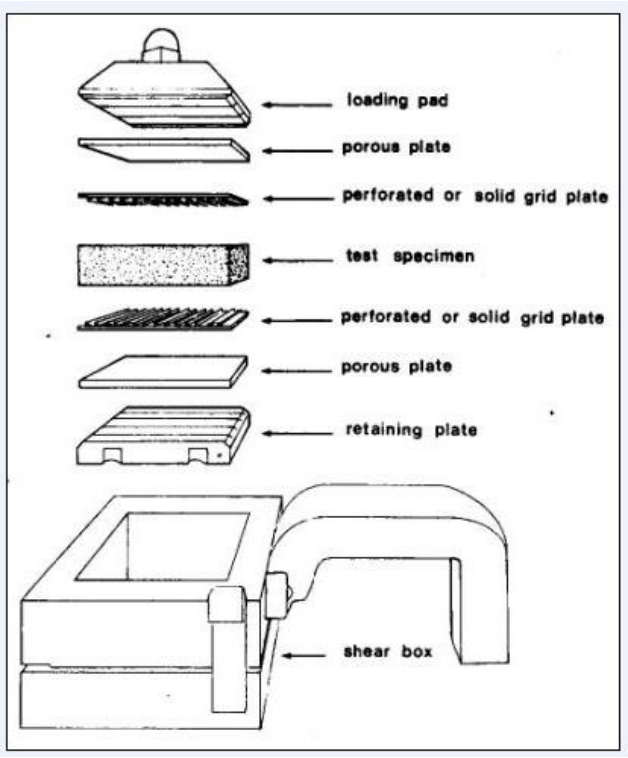

Figure 3.7 Apparatus of ınner box (Head, 1982)

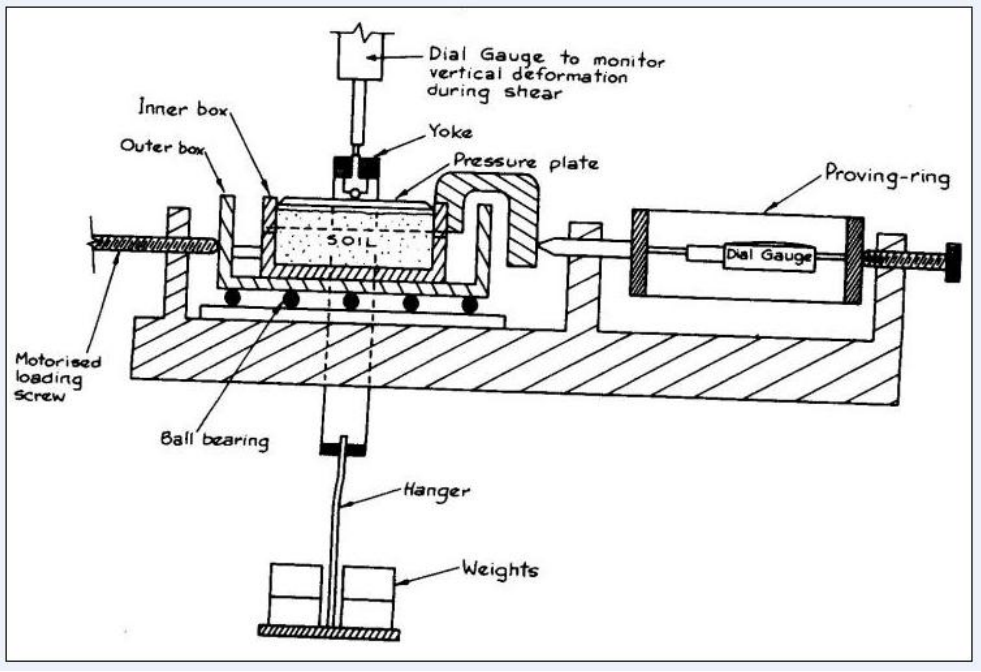

Figure 3.8 Shear box apparatus (not to scale) (Vickers, 1984)

Advantages:

1. There is some measure of control of drainage during testing, and both undrained and drained tests can be performed. The drained tests must be carried out at such a low rate of shearing that no excess pore-water pressures are allowed to develop.

2. In some cases the shear box can be of distinct advantage. With coarse-grained soils, provided that densities can be simulated, it can provide a relatively cheap means of estimating drained shear strength parameters. This is mainly because of the relative expense and difficulty of preparing samples of coarse-grained soils for other methods of shear-strength testing.

Disadvantages:

1. During testing there is no available means of measuring the pore-water pressure. In some particular field problems knowledge of pore-water pressure during shear is a distinct advantage and will aid field predictions of shear strength.

2. Other drawbacks to the shear box test are that the plane of shear is predetermined as horizontal by the split box; the area of shearing is constantly decreasing as the two halves of the soil separate; the results can be affected by end and side effects of the rigid box and there is subsequent doubt about the stress distributions within the sample (Vickers, 1984).

3.2.8 Triaxial Test Machine

The triaxial apparatus is possibly the most widely used and most versatile means of observing the shear-strength characteristics of soils. A cylindrical sample of soil is enclosed in a pressurised chamber which subjects the sample to compressive stresses in three mutually perpendicular directions. The vertical compressive stress is then increased in excess of the horizontal stresses until eventually the soil fails in shear or strains to such a point that excessive deformation results. Means are provided to vary the drainage conditions, to monitor vertical deformations, to observe volume change of the sample and to monitor pore-water pressures during testing. The basic Triaxial Cell set-up is shown in Figure 3.9.

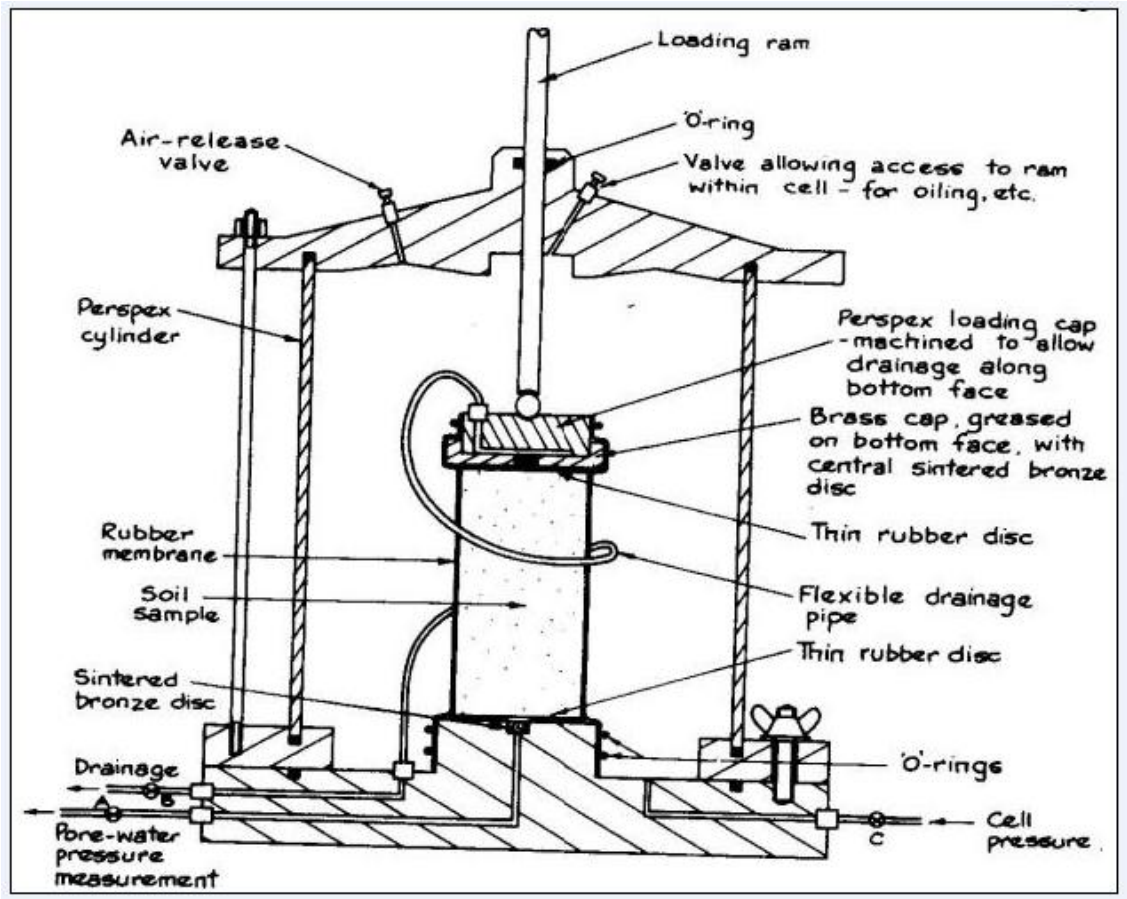

Figure 3.9 Triaxial cell set-ups (Vickers, 1984)

As shown in Figure 3.9, the soil sample is mounted on a pedestal base which is attached to the base plate of the triaxial cell. The cell is formed from a Perspex cylinder attached, usually by rods, to metal upper and lower plates. The whole assembly is able to withstand, without leakage, hydraulic pressures.

The pedestal base is such that it will receive cylindrical soil samples and the standard diameters are 38 mm and 100 mm, although some cells are manufactured to accommodate samples of 254 mm diameter. The heights of the samples are usually such as to give a height-to-diameter ratio of 2:1 (i.e. 76 mm and 200 mm).

The sample is enclosed in a thin rubber membrane so that it is effectively sealed from interaction with the fluid used to provide the all-round (cell) pressure. Water is the most commonly used to provide this all-round pressure although recent research has shown that there can be benefit from using other fluids, such as light oil, especially in long-term tests. The function of the surrounding membrane is to prevent moisture movement across it; any potential moisture seepage between the membrane and the upper platen and base pedestal is prevented by the clamping effect of two or more ‘O’-ring seals.

From the base pedestal a connection, via a Klinger valve (A), connects the pore water of the soil to a pore-water pressure measuring device; from the top platen (usually made of Perspex) is a connection via a Klinger valve (B) to a burette system to allow drainage and volume-change observations. A further Klinger valve (C) is connected to the base plate of the cell, allowing the fluid in the cell and surrounding the externally sealed sample to be pressurised.

A ball seating at the upper face of the top Perspex platen allows the vertical axial load to come into contact with the sample by means of a plunger fitted in a rotating bush in the top plate of the cell (Vickers, 1984).

Application of Cell Pressure:

The two most common means of supplying a constant fluid pressure to surround the sample are

(i) A constant-pressure mercury pot system

(ii) An air-water cylinder. Oil-water cylinder system is also used in the recent designs.

The most important requirements are that the pressure supply is maintained constant for the duration of the test (which may be up to or over one month) and that the supply system can accommodate the expected volume change of the sample. In addition it is necessary to have a connection from the cell pressure supply lines to a pressure gauge or, preferably, a manometer so that cell pressures can be adequately monitored. It should be noted that the datum for pressure observations is usually taken as the mid-height of the sample. Cell pressure systems are shown in Figure 3.10. (Vickers, 1984).

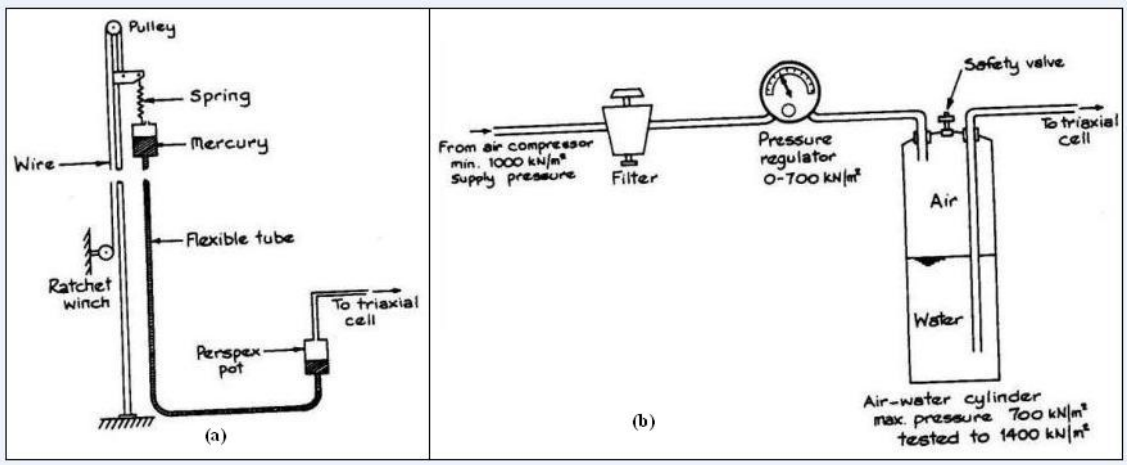

Figure 3.10 (a) Constant-pressure pot system, (b) Air-water cylinder (Vickers, 1984)

Application of Vertical Load:

The vertical load, transmitted to the sample via the plunger fitted into the top plate of the triaxial cell, is increased gradually to cause shear failure of the sample. Two systems of loading are generally available. The most common load system is one using a motorised load frame where the cell base is raised, pushing the sample and plunger against a proving-ring fixed to the load frame. This system is shown in Figure 3.11.

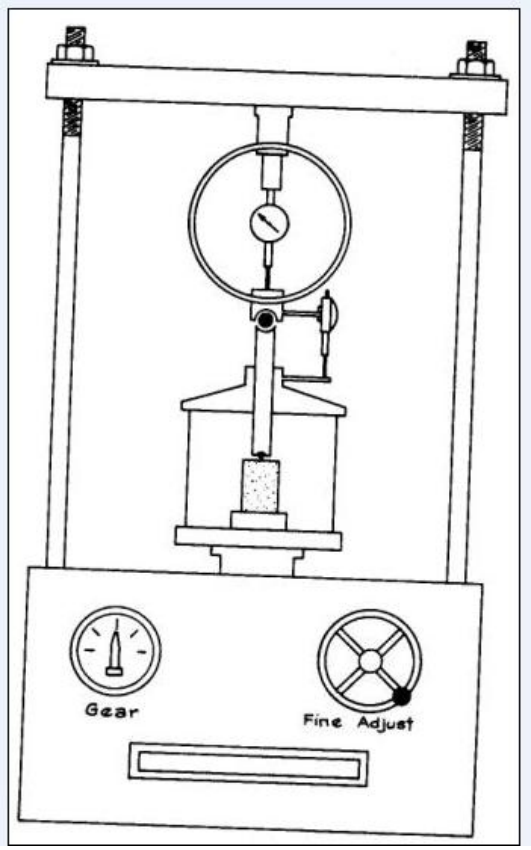

Figure 3.11 Motorised loading frame for strain-controlled test (Vickers, 1984)

The rate of loading can be varied by appropriate gear selection to give a variety of compressive strain rates. In undrained triaxial tests the rate of strain is often 2% per minute, thus producing 20% strain or failure within 10 minutes from the start of

loading; in drained tests the strain rate may be of the order of 0.001% per minute, giving a time to 20% strain of about 2 weeks. The actual rate of strain in drained test should be chosen so that no excess pore-water pressure builds up.

Tests where the load application is by a motorised loading frame are termed ‘strain-controlled’ tests, since the vertical compressive strain is set to a fixed rate and the vertical compressive stress is such as to allow the fixed strain rate.

The alternative type of loading system is that using hanger weights (as with the normal stress applied in the shear box), perhaps supplemented by a lever mechanism for large compressive loads. The load is incrementally applied at time intervals to suit the type of test being undertaken, i.e. relatively quickly in undrained triaxial tests and sufficiently slowly to allow dissipation of excess pore water pressures in drained triaxial tests. A typical arrangement is shown in Figure 3.12. This type of loading gives triaxial tests that are ‘stress-controlled’ in that the stress is being increased by specific increments at a chosen rate and this creates the subsequent strain.

The advantage of the strain-controlled tests is that, in the case of dense sand, peak shear resistance (that is, at failure) as well as lesser shear resistance (that is, at a point after failure called ultimate strength) can be observed and plotted. In stress-controlled tests, only peak shear resistance can be observed and plotted. Note that the peak shear resistance in stress-controlled tests can only be approximated. This is because failure occurs at a stress level somewhere between the prefailure load increment and the failure load increment. Nevertheless, stress-controlled tests probably simulate real field situations better than strain-controlled tests (Head, 1982).

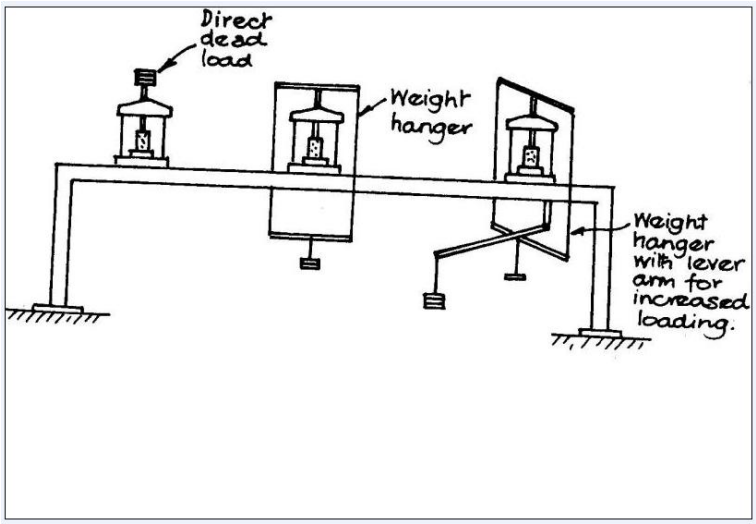

Figure 3.12 Dead loading frame for stress-controlled test (Vickers, 1984)

Vertical Deformation:

Usually vertical deformation of the sample is monitored by a dial gauge recording vertical movement of the loading piston. It is shown in Figure 3.13. In some cases lineal displacement transducers can also be installed to record vertical deformation. The transducers are electrically excited and can be installed to print out automatically the deformation of the sample at specified time intervals. This refinement can thus save attendant-time and is obviously of benefit in long-term tests running day and night.

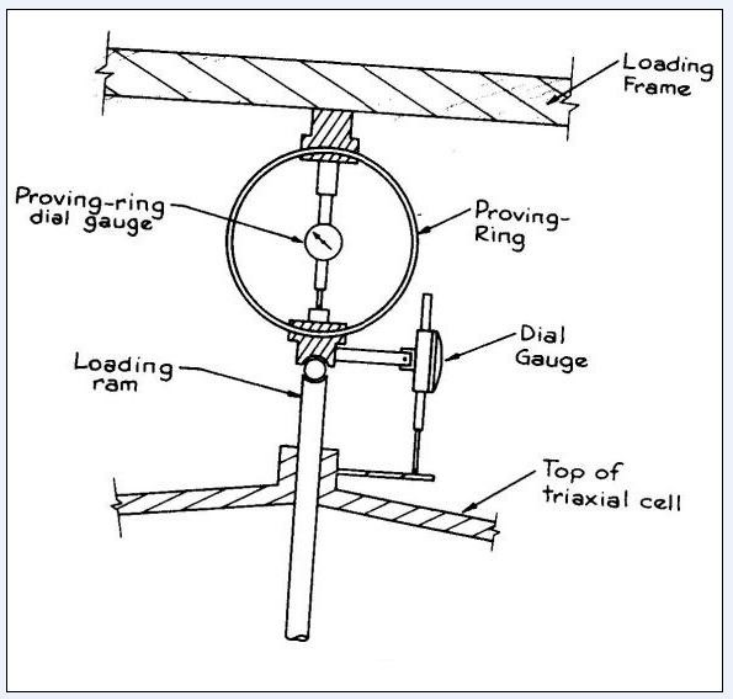

Figure 3.13 Proving-ring and dial-gauge set-up on triaxial cell (Vickers, 1984)

Advantages:

1. In spite of some inherent weakness, the triaxial test is still used on a commercial basis as the most sophisticated and versatile shear-strength test. Its versatilities are due to the facilities of drainage control which allows close correlation to field drainage conditions. The sophistication lies in the fact that pore-water pressures, during undrained testing, can be monitored and volume-change observations, during drained testing, can be made. In addition, field levels of all relevant pressures can be simulated, the applied stresses during testing are principal stresses and tests can be performed under controlled stress or controlled deformation rates.

2. Other important features are that failure can occur on any plane (whereas in the shear box test the failure plane is predetermined) and naturally occurring

features of the soil can be incorporated into the samples under tests if such samples are of sufficiently large diameter.

Disadvantages:

1. In the field the soil is in a state of anisotropic stress, i.e. the vertical pressure is in excess of the lateral pressure ($\sigma_1>\sigma_3$), and usually it has attained its state of full consolidation under similar stress conditions. However, in the test, the sample is consolidated under isotropic stress conditions ($\sigma_1=\sigma_3$), i.e. equal all-round cell pressure is applied to consolidate the sample before shearing.

2. In the triaxial cell the sample is axially symmetrical: ($\sigma_2=\sigma_3$) it is shown in Figure 3.14. However, most problems at field scale approximate to a condition of plane strain; the length-to-breadth ratio is large and consequently the problem can be treated as being two-dimensional, made up of a series of similar strips with no stresses assumed to act between these strips. The assumption of this condition also simplifies the analysis of the problem.

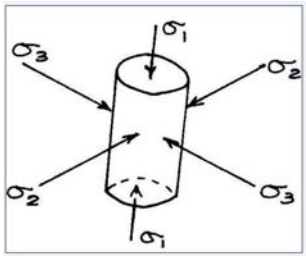

Figure 3.14 Axially symmetrical samples

The above differences between field and test conditions, however, appear to counterbalance each other in some way, since experience shows that triaxial test results generally correlate well with observed field values of shear strength.

3.3 Index Properties of the Samples Prepared

The following specified soil mixtures properties were determined after performing standard laboratory tests in accordance with TS 1900.

3.3.1 Grain Size Distributions

The particle size distribution of the soil mixtures were determined with the standard methods for coarse-grained soils (for particles having diameter > 0.074 mm, Sieve analysis was performed) and for fine-grained soils (for particles having diameter ≤ 0.074 mm, Hydrometer analysis was performed). The soil fractions of the specified soil mixtures with their percentages and the grain size distribution curves are given in Table 3.1 - 3.9 and Figure 3.15, as respectively.

Table 3.1 Soil fractions and their percentages for mixture having 0% kaolin fraction

Mixture having 0% kaolin fraction		
Soil Fraction	**Grain Size Range (μm)**	**Material Passing, %**
Coarse Sand	2000	99.74
Medium Sand	600	49.22
Fine Sand	200	14.63
Coarse Silt	60	3.12
Medium Silt	20	2.46
Fine Silt	6	0.41
Clay	<2	0.00

Table 3.2 Soil fractions and their percentages for mixture having 5% kaolin fraction

Mixture having 5% kaolin fraction		
Soil Fraction	**Grain Size Range (μm)**	**Material Passing, %**
Coarse Sand	2000	99.45
Medium Sand	600	53.20
Fine Sand	200	18.77
Coarse Silt	60	4.58
Medium Silt	20	4.20
Fine Silt	6	3.10
Clay	<2	2.33

Table 3.3 Soil fractions and their percentages for mixture having 10% kaolin fraction

Mixture having 10% kaolin fraction		
Soil Fraction	**Grain Size Range (μm)**	**Material Passing, %**
Coarse Sand	2000	99.62
Medium Sand	600	57.90
Fine Sand	200	25.90
Coarse Silt	60	9.38
Medium Silt	20	8.47
Fine Silt	6	6.22
Clay	<2	4.74

Table 3.4 Soil fractions and their percentages for mixture having 15% kaolin fraction

Mixture having 15% kaolin fraction		
Soil Fraction	**Grain Size Range (μm)**	**Material Passing, %**
Coarse Sand	2000	99.84
Medium Sand	600	59.40
Fine Sand	200	30.20
Coarse Silt	60	15.40
Medium Silt	20	12.88
Fine Silt	6	9.54
Clay	<2	7.67

Table 3.5 Soil fractions and their percentages for mixture having 20% kaolin fraction

Mixture having 20% kaolin fraction		
Soil Fraction	**Grain Size Range (μm)**	**Material Passing, %**
Coarse Sand	2000	99.44
Medium Sand	600	60.20
Fine Sand	200	34.97
Coarse Silt	60	20.20
Medium Silt	20	17.64
Fine Silt	6	13.10
Clay	<2	9.86

Table 3.6 Soil fractions and their percentages for mixture having 25% kaolin fraction

Mixture having 25% kaolin fraction		
Soil Fraction	**Grain Size Range (μm)**	**Material Passing, %**
Coarse Sand	2000	99.84
Medium Sand	600	62.60
Fine Sand	200	39.77
Coarse Silt	60	25.08
Medium Silt	20	22.11
Fine Silt	6	16.26
Clay	<2	13.04

Table 3.7 Soil fractions and their percentages for mixture having 30% kaolin fraction

Mixture having 30% kaolin fraction		
Soil Fraction	**Grain Size Range (μm)**	**Material Passing, %**
Coarse Sand	2000	99.54
Medium Sand	600	65.00
Fine Sand	200	44.63
Coarse Silt	60	29.34
Medium Silt	20	26.12
Fine Silt	6	17.46
Clay	<2	15.90

Table 3.8 Soil fractions and their percentages for mixture having 40% kaolin fraction

Mixture having 40% kaolin fraction		
Soil Fraction	**Grain Size Range (μm)**	**Material Passing, %**
Coarse Sand	2000	99.72
Medium Sand	600	67.54
Fine Sand	200	50.20
Coarse Silt	60	38.66
Medium Silt	20	31.30
Fine Silt	6	24.43
Clay	<2	20.12

Table 3.9 Soil fractions and their percentages for 100% kaolin

100% kaolin		
Soil Fraction	**Grain Size Range (μm)**	**Material Passing, %**
Coarse Silt	60	94.51
Medium Silt	20	85.74
Fine Silt	6	62.79
Clay	<2	31.92

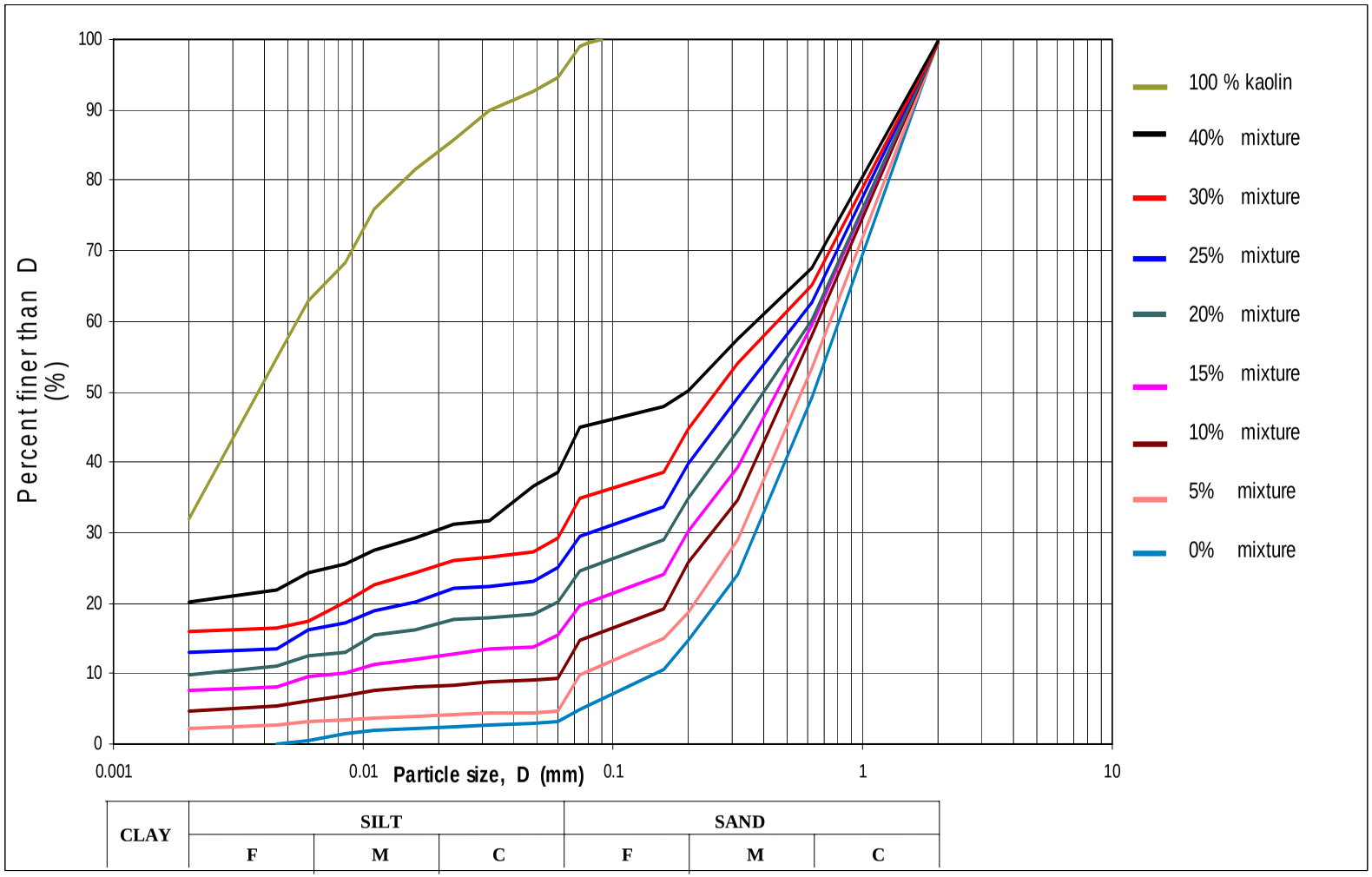

Figure 3.15 Grain Size Distribution Curves

3.3.2 Atterberg Limits and Specific Gravities (G_s Analyses)

The Atterberg limits tests and G_s analyses were performed on the specified soil mixtures and kaolin clay. For Atterberg limits tests, specimens were left for three days so that they become mature and a homogeneous batch. Results are given in Table 3.10.

Table 3.10 Properties of specified soil mixtures

% Fines	% Kaolin	% Clay	LL %	PL %	PI %	G_s	Soil Type
4.90	0	0.00	NP	NP	NP	2.67	SP
9.80	5	2.33	NP	NP	NP	2.66	SM
14.80	10	4.74	NP	NP	NP	2.68	SM
19.56	15	7.67	NP	NP	NP	2.67	SM
24.46	20	9.86	NP	NP	NP	2.67	SM
29.50	25	13.04	22.40	12.86	9.54	2.67	SC
34.88	30	15.90	23.29	13.15	10.14	2.67	SC
44.94	40	20.12	24.74	13.59	11.15	2.65	SC
100	99	31.92	40.80	22.37	18.43	2.60	CL

3.4 Testing

The aim of this section is to determine shear strength of the specified specimens. To do this three series of experiments are performed.

3.4.1 Series 1 Experiments

In series 1 experiments, soil mixtures at specified kaolin fractions were consolidated under 50 kPa vertical pressure in a cube box (at initial consolidation stage). Specimens are formed by mixing kaolin clay and poorly graded sand with adding some water. In this series of experiments, soil mixtures were not kept under water at initial consolidation stage and triaxial unconsolidated-undrained compression tests (UU) were performed. These tests were applied for the specified soil mixtures having a variety of kaolin fractions which are 5%, 10%, 15%, 20%, and 25% of soil mixture weight. For each soil mixture, triaxial UU tests were performed under 35 kPa, 60 kPa, and 85 kPa cell pressures. Testing program for this series is shown in Table 3.11.

Table 3.11 Testing program for series 1 experiments

	TRIAXIAL UU TESTS
KAOLIN CONTENT	**Number of tests performed**
%5	3
%10	3
%15	3
%20	3
%25	3

The moisture contents, bulk, and dry unit weights and initial void ratios of specimens in the 1st series experiments are shown in Table 3.12.

Table 3.12 Sample properties of the series 1 experiments

PROPERTIES OF SAMPLES IN TRIAXIAL UU TEST IN THE 1ST SERIES OF EXPERIMENTS													
Kaolin (%)	**w_i (%)**			**w_f (%)**			**ρ_{bulk} (Mg/m^3)**			**ρ_{dry} (Mg/m^3)**			**e_o**
Cell Pressure	**35 kPa**	**60 kPa**	**85 kPa**	**35 kPa**	**60 kPa**	**85 kPa**	**35 kPa**	**60 kPa**	**85 kPa**	**35 kPa**	**60 kPa**	**85 kPa**	
5	16.30	16.83	16.70	14.53	14.85	14.40	1.82	1.77	1.78	1.56	1.52	1.53	0.44
10	15.70	16.02	15.95	14.32	15.10	15.48	1.97	1.98	1.98	1.70	1.71	1.71	0.43
15	14.74	14.36	14.58	13.62	13.58	14.08	1.99	2.00	1.98	1.73	1.75	1.73	0.39
20	12.60	13.03	12.71	11.74	12.38	12.26	2.02	1.99	1.99	1.80	1.76	1.77	0.34
25	14.50	14.20	14.21	13.20	13.80	13.86	2.02	2.04	2.04	1.76	1.79	1.79	0.38

The procedure of the sample preparation is as follows:

a. Poorly-graded sand and kaolin clay powder are dried in the oven.
b. Specimens are formed by mixing kaolin powder and poorly-graded sand with adding some water which is about 20% of soil mixture weight.
c. The Kaolin powder, poorly-graded sand, and water are mixed until getting a homogeneous soil mixture at specified kaolin contents which are 5%, 10%, 15%, 20%, and 25%.
d. Inside the plexiglas boxes, geotextile sheets, which are cut in appropriate width and length, were placed for proper drainage and also for prevention of drying of the soil during initial consolidation period. (Figure 3.16).
e. Then the prepared soil mixture is placed in the plexiglas boxes layer by layer manually, and then surface is smoothened. Thereafter, the top portion is covered with the geotextile sheets and plexiglas cover, which has small holes for drainage, is placed.
f. The plexiglas box is placed under the loading jack. Then, the displacement dial is placed on the plexiglas cover in order to read settlements. (Figure 3.17).
g. 50 kPa vertical consolidation pressures are applied for a consolidation time of one week at least.

h. The samples are wetted from top periodically to prevent drying during the consolidation period.

i. After consolidation period, 40 mm portion of the soil is removed in order to reduce negative effects of surface drying and samples are taken into the sampling molds (Figure 3.18).

j. The prepared samples are then placed in plastic bags, and they are kept in dessiccator.

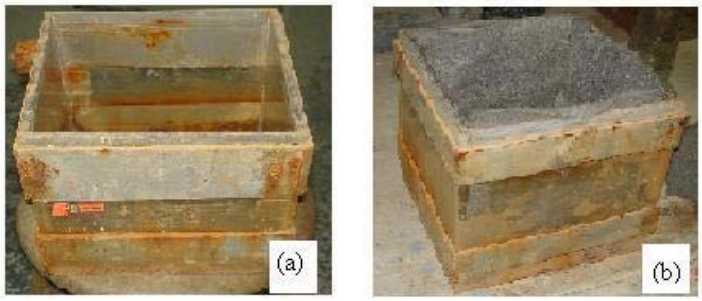

Figure 3.16 (a) Plexiglas box empty, (b) After geotextile sheets placed

Figure 3.17 Plexiglas box is placed under loading jack with displacement dial

Figure 3.18 After taking samples from the plexiglas box

The procedure of the Triaxial (UU) test is as follows:

a. The sample is extruded from the sampling tube, in which it has been stored, and trimmed to suit a split mould of the required sample size. (Figure 3.19 and Figure 3.20). Standard test conditions for triaxial UU test are summarized in Table 3.13
b. The split mold containing the sample is then mounted on the base pedestal of the cell. A rubber sleeve or membrane of the appropriate size is stretched in a 'membrane stretcher', which is simply a tube with a pipe connection at its mid-height to enable a suction to be applied to the air gap between the membrane and the tube membrane stretcher. The split mold is removed from the sample and the stretched membrane is placed around the sample and over the base pedestal. (Figure 3.21 and Figure 3.22). The top platen is then carefully placed into contact with the top of the sample, the suction on the membrane is released and totally encloses the sample and the sides of the upper and lower platens. 'O'-ring seals are then placed over the membrane by using a cylindrical stretcher and these rings are carefully rolled from the stretcher to the sides of the lower and upper loading platens. The rings then securely clamp the membrane and prevent any seepage of water between the membrane and the sides of the platens.
c. Any porous discs used must be saturated by boiling in water. The Perspex cell is then assembled over the sample and securely tightened to the base plate of the cell. The piston or ram is carefully lowered to rest on the ball

seating on top of the sample, clamped in such a position that it just touches the ball seating. Extreme care is needed at this stage to ensure that no vertical load is applied to the sample. Then triaxial cell is filled water from a header bottle, the air release valve at the top of the cell is being kept open to allow filling. When the cell is full this valve is closed. (Figure 3.23 a.).

d. The cell is then pressurized from the pressure cylinder, preset to the required equal all-round cell pressure or confining pressure.
e. In triaxial (UU) tests, there is no need to consolidation stage. For this reason, immediately after giving cell pressure sample is loaded quickly. Moreover there is no a drainage facility at loading because of undrained conditions. In general if the vertical strain of the sample is higher than 20%, it is accepted as to be of in failure. By means of this, appropriate loading rate is computed. Generally, failure takes place in 10 minutes. Recordings of the data that are taken from proving ring dial gauge and vertical deformation dial gauge are performed when each of ten unit's increment takes place on vertical-deformation dial gauge. The point of failure is signified by a fall-off in recorded shear load (from proving ring dial gauge). Termination of the test is made when values in the recorded shear load decrease or give the same number at last three recordings (Mirata, 2001).
f. After shearing, specimen is shown in Figure 3.23 b.

Table 3.13 A summary of standard test conditions for triaxial UU test

Sample height (mm)	71
Sample diameter (mm)	36
Sample cross-sectional area (mm^2)	1017.88
Sample volume (10^{-6} x m^3)	72.27
Proving ring constant (kN/div.)	0.000995
Shearing Rate (mm/min)	1.52

Figure 3.19 Replacement apparatus

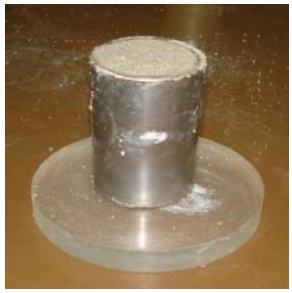

Figure 3.20 After trimming to suit the required sample size

Figure 3.21 Sample is carried on the base pedestal of the cell

Figure 3.22 Sample is mounted on the base pedestal of the cell

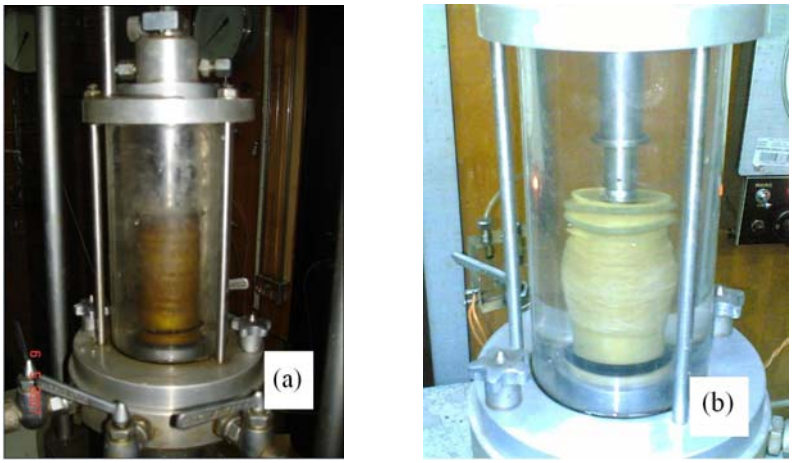

Figure 3.23 a) After filling water in cell, b) Sample at the end of the test

3.4.2 Series 2 Experiments

In this series of experiments, soil mixtures were consolidated under 100 kPa vertical pressure in the cubical box (at initial consolidation stage) with keeping under water in a water tank and triaxial (UU) compression tests were performed again. These tests were performed under 50 kPa and 100 kPa cell pressures and they were repeated two times at each cell pressure. Triaxial (UU) tests were applied for soil mixtures having kaolin contents that are 10%, 20%, 30%, and 40% of soil mixture weight. Testing program for this series is shown in Table 3.14.

Table 3.14 Testing program for series 2 experiments

	TRIAXIAL UU TESTS
KAOLIN CONTENT	**Number of tests performed**
%10	4
%20	4
%30	4
%40	4

The moisture contents, bulk, and dry unit weights and initial void ratios of specimens in the 2nd series experiments are shown in Table 3.15.

Table 3.15 Sample properties of the series 2 experiments

PROPERTIES OF SAMPLES IN TRIAXIAL UU TEST IN THE 2ND SERIES OF EXPERIMENTS																	
Kaolin (%)	**w_i (%)**				**w_f (%)**				**ρ_{bulk} (Mg/m^3)**				**ρ_{dry} (Mg/m^3)**				**e_o**
Cell Pressure	**50 kPa**	**50 kPa**	**100 kPa**	**100 kPa**	**50 kPa**	**50 kPa**	**100 kPa**	**100 kPa**	**50 kPa**	**50 kPa**	**100 kPa**	**100 kPa**	**50 kPa**	**50 kPa**	**100 kPa**	**100 kPa**	
10	17.62	17.30	17.39	17.74	16.03	15.86	16.64	17.16	1.94	1.94	1.91	1.94	1.65	1.65	1.63	1.65	0.44
20	15.50	15.92	15.37	14.82	14.52	15.20	14.52	14.17	2.11	2.09	2.08	2.03	1.83	1.80	1.80	1.77	0.39
30	16.50	17.03	16.52	15.96	14.70	15.13	15.22	14.72	2.11	2.10	2.08	2.10	1.81	1.79	1.79	1.81	0.39
40	14.11	13.50	13.90	14.20	13.67	12.95	13.43	13.58	2.06	2.03	2.06	2.09	1.81	1.79	1.81	1.83	0.36

The procedure of the sample preparation is as follows:

As it was mentioned before, soil mixtures were consolidated under 100 kPa vertical pressure in the cube box (at initial consolidation stage) with keeping under water in the water tank. (Figure 3.24). The remaining part is in the same procedure with the 1st series experiments have.

Figure 3.24 Plexiglas box in water tank is placed under loading jack

3.4.3 Series 3 Experiments

In this series initial consolidation stage was not performed. Soil mixtures at specified kaolin contents were directly prepared and specimens were placed on the test machine by manually. Only direct shear CD tests were performed. Direct shear tests were applied for the specified soil mixtures having kaolin fractions which are 0%, 10%, 20%, 30%, and 40% of soil mixture weight. These tests were performed for each soil mixture under 50kPa, 100kPa, and 150kPa vertical pressures and they were repeated two times at each pressure. Testing program for this series is shown in Table 3.16.

Table 3.16 Testing program for series 3 experiments

	DIRECT SHEAR TESTS
	CD
KAOLIN CONTENT	**Number of tests performed**
%0	6
%10	6
%20	6
%30	6
%40	6

The moisture contents, bulk, and dry unit weights and initial void ratios of specimens in the 3rd series experiments are shown in Table 3.17.

Table 3.17 Sample features of the series 3 experiments

	PROPERTIES OF SAMPLES IN DIRECT SHEAR CD TEST IN THE 3RD SERIES OF EXPERIMENTS				
Kaolin (%)	**0**	**10**	**20**	**30**	**40**
ρ_{bulk}**(Mg/m^3)**	1.74	1.91	2.30	2.33	2.23
ρ_{dry}**(Mg/m^3)**	1.60	1.75	2.09	2.07	1.94
w_i **(%)**	8.67	9.20	10.10	12.52	14.88
e_0	0.23	0.25	0.27	0.33	0.39

The procedure of the sample preparation is as follows:

a. Initial consolidation stage was not performed.
b. Soil mixtures were directly prepared at desired kaolin contents with adding some water. (Figure 3.25).
c. Prepared mixtures were then placed in the shear box layer by layer manually with tamping slightly.

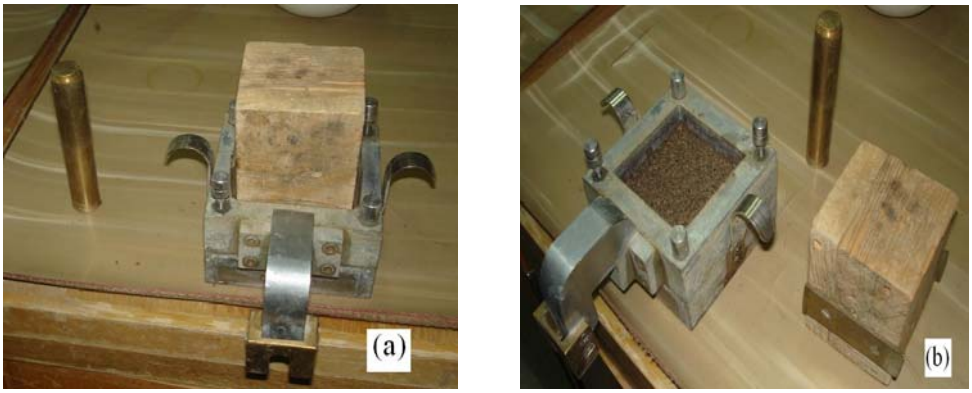

Figure 3.25 (a) Before placing in the shear box, (b) After placing in the shear box

The procedure of the Direct Shear CD test is as follows:

a. Standard test conditions for direct shear CD test are summarized in Table 3.18 and 3.19.
b. They are placed carefully to suit the plan dimensions of the box which can be square or circular in shape. (Figure 3.26).
c. According to drainage conditions of the test (CD tests or UU tests) have been predetermined; the corresponding metal plates (Figure 3.7) are inserted into the shear box adjacent to the upper and lower faces of the sample. (Figure 3.26).
d. The hanger weight applying the vertical normal stress to the sample is then assembled, together with the dial gauge monitoring vertical displacements. Then, outer box is filled with water in order to make the plane of shear smoother. (Figure 3.27).
e. Thereafter, consolidation stage is applied.
f. Consolidation stage of the sample takes up one day utmost, because the sample thickness is of 2 cm and two ways drainage condition is applied. These factors decrease the consolidation time.
g. Before beginning shear of the specimen, locating screws which align the two split halves of the box are removed and an appropriate gear is selected for the required rate of application of the horizontal shear force. In these tests (CD), rate of shear strain was selected as 0.00048 (inches/minute). This shearing rate was computed by using root-time method depended upon consolidation graph, which is shown in Figure 3.29, belonged the soil mixture having the maximum kaolin content (40%) in the 3rd series of experiments and applied for all soil mixtures in this series. These kinds of tests are called ‘slow’ tests and dissipation of pore-water pressures are achieved in this way.
h. Shearing of the sample is then begun and records of time, proving-ring dial gauge, vertical-deformation dial gauge, and horizontal-deformation dial gauge are kept throughout the test until shear failure of the sample takes

place. Reading of these dial gauges are performed in CD tests at each 15 minutes time intervals.

i. The point of failure is signified by a fall-off in recorded shear load (or proving-ring dial gauge) with continued separation of the two halves.
j. Termination of the test is performed when values in recorded shear load are in decrease or give the same number at least last three recordings (Vickers, 1984).
k. The whole test procedure is then repeated with at least three similar samples of the same soil, each with an increase normal load applied during horizontal shearing of the sample. After shearing, specimen is shown in Figure 3.28.

Table 3.18 A summary of standard test conditions for direct shear CD test in square box

Sample height (mm)	20
Sample dimensions (mm)	60 x 60
Sample cross-sectional area (mm^2)	3600
Sample volume (10^{-6} x m^3)	72
Proving ring constant (kg/div.)	0.212
Shearing Rate (in/min)	0.00048

Table 3.19 A summary of standard test conditions for direct shear CD test in circular box

Sample height (mm)	19
Sample diameter (mm)	63.5
Sample cross-sectional area (mm^2)	3166.9
Sample volume (10^{-6} x m^3)	60.17
Proving ring constant (kg/div.)	0.207
Shearing Rate (in/min)	0.00048

Figure 3.26 The sample is placed into the shear box

Figure 3.27 Direct shear test machine during shear

Figure 3.28 Immediately after testing

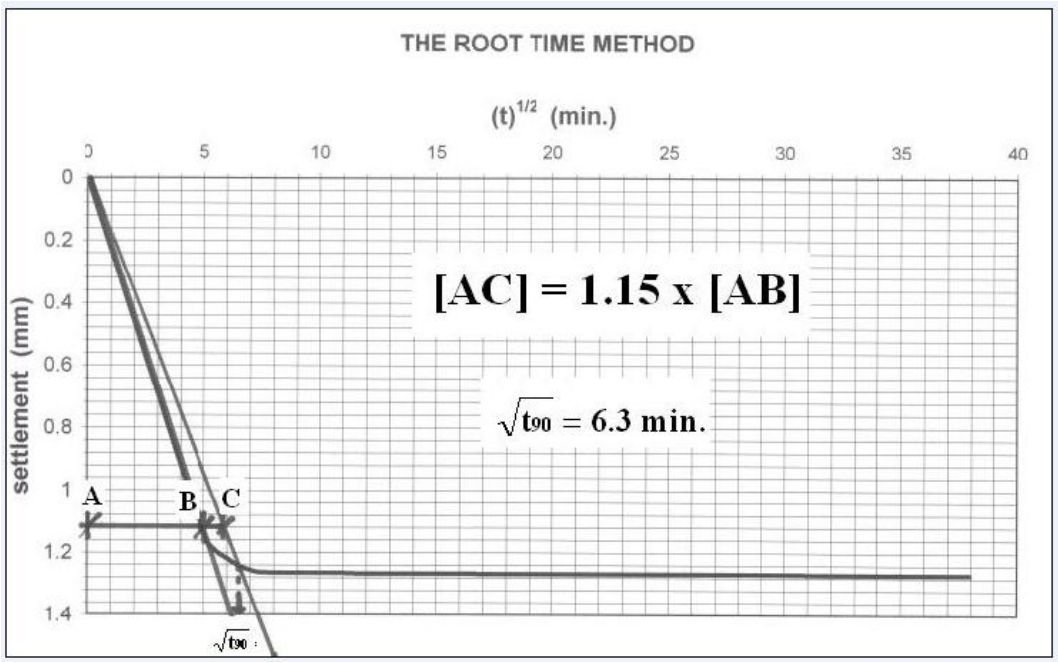

Figure 3.29 Settlement-$\sqrt{\text{time}}$ graph for soil mixture having 40% kaolin fraction

According to Jean Pierre Bardet, (Experimental Soil Mechanics),

$t_f = 11.7 \times t_{90}$ (3.1)

where t_f = the minimum time required for failure,

t_{90} = time for reaching 90% of the primary consolidation.

$$V_{max} = \frac{\delta_f}{t_f} \tag{3.2}$$

where V_{max} = maximum rate of shearing

δ_f = lateral displacement required to reach the soil peak strength, δ_f = 8 to 10 mm for plastic clay, δ_f is taken as 7 mm in order to stay in safer side so that dissipation of pore-water pressure during shear can be highly achieved.

Relationship between kaolin fractions, initial water contents, bulk and dry densities and initial void ratios for Series 1, 2, and 3 series are also shown respectively in Figures 3.30 – 3.33.

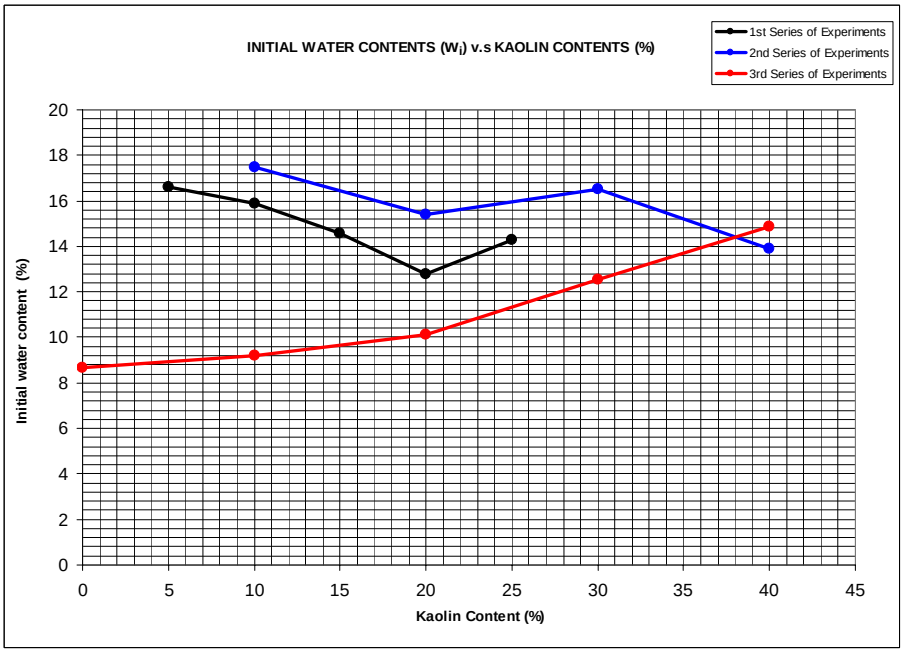

Figure 3.30 Relationship between kaolin fractions and initial water content

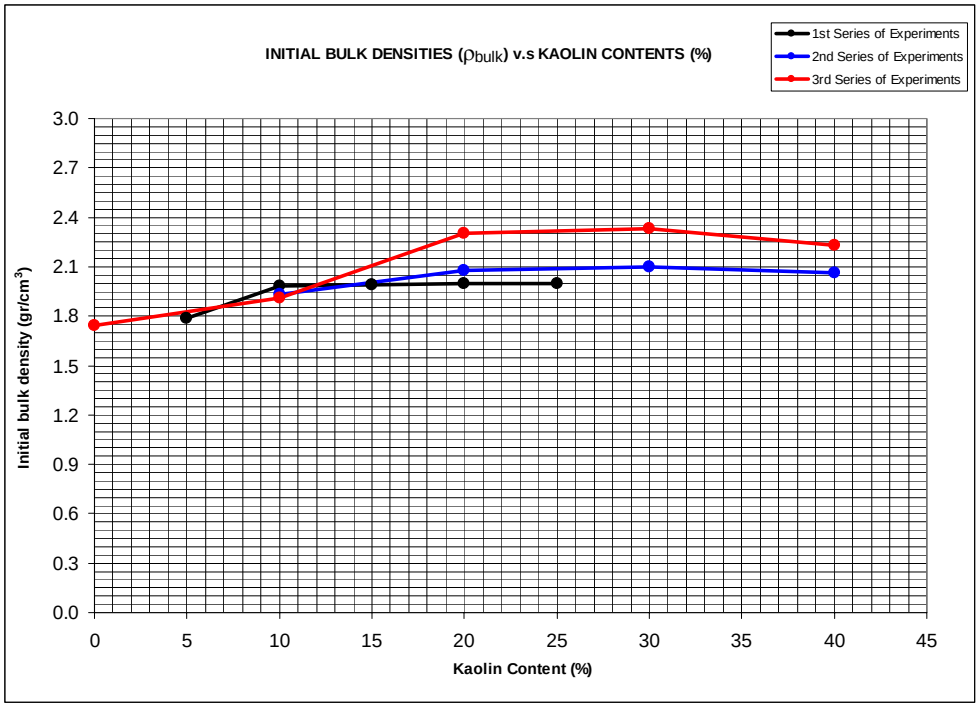

Figure 3.31 Relationship between kaolin fractions and initial bulk densities

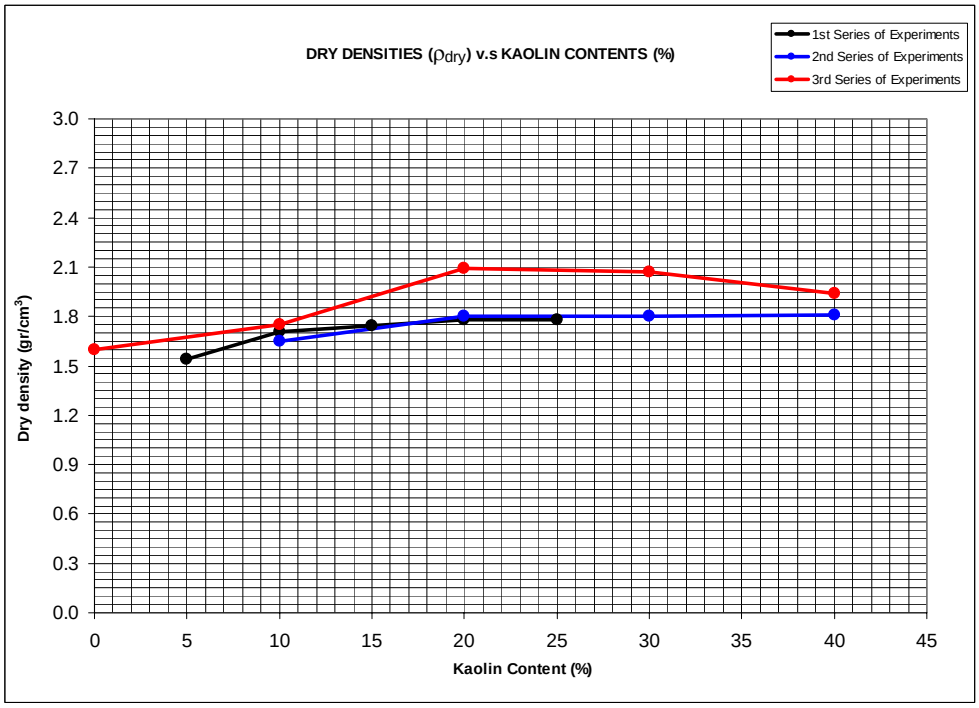

Figure 3.32 Relationship between kaolin fractions and dry densities

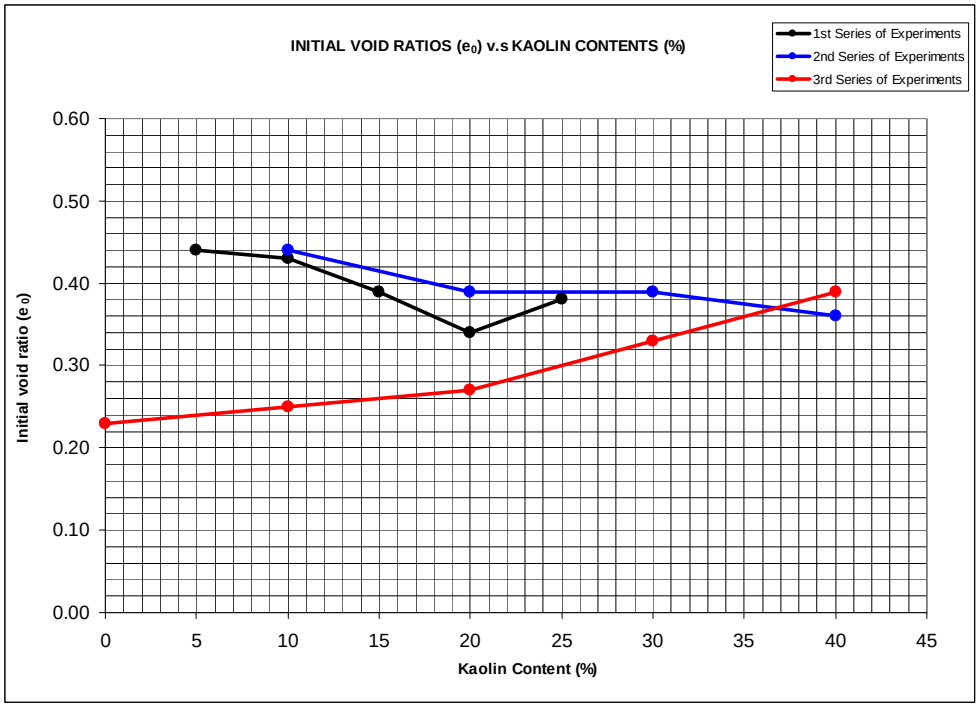

Figure 3.33 Relationship between kaolin fractions and initial void ratios

CHAPTER 4

TEST RESULTS

4.1. General

In this study, effects of increasing kaolin content on the shear strength behaviour of soil mixtures were investigated.

Three series of experiments were performed. In the first and second series triaxial compression UU tests and in the third series direct shear CD tests were performed. For each series of experiment, test results include mainly two components that are shear strength behaviour and stress-strain relations. Variations in secant moduli, which is a ratio of stress at any point on curve in a stress-strain diagram and it is the slope of a line from the origin to any point, corresponding to 55 % of failure strain on the diagram in this study, on a stress-strain curve, and failure strains were also presented for each of them. These mentioned test results were exhibited in graphs and tables.

The results of the tests given in this Chapter are:

1. Results of the 1st series of experiments
2. Results of the 2nd series of experiments
3. Results of the 3rd series of experiments

4.2 Results of the 1st series of experiments

In this series, undrained shear strength values under 35, 60, and 85 kPa cell pressures for different kaolin contents that are 5, 10, 15, 20, and 25 % are presented in Table

4.1. Relations between undrained shear strength, τ_u (as given on page 17) and vertical strain under specified cell pressures of the tests are presented for specified kaolin contents of the mixtures in Figure 4.1 and Figure 4.5. Values of failure strains and secant moduli for this series are presented in Table 4.2 and Table 4.3.

Table 4.1 Undrained shear strength values from triaxial UU tests, in series 1

			Undrained shear strength (τ_u) values taken from Triaxial UU tests (1st series) under different cell pressures kPa		
Average of initial water contents (%)	% Kaolin	% Clay	σ_{cell} = 35 kPa	σ_{cell} = 60 kPa	σ_{cell} = 85 kPa
16.60	5	2.33	79.39	111.35	150.89
15.90	10	4.74	75.59	121.19	160.97
14.56	15	7.67	77.07	115.49	148.51
12.78	20	9.86	80.72	110.73	134.86
14.30	25	13.04	39.48	84.42	99.47

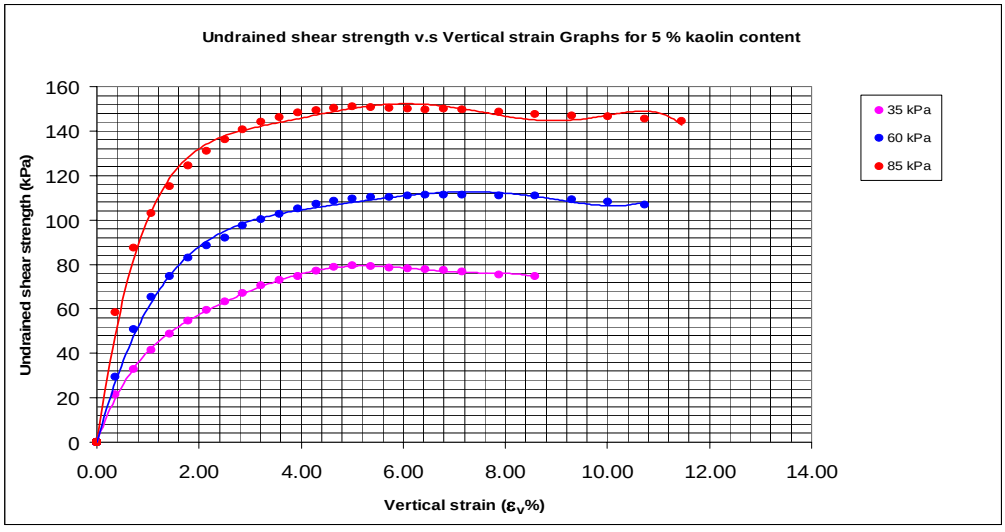

Figure 4.1 Undrained shear strength-vertical strain relationships for 5 % kaolin content, in series 1

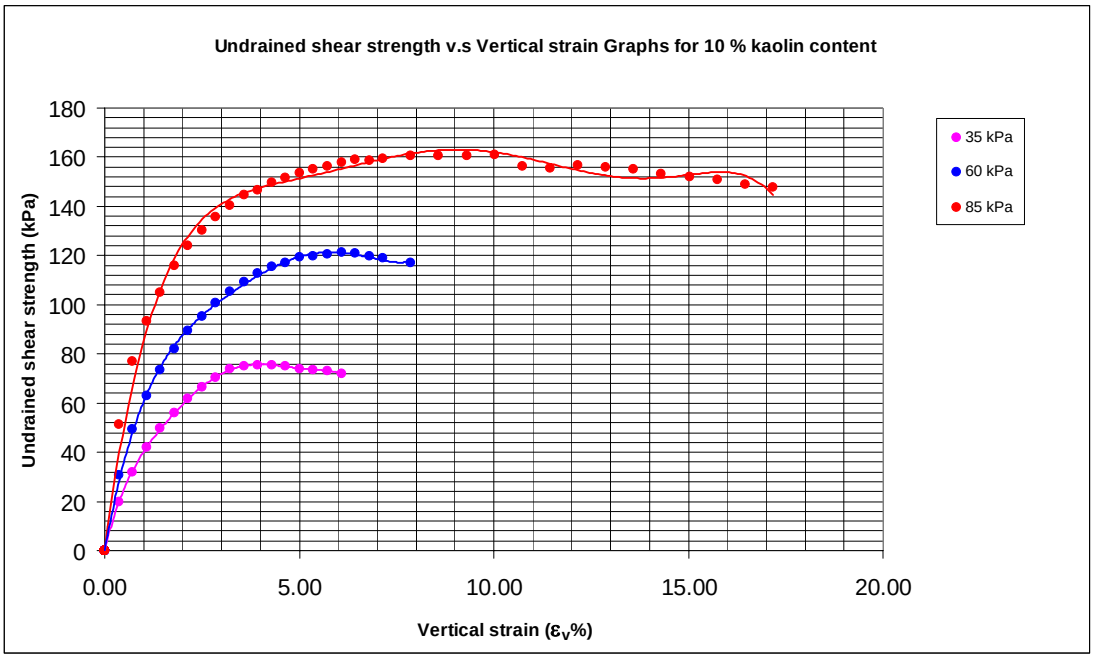

Figure 4.2 Undrained shear strength-vertical strain relationships for 10 % kaolin content, in series 1

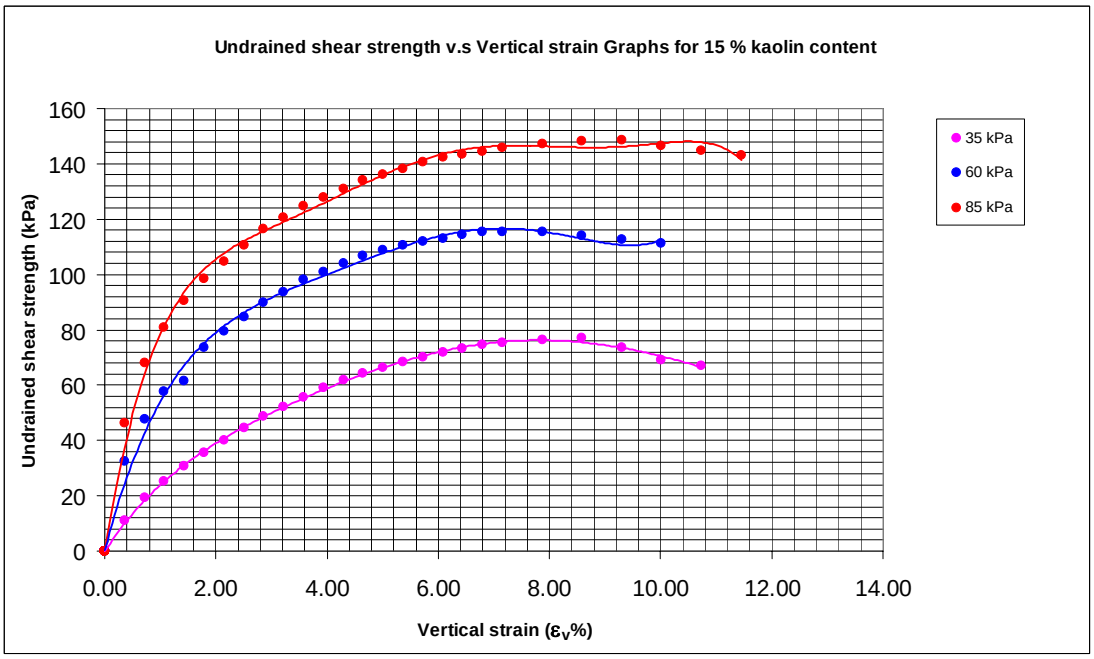

Figure 4.3 Undrained shear strength-vertical strain relationships for 15 % kaolin content, in series 1

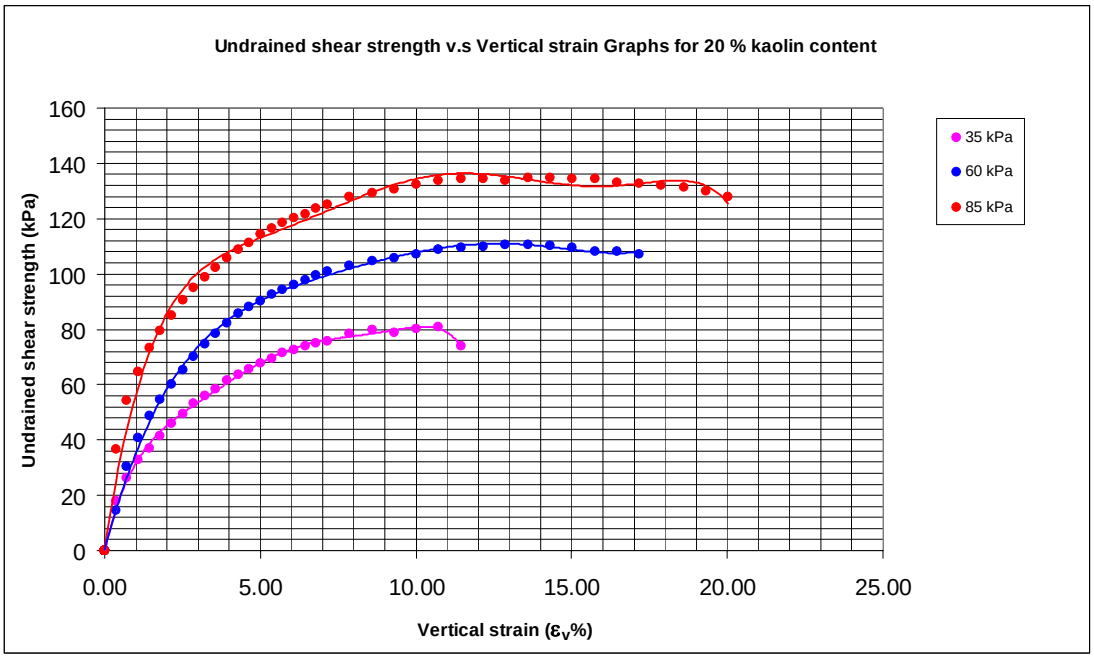

Figure 4.4 Undrained shear strength-vertical strain relationships for 20 % kaolin content, in series 1

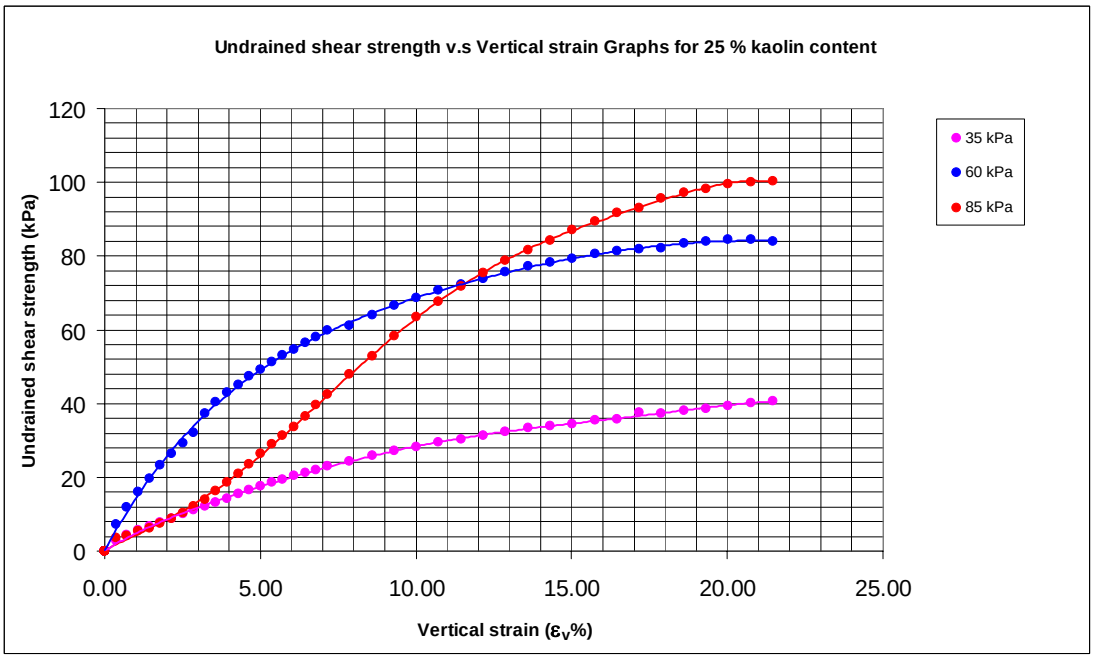

Figure 4.5 Undrained shear strength-vertical strain relationships for 25 % kaolin content, in series 1

Table 4.2 Failure strain values from triaxial UU tests, in series 1

			Failure strain (%)		
Initial water contents (%)	% Kaolin	% Clay	σ_c = 35 kPa	σ_c = 60 kPa	σ_c = 85 kPa
16.60	5	2.33	5.01	6.44	5.01
15.90	10	4.74	3.94	6.08	7.87
14.56	15	7.67	8.59	7.15	9.30
12.78	20	9.86	10.73	13.59	14.31
14.30	25	13.04	20	20	20

Table 4.3 Values of secant modulus from triaxial UU tests, in series 1

			Secant Moduli (MPa)		
Initial water contents (%)	% Kaolin	% Clay	σ_c = 35 kPa	σ_c = 60 kPa	σ_c = 85 kPa
16.60	5	2.33	4.40	6.22	12.67
15.90	10	4.74	4.22	6.10	9.11
14.56	15	7.67	2.11	5.27	8.22
12.78	20	9.86	2.67	2.95	5.23
14.30	25	13.04	0.33	1.10	0.61

4.3 Results of the 2nd series of experiments

In this series, undrained shear strength values under 50 and 100 kPa cell pressures are presented in

. Relations between undrained shear strength and shear strain under specified cell pressures of the tests are presented for specified kaolin contents of the mixtures in Figure 4.6-Figure 4.9. Values of failure strains and secant moduli for this series are presented in Table 4.5 and 4.6.

Table 4.4 Undrained shear strength values from triaxial UU tests, in series 2

			Undrained shear strength (τ_u) values taken from Triaxial UU tests (2nd series) under different cell pressures kPa				**Averages of τ_u values for similar cell pressure kPa**	
Average of initial water contents (%)	**% Kaolin**	**% Clay**	**σ_{cell} = 50 kPa**	**σ_{cell} = 50 kPa**	**σ_{cell} = 100 kPa**	**σ_{cell} = 100 kPa**	**σ_{cell} = 50 kPa**	**σ_{cell} = 100 kPa**
17.50	10	4.74	103.83	108.79	157.54	160.56	106.30	159.10
15.40	20	9.86	104.35	97.24	158.13	154.73	100.80	156.43
16.50	30	15.90	74.46	68.00	109.60	111.60	71.23	110.60
13.90	40	20.12	40.70	40.26	49.64	53.54	40.50	51.60

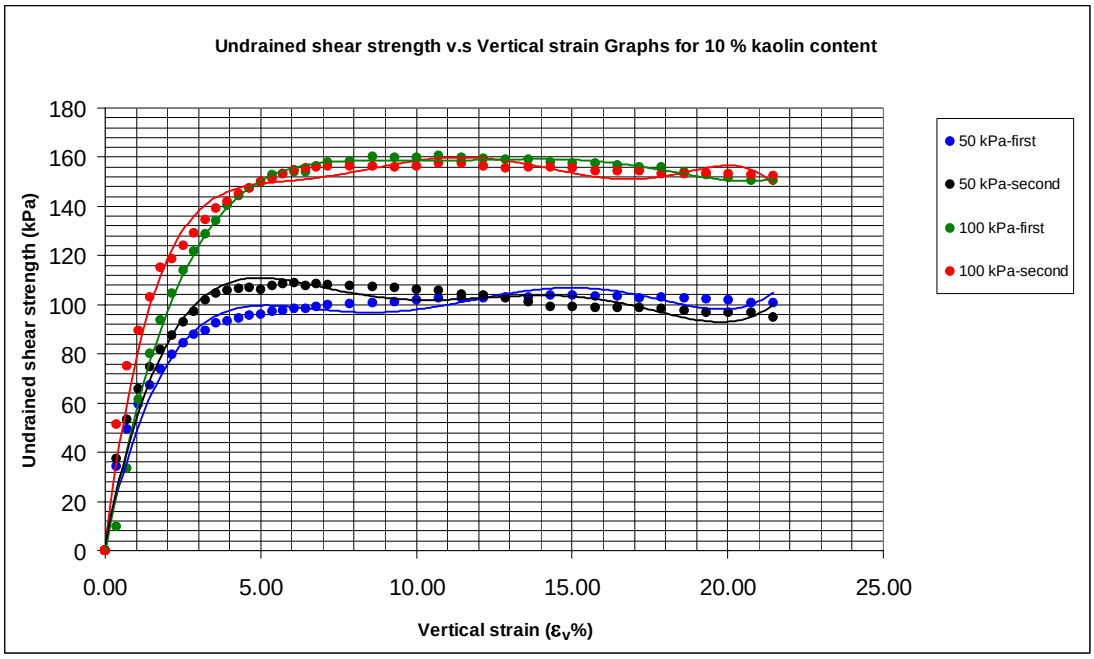

Figure 4.6 Undrained shear strength-vertical strain relationships for 10 % kaolin content, in series 2

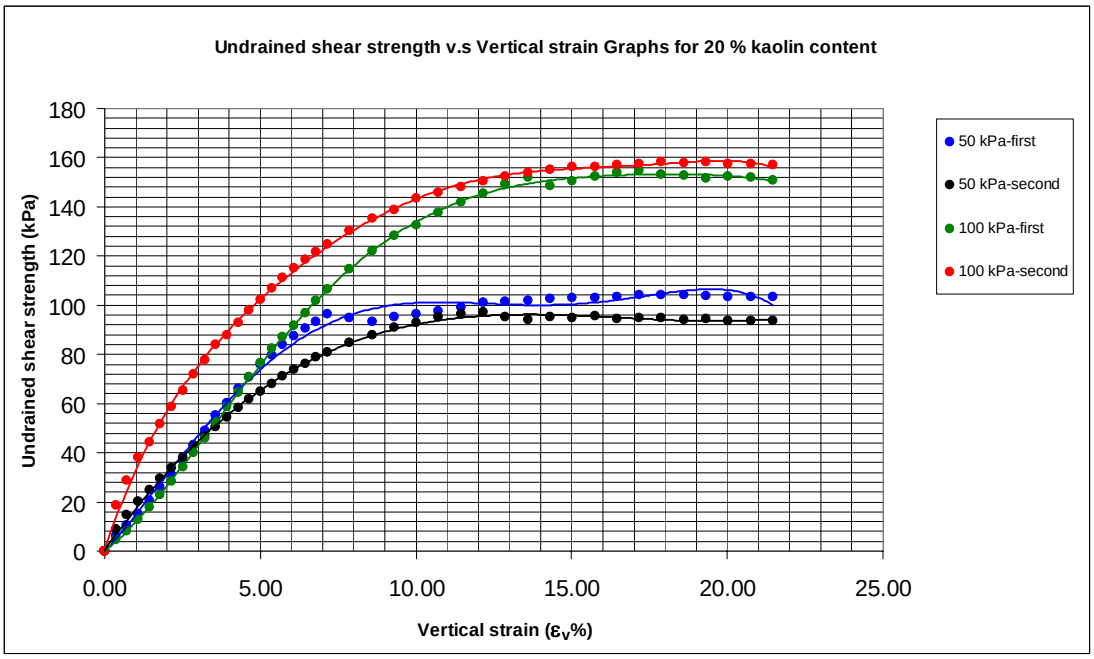

Figure 4.7 Undrained shear strength-vertical strain relationships for 20 % kaolin content, in series 2

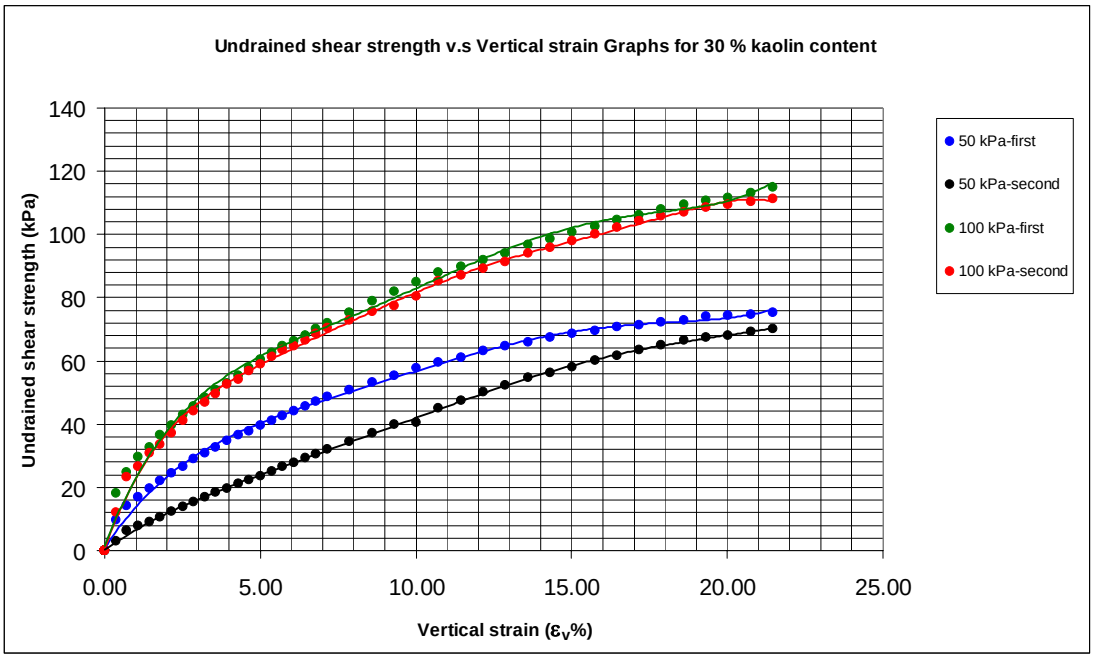

Figure 4.8 Undrained shear strength-vertical strain relationships for 30 % kaolin content, in series 2

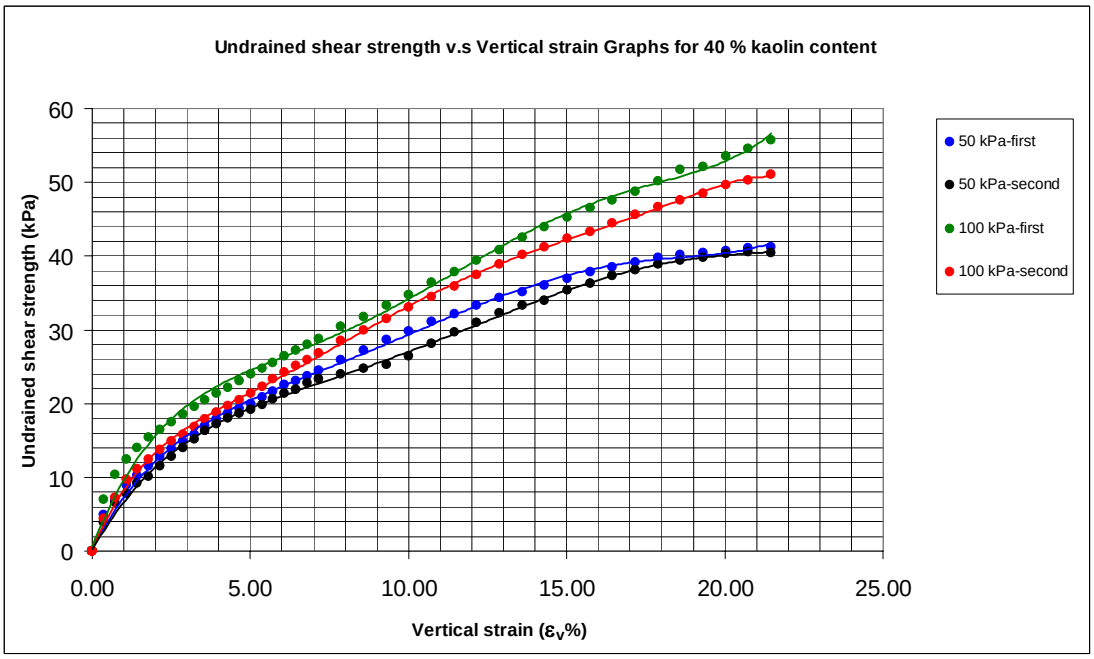

Figure 4.9 Undrained shear strength-vertical strain relationships for 40 % kaolin content, in series 2

Table 4.5 Failure strain values from triaxial UU tests, in series 2

			Failure strain (%)	
Initial water contents (%)	% Kaolin	% Clay	σ_c = 50 kPa	σ_c = 100 kPa
17.50	10	4.74	10.56	11.10
15.40	20	9.86	15.03	18.25
16.50	30	15.90	20	20
13.90	40	20.12	20	20

Table 4.6 Values of secant modulus from triaxial UU tests, in series 2

			Secant Moduli (MPa)	
Initial water contents (%)	% Kaolin	% Clay	σ_c = 50 kPa	σ_c = 100 kPa
17.50	10	4.74	5.30	6.67
15.40	20	9.86	1.49	1.98
16.50	30	15.90	0.64	0.86
13.90	40	20.12	0.41	0.54

4.4 Results of the 3rd series of experiments

Drained direct shear tests were performed in the 3rd series. In this series, drained shear strength values under 50, 100, and 150 kPa vertical consolidation pressures were measured for different kaolin contents of the kaolin-sand mixtures (0, 10, 20, 30, and 40 %). The results are presented in . The tests were repeated at each kaolin content. Values of drained friction angle and cohesion parameters against increasing kaolin contents are shown in Table 4.8. Effective failure envelopes for direct shear CD tests are shown in Figure 4.10. Relations between drained shear strength and shear strain, ε_h (as defined on page 12) for specified kaolin contents of the mixtures are presented in Figure 4.11, 13, 15, 17, and 19. Relations between vertical strain and shear strain are also shown in Figure 4.12, 14, 16, 18, and 20. Values of failure strains and secant moduli for this series are presented in Table 4.9 and 4.10.

Table 4.7 Drained shear strength values from direct shear CD tests, in series 3

			Drained shear strength (τ) values taken from Direct Shear CD tests (3rd series) under different vertical pressures kPa						**Average of (τ) values under the same vertical pressure kPa**		
Average of initial water contents (%)	**% Kaolin**	**% Clay**	**σ_v = 50 kPa**	**σ_v = 50 kPa**	**σ_v = 100 kPa**	**σ_v = 100 kPa**	**σ_v = 150 kPa**	**σ_v = 150 kPa**	**σ_v = 50 kPa**	**σ_v = 100 kPa**	**σ_v = 150 kPa**
8.67	0	0	44.77	42.23	84.11	80.26	126.32	129.63	43.50	82.20	128
9.20	10	4.74	41.39	37.84	78.12	75.63	114.30	110.19	40	76.90	112.25
10.10	20	9.86	36.15	35	67.11	64.23	94.26	90.21	35.60	65.67	92.24
12.52	30	15.90	31.48	33.63	51.22	55.40	78.19	78	32.60	53.31	78.10
14.88	40	20.12	28.16	27.43	49.75	50.41	67.63	65.34	27.80	50.10	66.50

Table 4.8 Drained friction angle and cohesion values from direct shear CD tests, in series 3

Initial water contents (%)	% Kaolin	% Clay	ϕ' (deg.)	c' (kPa)
8.67	0	0	40.20	0.10
9.20	10	4.74	36	3.60
10.10	20	9.86	29.50	7.80
12.52	30	15.90	24.50	9.10
14.88	40	20.12	21.20	9.40

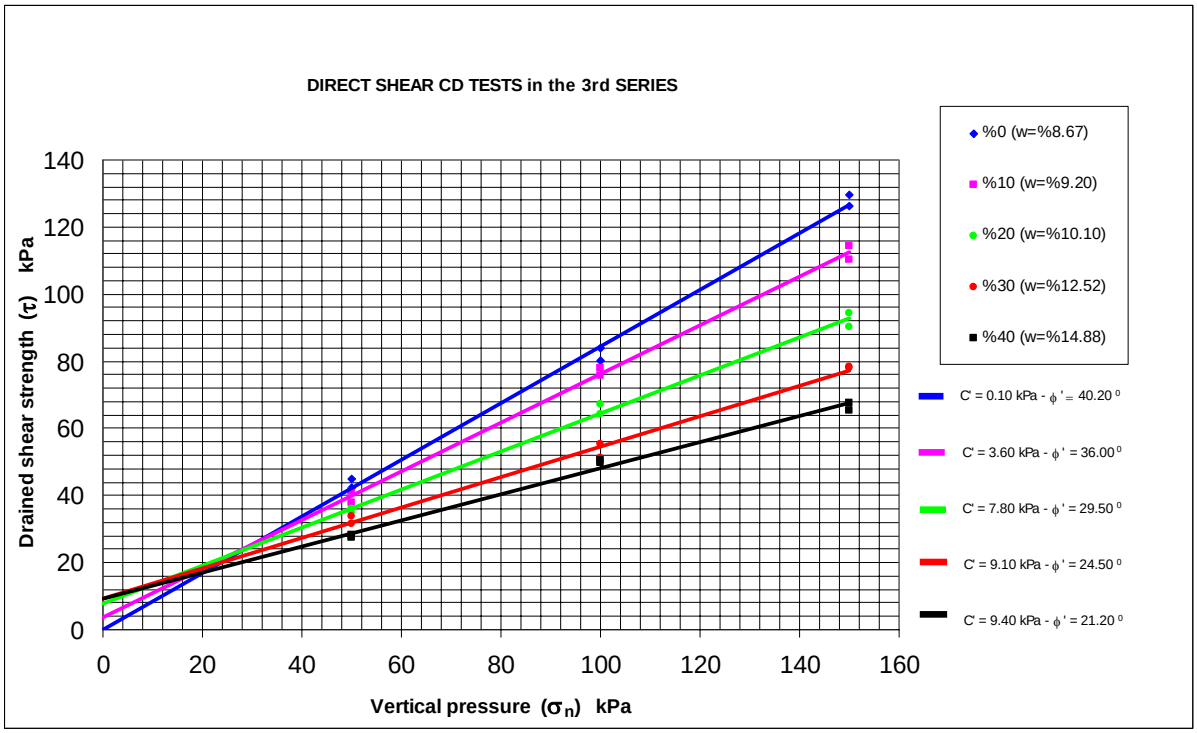

Figure 4.10 Effective failure envelopes for direct shear CD, in series 3

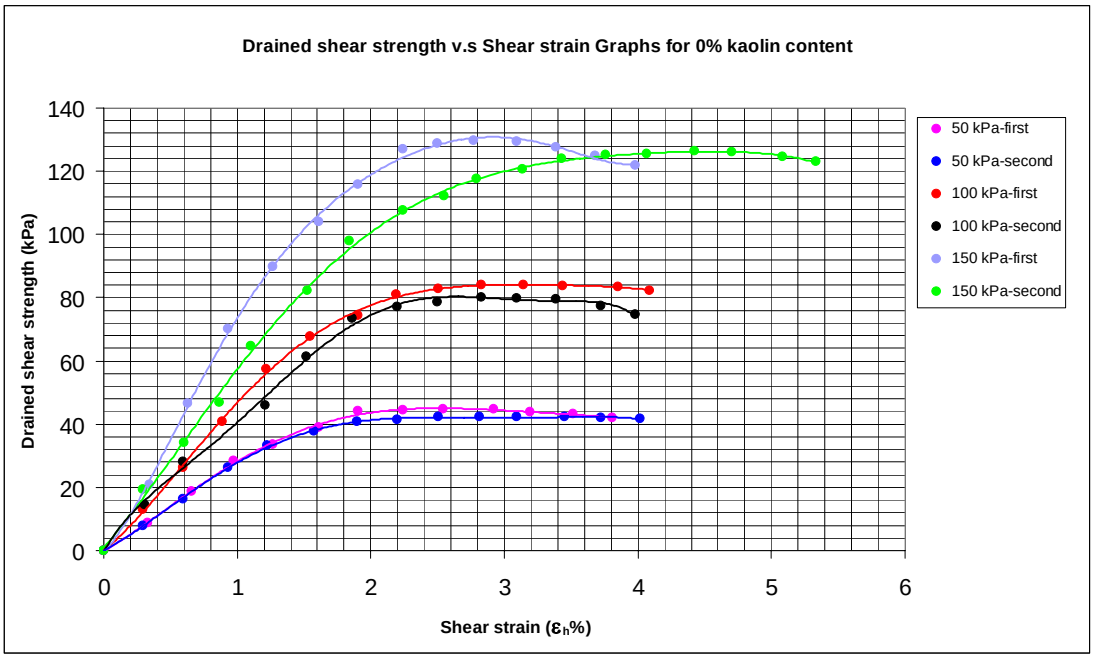

Figure 4.11 Drained shear strength-shear strain relationships for 0 % kaolin content, in series 3

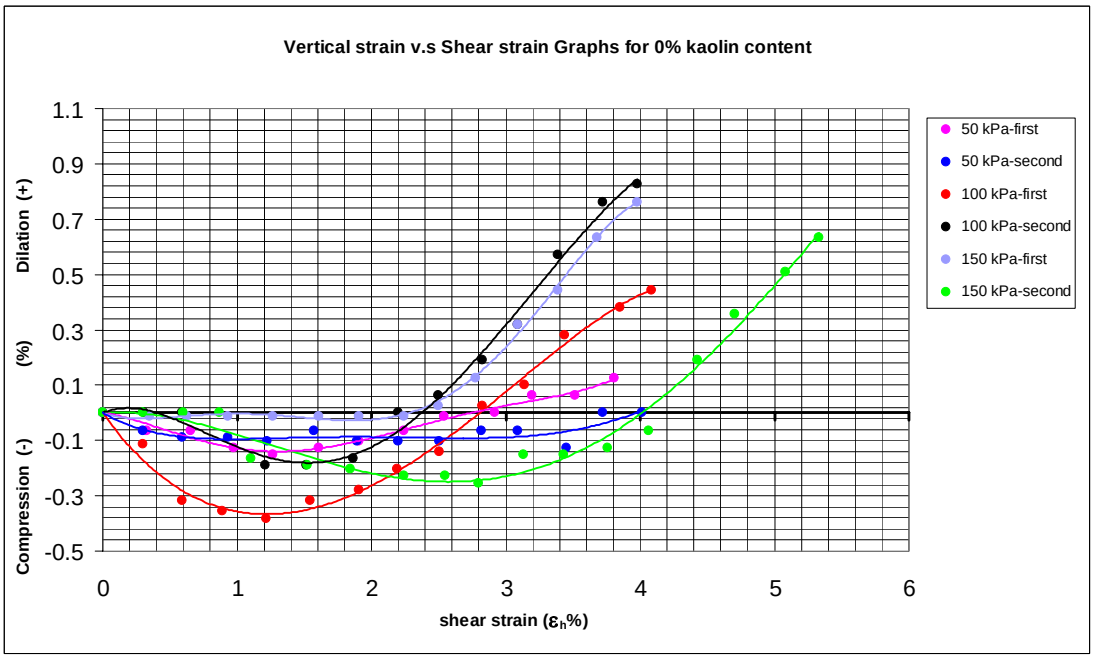

Figure 4.12 Vertical strain-shear strain relationships for 0 % kaolin content, in series 3

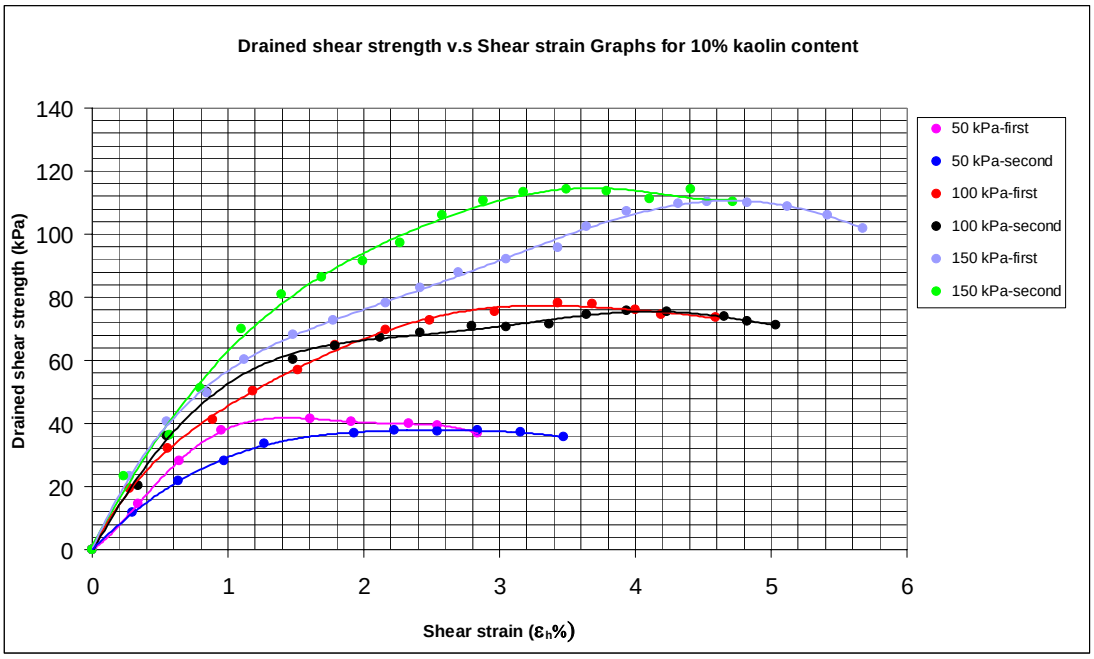

Figure 4.13 Drained shear strength-shear strain relationships for 10 % kaolin content, in series 3

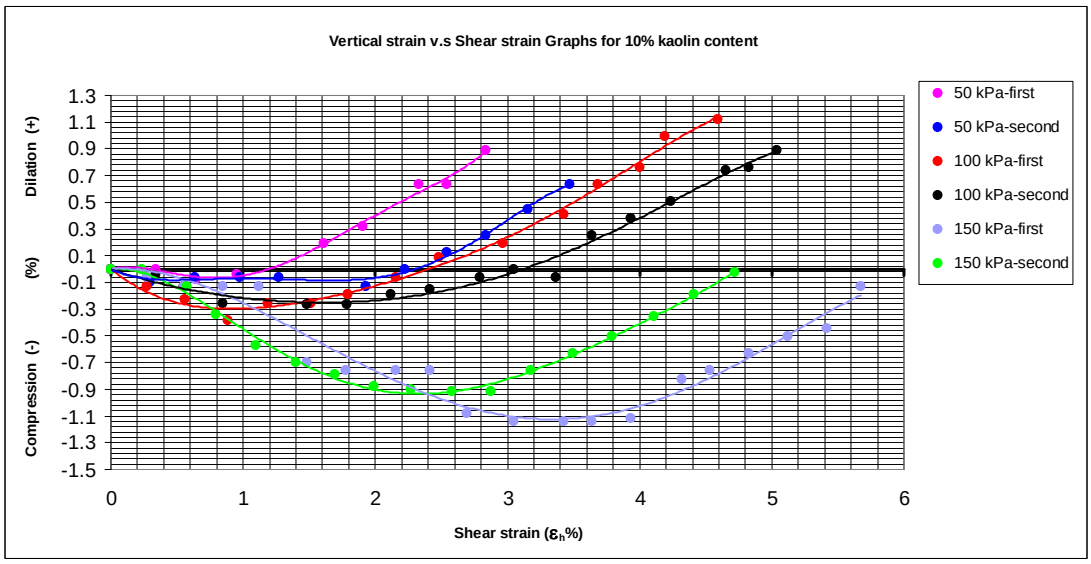

Figure 4.14 Vertical strain-shear strain relationships for 10 % kaolin content, in series 3

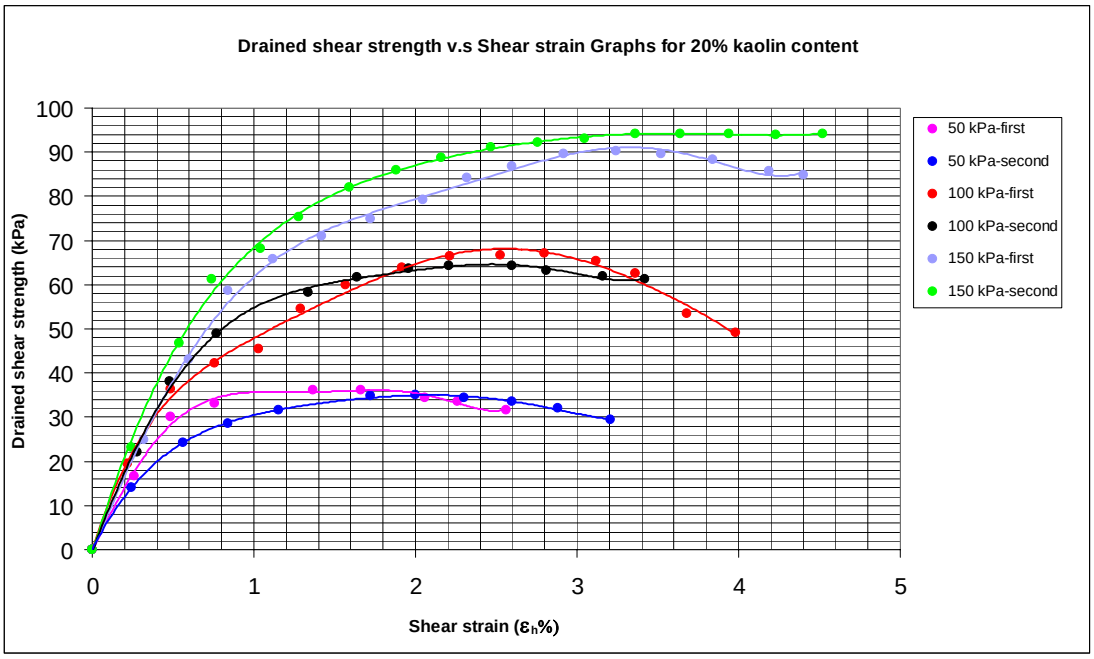

Figure 4.15 Drained shear strength-shear strain relationships for 20 % kaolin content, in series 3

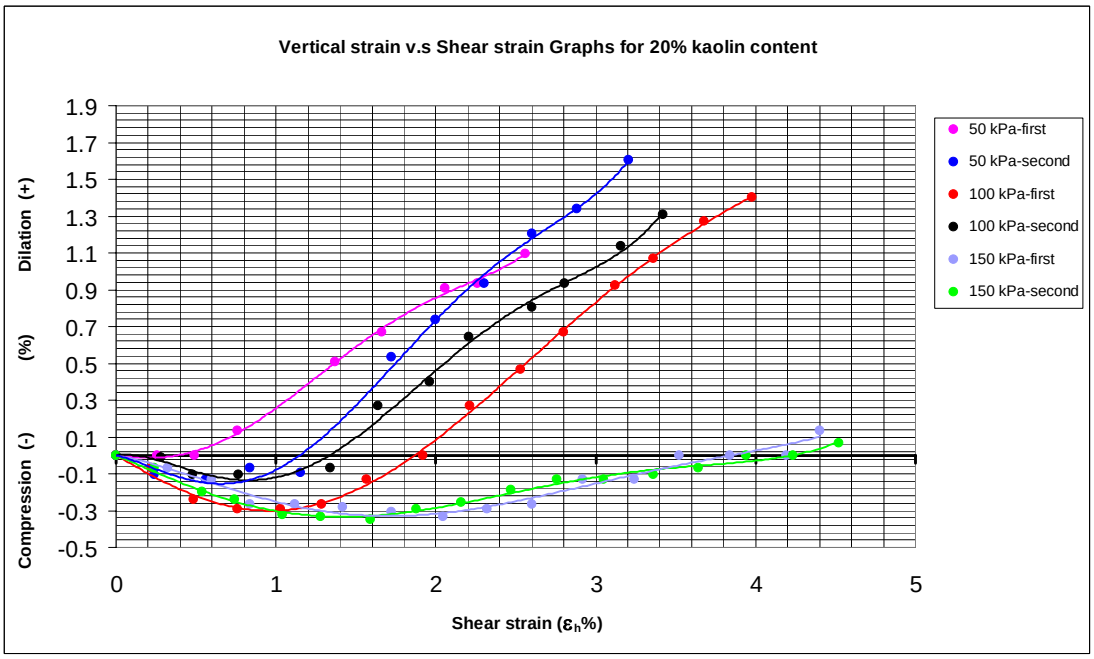

Figure 4.16 Vertical strain-shear strain relationships for 20 % kaolin content, in series 3

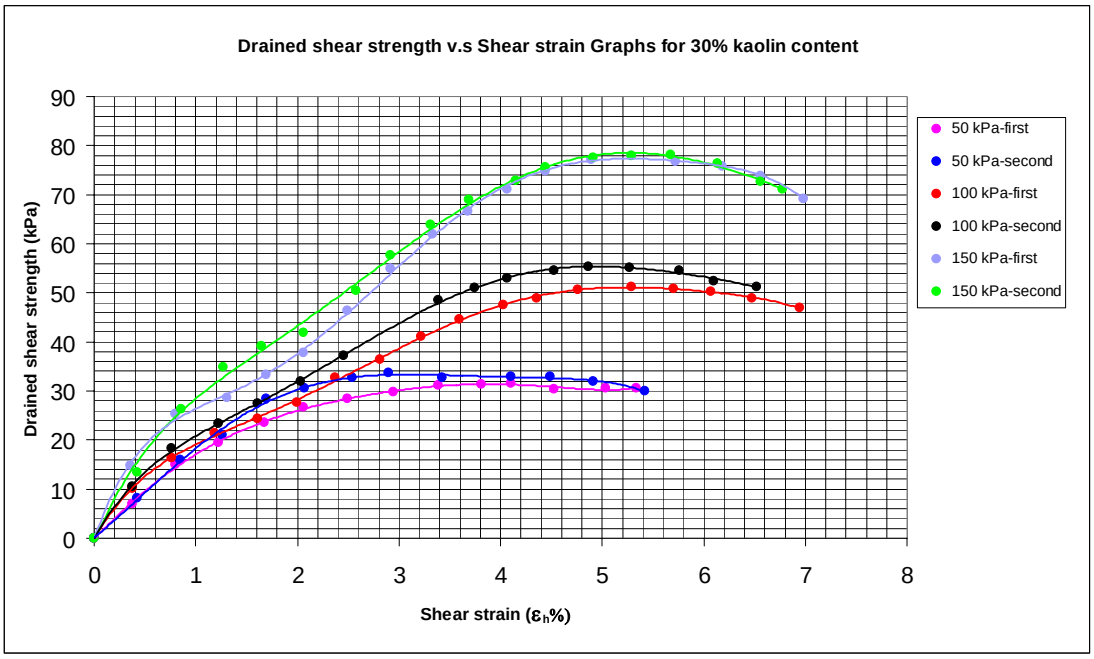

Figure 4.17 Drained shear strength-shear strain relationships for 30 % kaolin content, in series 3

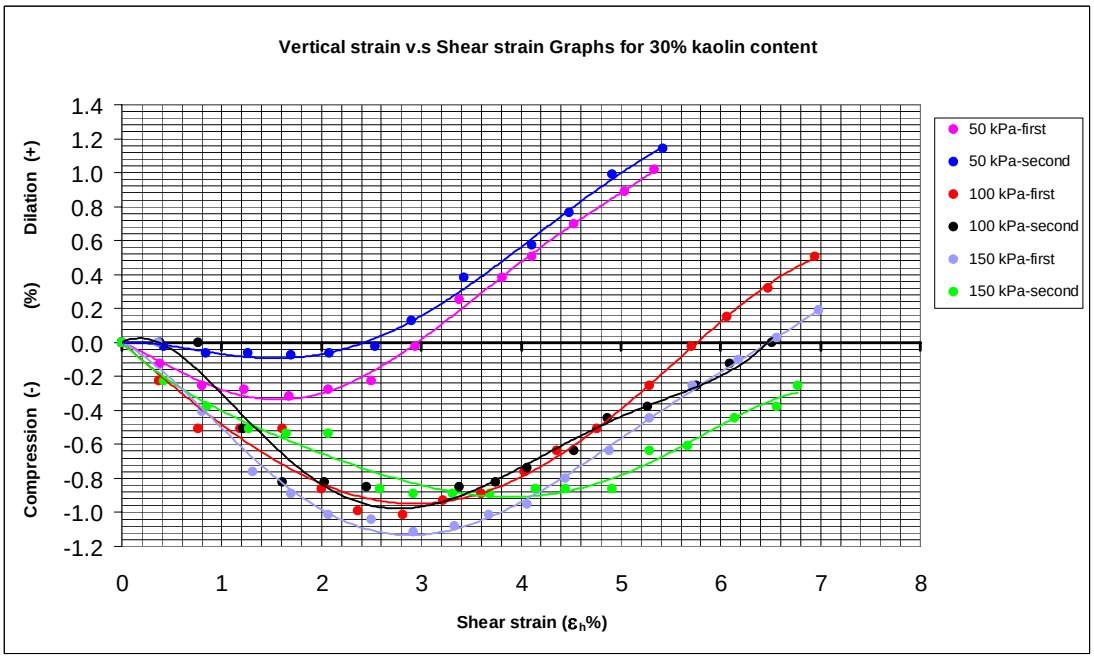

Figure 4.18 Vertical strain-shear strain relationships for 30 % kaolin content, in series 3

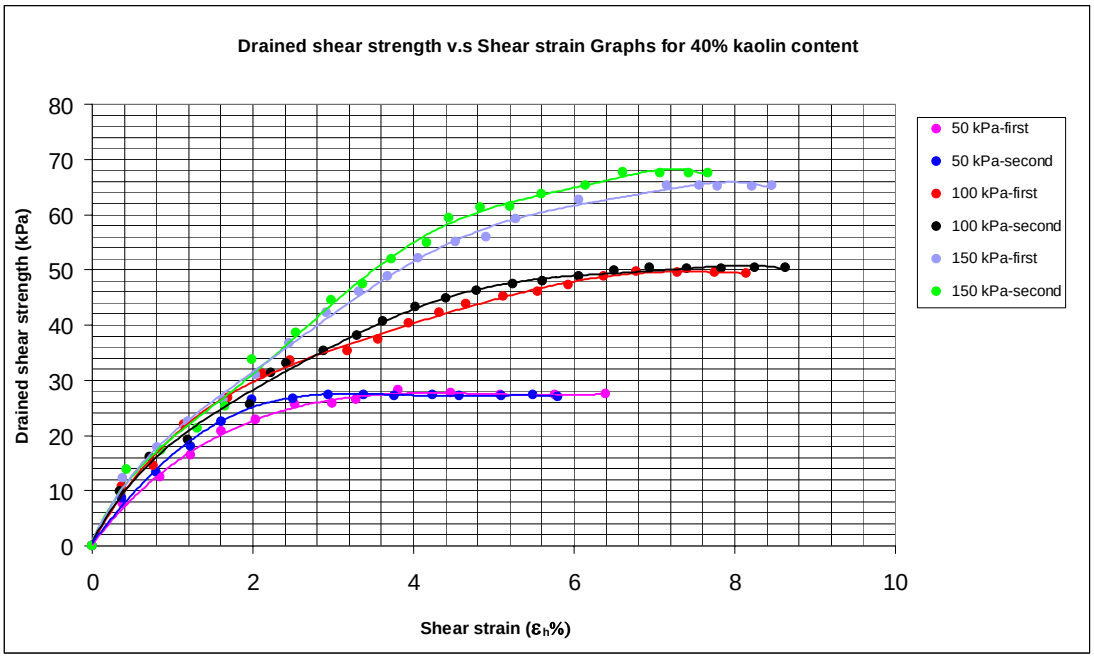

Figure 4.19 Drained shear strength-shear strain relationships for 40 % kaolin content, in series 3

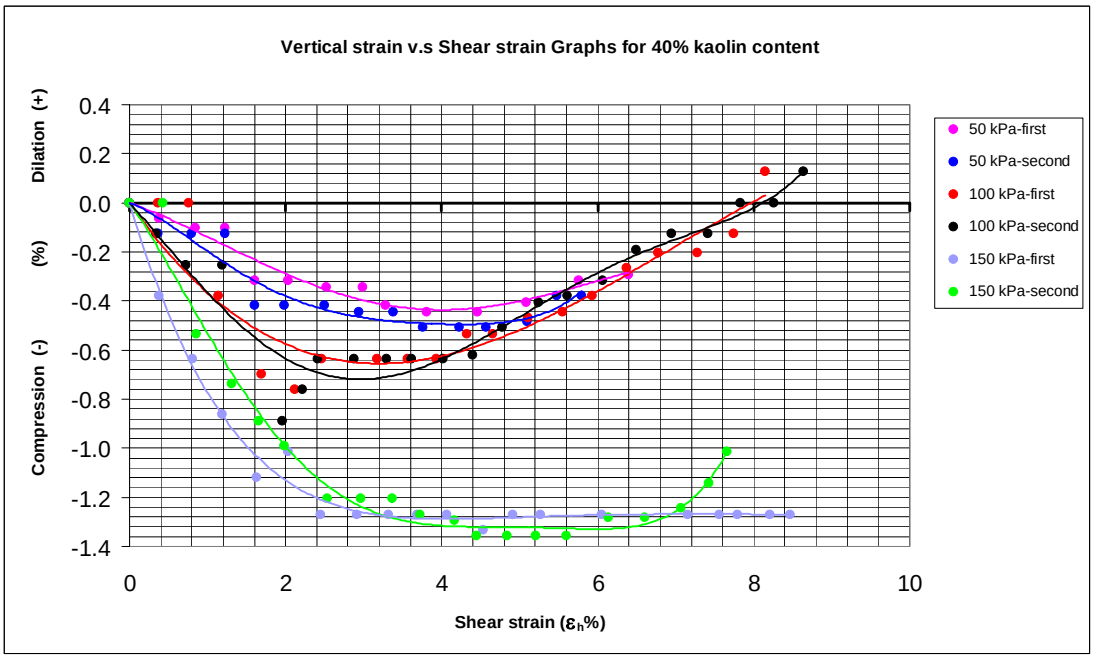

Figure 4.20 Vertical strain-shear strain relationships for 40 % kaolin content, in series 3

Table 4.9 Failure strain values from direct shear CD tests, in series 3

			Failure strain (%)		
Initial water contents (%)	% Kaolin	% Clay	σ_v = 50 kPa	σ_v = 100 kPa	σ_v = 150 kPa
8.67	0	0	2.53	2.83	3.60
9.20	10	4.74	1.92	3.69	4.01
10.10	20	9.86	1.69	2.51	3.30
12.52	30	15.90	3.51	5.10	5.48
14.88	40	20.12	3.38	6.86	6.88

Table 4.10 Values of secant modulus from direct shear CD tests, in series 3

			Secant Moduli (MPa)		
Initial water contents (%)	% Kaolin	% Clay	σ_v = 50 kPa	σ_v = 100 kPa	σ_v = 150 kPa
8.67	0	0	2.98	4.34	6.56
9.20	10	4.74	3.83	5.36	5.94
10.10	20	9.86	5.70	7.56	7.90
12.52	30	15.90	1.78	1.63	2.05
14.88	40	20.12	1.61	1.63	1.56

CHAPTER 5

DISCUSSION OF TEST RESULTS

5.1. Review of the Test Series

This chapter presents results of various series of tests on kaolin - sand mixtures. Shear strength and stress - strain behavior of the samples are presented. As it is described in Chapter 3, three series of experiments are performed. Mainly effects of increasing percentage of kaolin in the kaolin - sand mixtures are investigated.

In series 1 experiments, all of the specimens are consolidated under 50 kPa vertical pressures in a cubical box that has 20x20x20 cm dimensions. Specimens are formed by mixing kaolin and poorly graded sand with some water which is about 20% of soil mixture dry weight. Kaolin, poorly graded sand and water are mixed until getting a homogeneous soil mixture. Thereafter, it is placed in the cubical box and then consolidation stage is started. In this series of experiments, soil mixture is not kept under water. Triaxial unconsolidated – undrained tests (UU) were performed in this series. These applications were performed under 35 kPa, 60 kPa, and 85 kPa cell pressures and they were repeated for a variety of kaolin fractions which are 5%, 10%, 15%, %20, and 25% of soil mixture dry weight.

In series 2 experiments, all of the specimens are consolidated under 100 kPa vertical pressures in the cubical box. At the consolidation stage soil mixture is kept under water. Triaxial unconsolidated – undrained tests (UU) were performed in this series again. These tests were performed under 50 kPa, and 100 kPa cell pressures and they were repeated two times at each pressure. These tests were repeated for 10%, 20%, 30%, and 40% kaolin fractions that are based on dry weight of soil mixture. Except

for these, the methodology in the series 1 experiments was used to prepare samples in the series 2.

In series 3 experiments, initial consolidation stage is not applied. Direct shear (CD) tests were performed at this series. These tests were performed under 50 kPa, 100 kPa, and 150 kPa vertical pressures and they were repeated two times at each pressure. These tests were repeated for 0%, 10%, 20%, 30%, and 40% kaolin fractions that are based on dry weight of soil mixture.

5.2. Undrained Shear Strength

In this part of the study, the results of series 1 and 2 experiments are analyzed for shear strengths. Behavior of the specimens under unconsolidated - undrained conditions at triaxial compression test is examined.

5.2.1. Results of Series 1 Experiments

Relation between undrained shear strength and specified kaolin contents of the mixtures is represented in Figure 5.1. Under all cell pressures (35, 60, and 85 kPa) undrained shear strength variations show some fluctuations up to 20 % kaolin content (end of non-plastic range) and changes in undrained strength are insignificant. After 20 %, strength reduction increases with the increase in kaolin content (plastic samples).

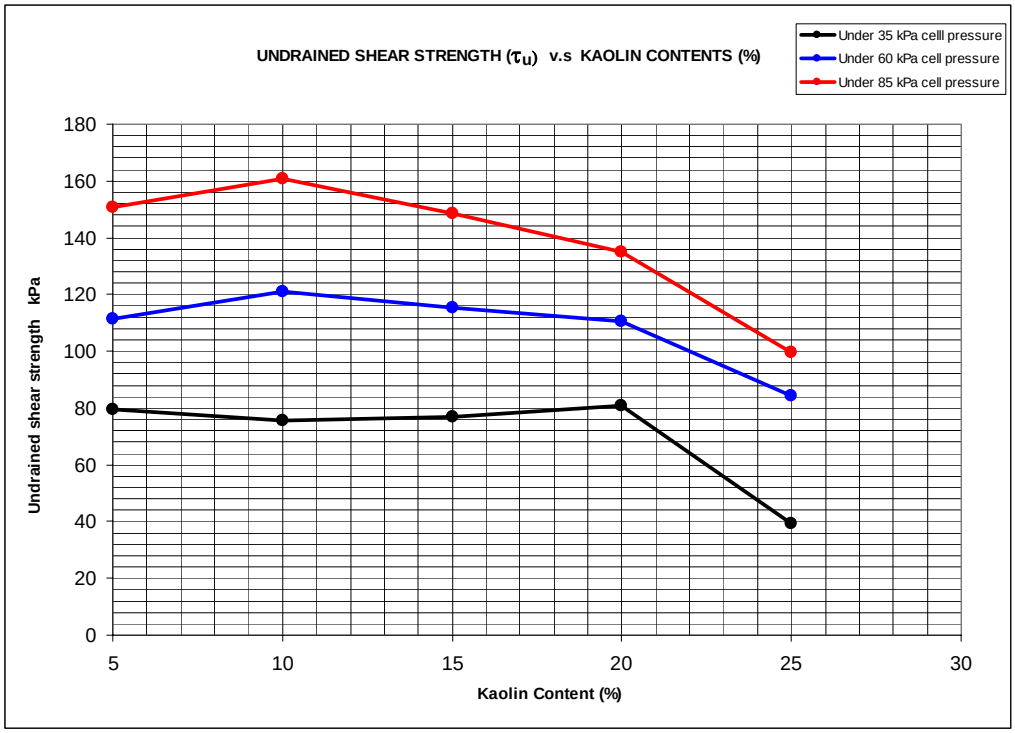

Figure 5.1 Relations between undrained shear strength and kaolin contents, in series1

5.2.2. Results of Series 2 Experiments

In this series of experiments, the behavior of the specimens under unconsolidated - undrained conditions in triaxial compression test is examined again. Relation between undrained shear strength and specified kaolin contents is represented in Figure 5.2. Under both 50 kPa and 100 kPa cell pressures undrained shear strength variations show similar trends. Up to 20% kaolin content (end of non - plastic range) decrease in undrained strength is marginal. After 20%, strength reduction increases with the increase in kaolin content (plastic samples).

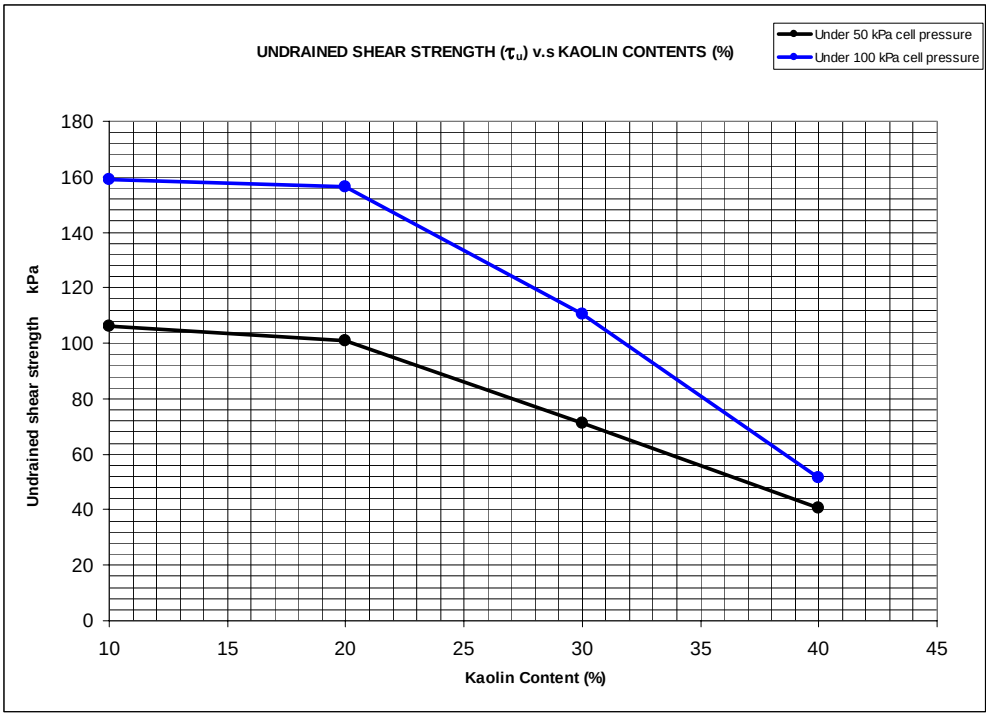

Figure 5.2 Relations between undrained shear strength and kaolin contents, in series2

5.3. Drained Shear Strength

Relation between effective cohesion and specified kaolin contents is represented in Figure 5.3. Effective cohesion increases as the kaolin content is increased. Increment rate in the cohesion starts decreasing after 20 % kaolin content. The rate of increase almost diminishes after about 30%. Change of angle of shearing resistance with increasing kaolin content is shown in Figure 5.4. It seems that this figure, effective angle of shearing resistance decreases as kaolin content is increased. Reduction rate in the friction angle is approximately uniform but the rate of decrease decreases with increasing kaolin content. A reasonable agreement of the trend of drained friction angles against increasing % fines and clay fractions % proposed by Bayoğlu et al. (1995) can also be observed in Figures 2.14 and 2.15.

Relation between drained shear strength at 50, 100, and 150 kPa vertical pressures and specified kaolin fractions is presented in Figure 5.5. Shear strengths decrease with increasing kaolin contents.

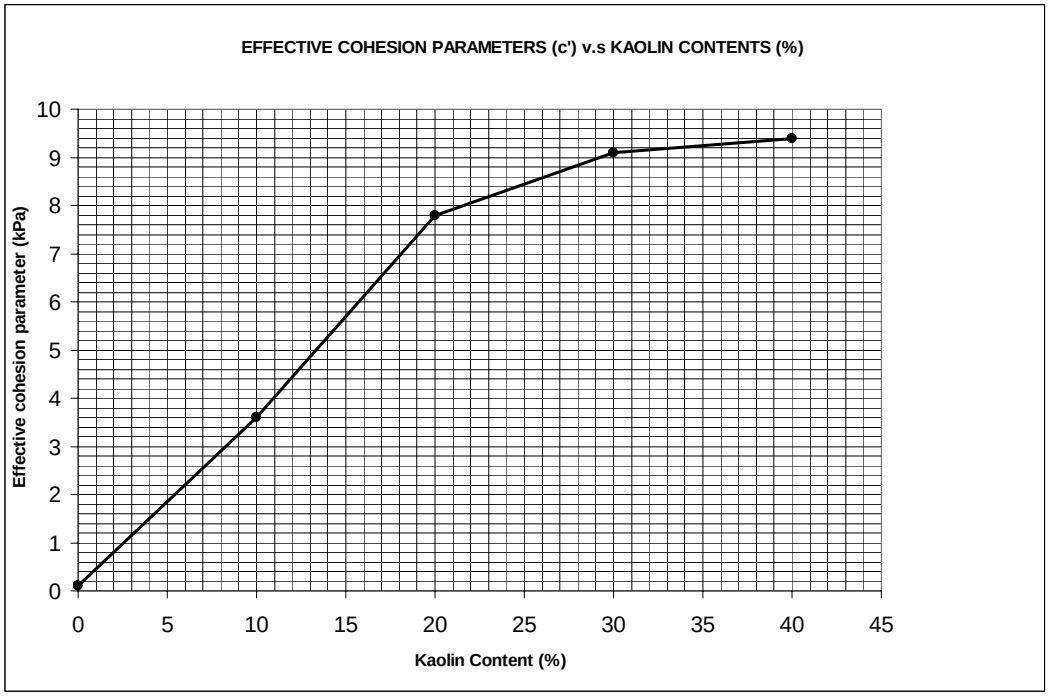

Figure 5.3 Relation between drained cohesion and kaolin content, in series 3

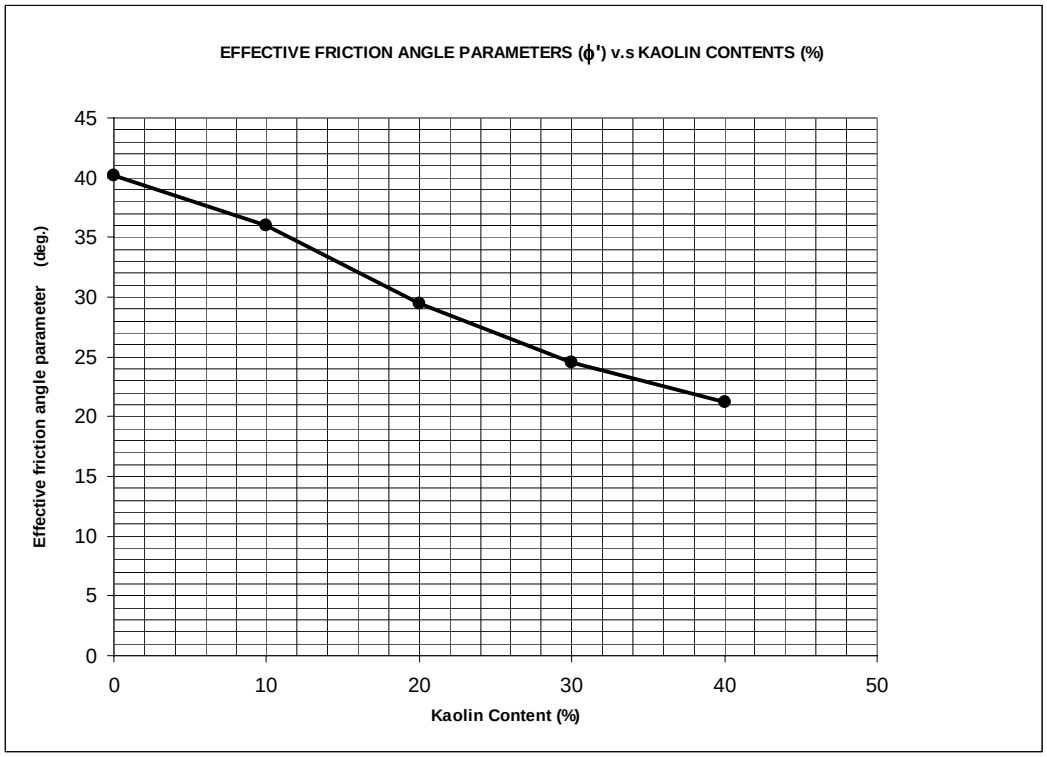

Figure 5.4 Relation between drained friction angle and kaolin content, in series 3

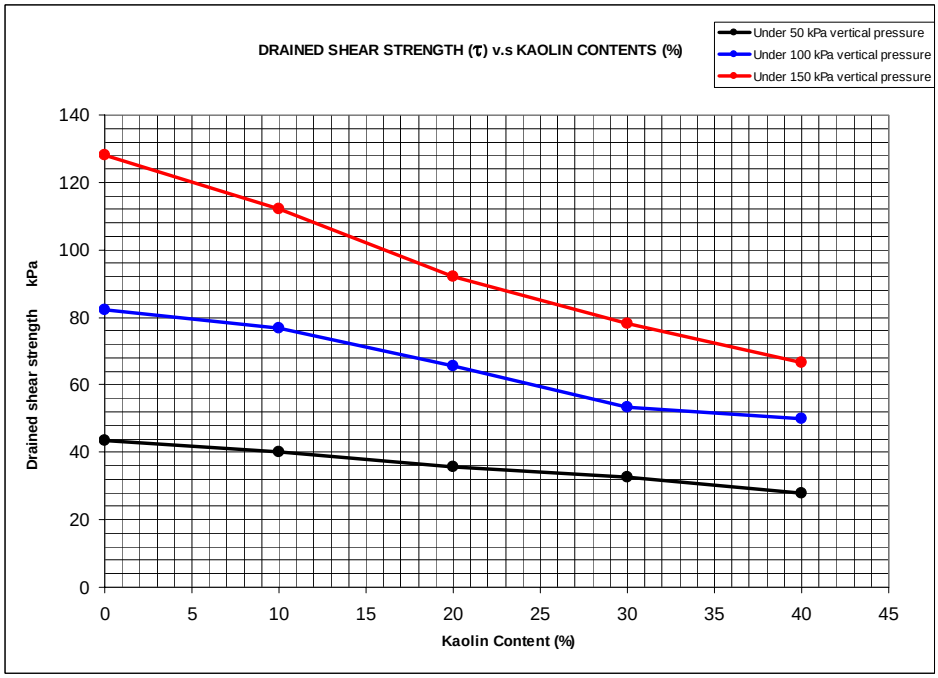

Figure 5.5 Relations between drained shear strength and kaolin contents, in series 3

5.4. Stress - Strain Behavior

In this part of the study, results of three series of experiments are analyzed for stress - strain behavior such as shear strength - shear strain, vertical strain - shear strain relationships. Relations between secant moduli and kaolin contents and relations between failure strains and kaolin contents are also investigated.

5.4.1 Results of Series 1 Experiments

In 5 % kaolin content series, undrained shear strength- vertical strain relationships are shown in Figure 4.1. There are no a distinct peaks and shear resistances remain the same after a certain level. Similar relationships are obtained for 10, 15, 20, and 25 % mixtures, which are shown in Figures 4.2 to 4.5

Variations in failure strains against increasing kaolin content are shown in Figure 5.6. Rate of increase in failure strains for all specimens are noticeable after 15 % kaolin content. Variations in secant moduli against increasing kaolin content are shown in Figure 5.7. Reductions in stiffness of the specimens become pronounced after about % 15 kaolin content.

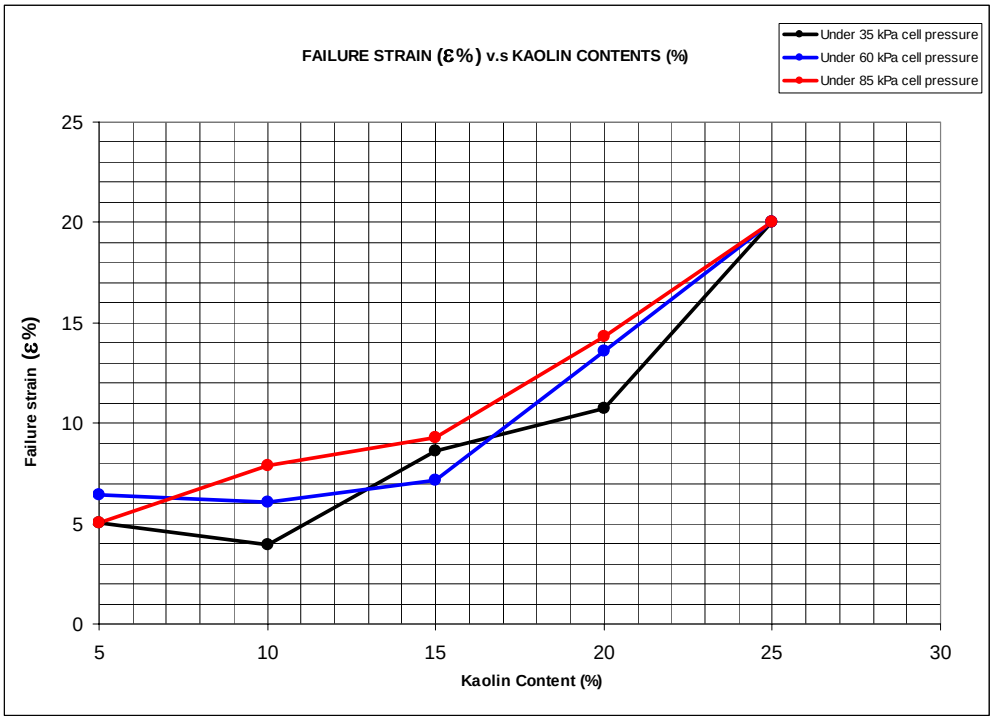

Figure 5.6 Failure strain and kaolin content relationships, in series 1

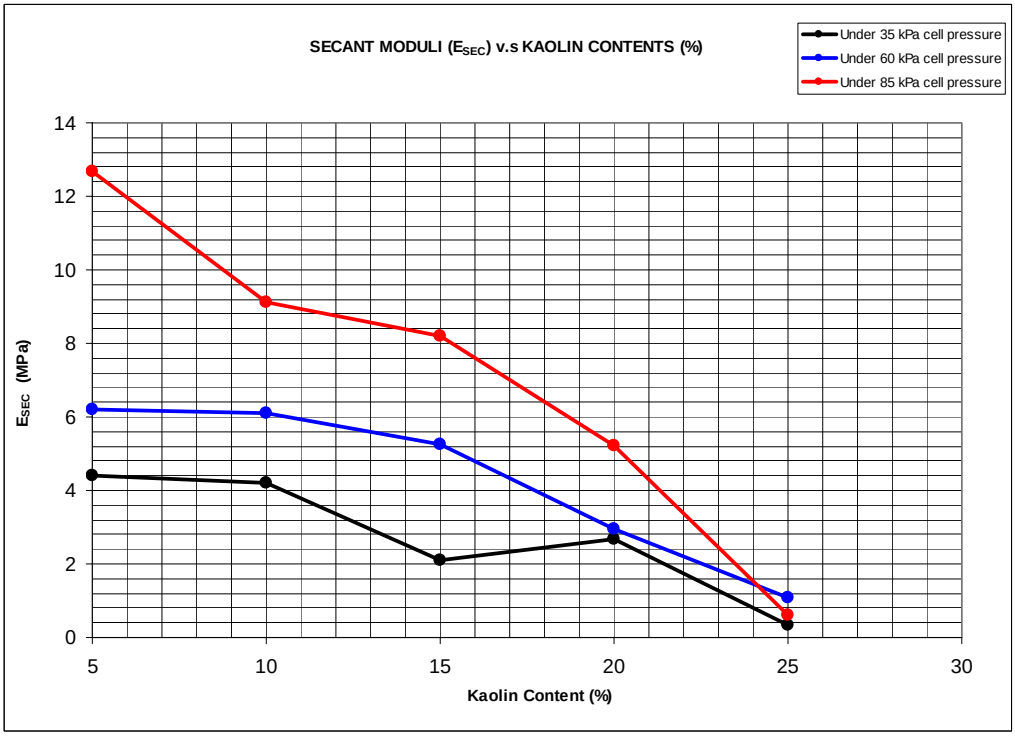

Figure 5.7 Secant moduli and kaolin content relationships, in series 1

5.4.2 Results of Series 2 Experiments

Undrained shear strength-vertical strain relationships are shown in Figures 4.6, 4.7, 4.8, and 4.9 for kaolin contents 10, 20, 30, and 40 % respectively.

Variations in failure strains against increasing kaolin content are shown in Figure 5.8. At 30 % kaolin content, strains in specimens reach its maximum value. After 30 %, this behavior does not change. Variations in secant moduli against increasing kaolin content are shown in Figure 5.9. Up to 20 % kaolin content reduction rate in the secant moduli are significant. After 20 %, decrease in this rate decreases.

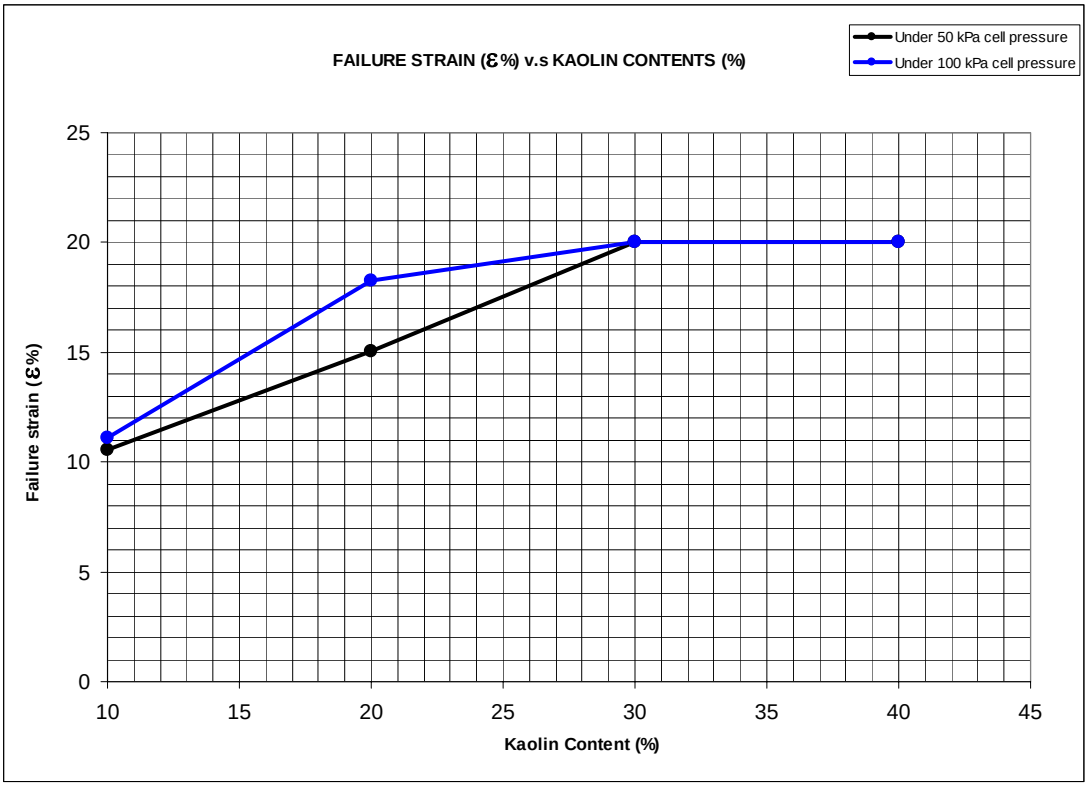

Figure 5.8 Failure strain and kaolin content relationships, in series 2

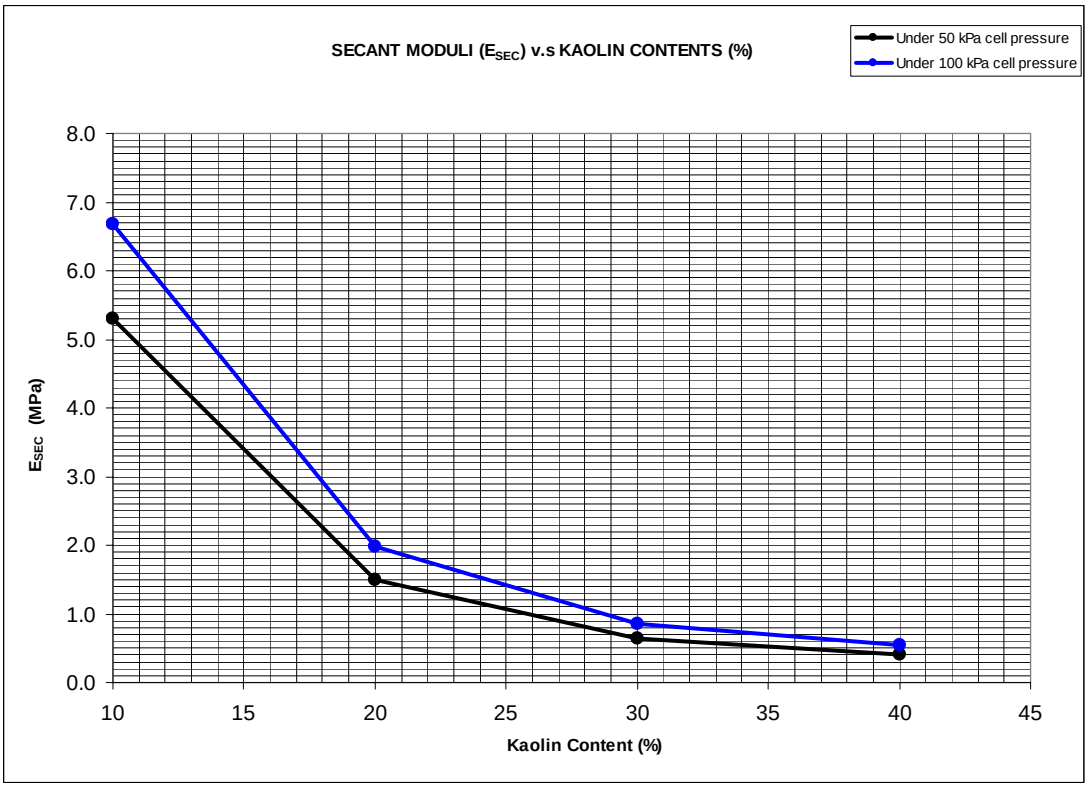

Figure 5.9 Secant moduli and kaolin content relationships, in series 2

5.4.3 Results of Series 3 Experiments

Shear strength-strain and shear strain-vertical strain relationships for 0, 10, 20, 30, and 40 % kaolin contents are shown in Figures 4.11 to 4.20. A reasonable agreement of the behavior of shear strain- vertical strain at 40 % kaolin content proposed by Georgiannou et al. (1988) can be seen. (page-22).

Variations in failure strains against increasing kaolin content are shown in Figure 5.10. Up to 20 % kaolin contents, variations in the strains are marginal. After 20 %, failure strains increase as kaolin content is increased. Variations in secant moduli against increasing kaolin content are shown in Figure 5.11. Up to 20 % kaolin

contents, values of secant moduli show some fluctuating trend especially in specimen under 150 kPa vertical pressures. After 20 %, stiffness of the specimens decreased significantly and after 30 %, rate of decrease decreases with increasing kaolin content.

Rate of volume change - kaolin content relationships are shown in Figure 5.12. Vertical compression - kaolin content relationships are also presented in Figure 5.13.

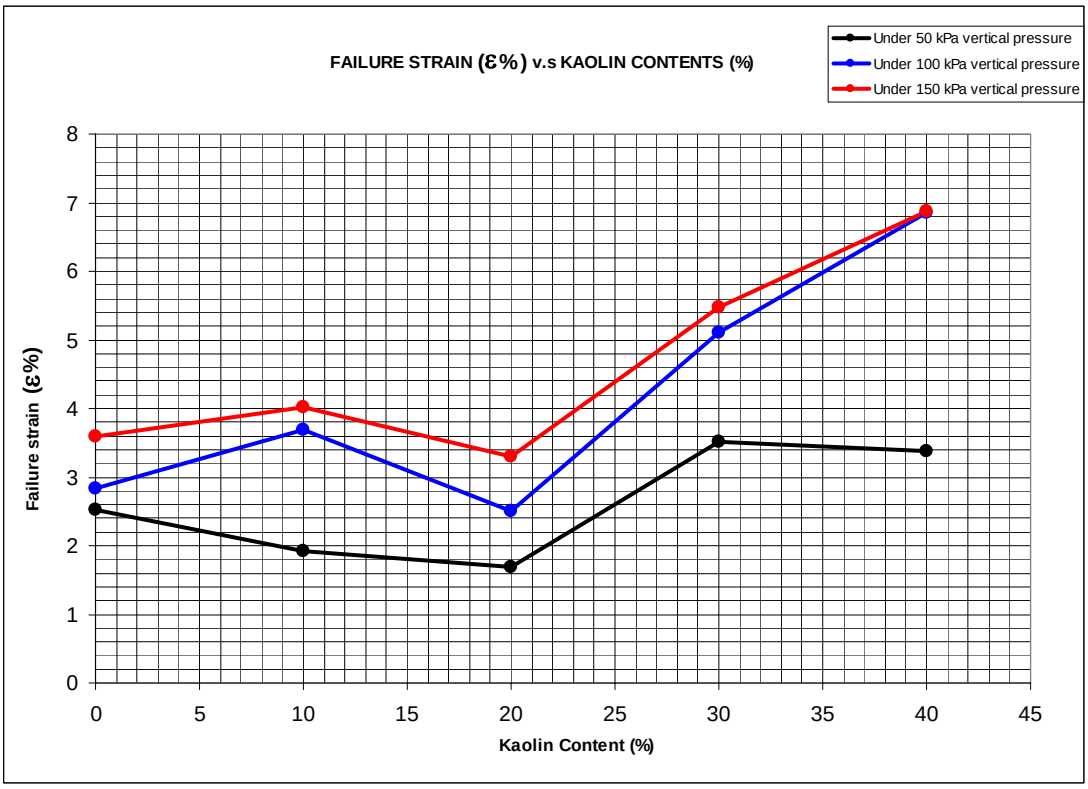

Figure 5.10 Failure strain and kaolin content relationships, in series 3

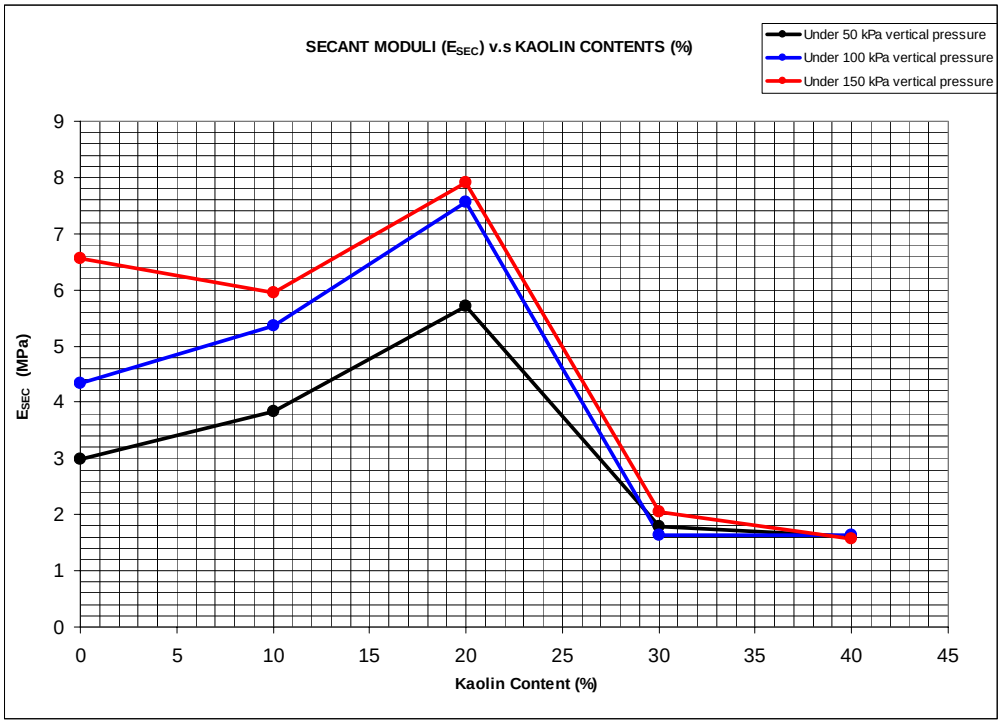

Figure 5.11 Secant moduli and kaolin content relationships, in series 3

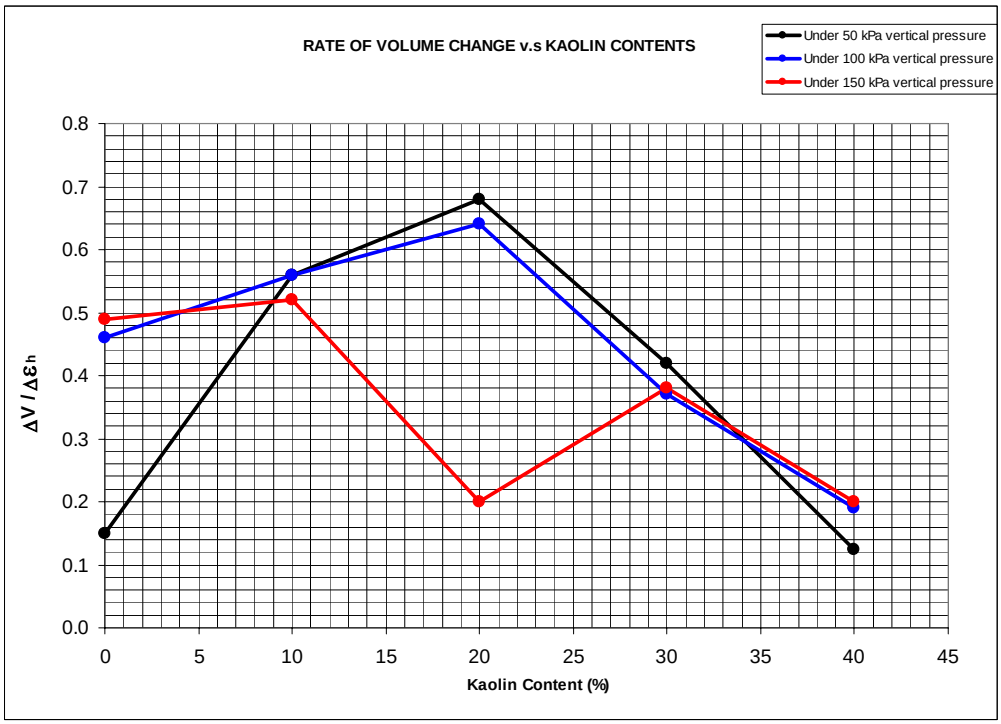

Figure 5.12 Rate of volume change and kaolin content relationships, in series 3

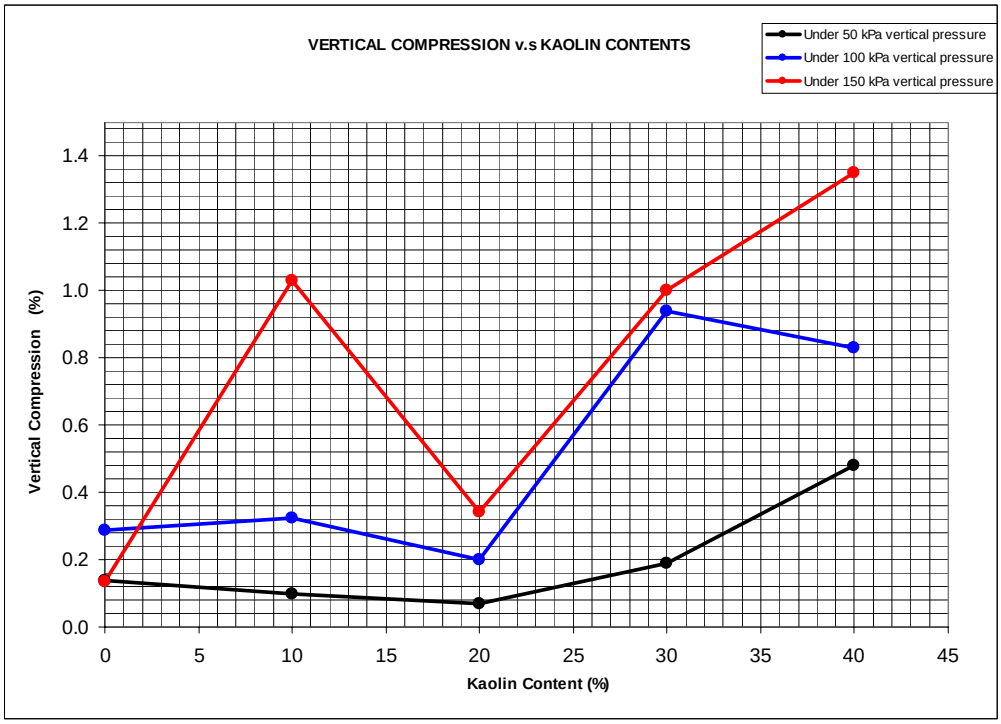

Figure 5.13 Vertical compression and kaolin content relationships, in series 3

CHAPTER 6

CONCLUSIONS

In this experimental study, the purpose of performing three series of experiments is to observe the effect of the kaolin content in the kaolin-sand mixtures on the behavior of shear strength. Both undrained shear strength and effective shear strength parameters are measured. Stress-strain characteristics are also investigated in all series. The following conclusions can be obtained from the results of the experimental work.

1. Shear strength properties and stress-strain characteristics of the kaolin-sand mixtures show noticeable changes at about 20 % kaolin-sand composition. This value seems to be as approximate limiting value at which all properties experience changes (physical explanations about this limiting value are given in Appendix A).

2. Undrained shear strength decreases significantly after 20 % kaolin content in both 1^{st} and 2^{nd} series of experiments. It seems to be a threshold value for undrained shear strength behavior against increasing kaolin content.

3. Angle of drained shear strength and drained shear strength decrease with increasing kaolin contents.

4. Drained (effective) cohesion against kaolin content relationship is linear up to 20 % and then it decreases markedly towards 30 %. Change in the drained shear angle is less marked.

5. Strains at failure in drained tests markedly increase in the specimens with 20 % kaolin content. Similar trends are also observed in the undrained series although less marked.

6. In the undrained triaxial compression tests stiffness of the specimens decrease after about 15-20 % kaolin content.

7. In drained tests the decrease in stiffness of the specimens can also be seen after 20 % kaolin content.

8. Rate of volume change of the samples against shear strain and amount of vertical compression also show noticeable changes at 20 % kaolin-sand mixtures.

REFERENCES

1. Bardet, J. P. (1997). Experimental Soil Mechanics, Prentice-Hall, Inc, United States.

2. Bayoğlu, Esra (1995). Shear Strength and Compressibility Behavior of Sand-Clay Mixtures, M.S. Thesis, Middle East Technical University, Turkey.

3. Cernica, J. N. (1995). Geotechnical Engineering: Soil Mechanics, John Wiley & Sons, Inc, United States.

4. Craig, R. F. (1997). Soil Mechanics, Sixth Edition, Spon Press, London.

5. Das, M. B. (1983). Advanced Soil Mechanics, Hemisphere Publishing Corp., McGraw Hill, London.

6. Das, M. B. (2005). Fundamentals of Geotechnical Engineering, Nelson, Toronto, Canada.

7. Georgiannou, V. N. 1988. Behavior of Clayey Sands under Monotonic and Cyclic Loading. Ph.D. thesis, Department of Civil Engineering, Imperial College of Science, Technology and Medicine, London, England.

8. Georgiannou, V. N., Burland, J.B. and Hight, D. W. (1990). The Undrained Behaviour of Clayey Sands in Triaxial Compression and Extension, Geotechnique 40, No.30, 431-449.

9. Georgiannou, V. N., Burland, J.B. and Hight, D. W. (1991a). Undrained Behaviour of Natural and Model Clayey Sands. Soils Found. 31, No.3, 17-29.

10. Head, K. H. (1982). Manual of Soil Laboratory Testing, Volume 2: Permeability, Shear Strength & Compressibility Tests, Robert Hartnoll Ltd., Bodmin, Cornwall.

11. Mirata, T. (2001). Laboratory Instructions for Soil Mechanics Students, Department of Civil Engineering, M.E.T.U. Ankara.

12. Novais-Ferreira, H. (1971). The Clay Content and the Shear Strength in Sand-Clay Mixtures. Proc. 5th African Reg. Conf. Soil Mech. Found. Engrng. Luanda. Vol 1, p.3-9, Theme 3.

13. Pitman, T.D., Robertson, P.K. & Sego, D.C. (1994). Influence of Fines on the Collapse of Loose Sands. Can. Geotech. J.31, 728-739.

14. R. Salgado (2000). Shear Strength and Stiffness of Silty Sand. Journal of Geotechnical and Geoenvironmental Engineering, ASCE, Vol.126, May. No.5, 451-462.

15. Thevanayagam, S. (1998). Effect of Fines and Confining Stress on Undrained Shear Strength of Silty Sands. J. Geotech. Geoenviron. Engng Div, ASCE 124, No.6, 479-491.

16. Vickers, B. (1984). Laboratory Work in Soil Mechanics, Granada Publishing Ltd., London.

17. Wasti, Y. and Alyanak, I. (1968). Kil Muhtevasının Zeminin Davranışına Tesiri. İnşaat Mühendisleri Odası, Türkiye İnşaat Mühendisliği 4. Teknik Kongresi. Ankara.

APPENDIX A

EFFECTS OF CLAY FRACTION ON THE BEHAVIOUR OF SAND-CLAY MIXTURES

According to Wasti and Alyanak (1968), when the clay content is just enough to fill the voids of the granular portion at its maximum porosity, the structure of the mixture changes and the linear relationship between the Atterberg Limits and the clay content ceases to be valid, and the compressional behavior of the soil also changes (see Figure A.1). In Figure A.1.a., clay content is just enough to fill the voids of the granular part. In Figure A.1.b., clay content is much more than the voids of the granular part. The clay content at which this change occurs has also been calculated for soils containing kaolin clay minerals in this study and this calculated clay fraction was compared the conclusions.

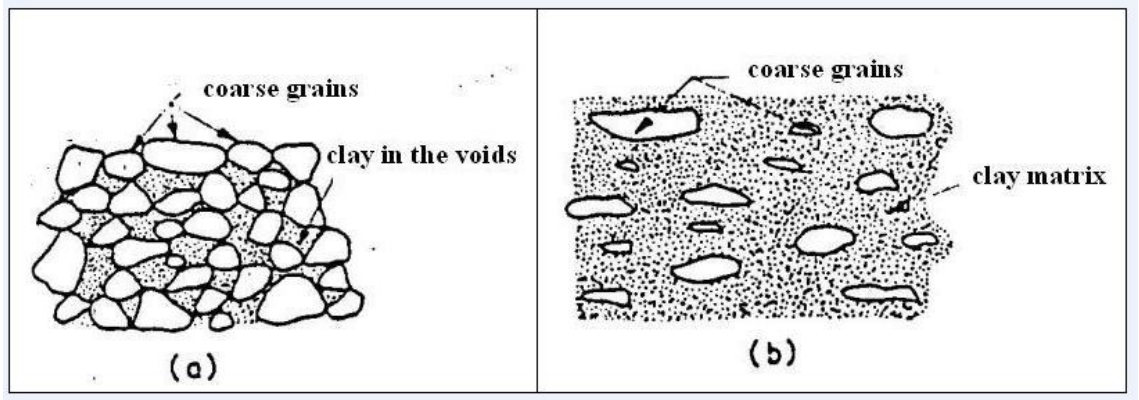

Figure A.1 Structures of the Soil Mixtures

$$C_{fv} = \frac{X}{X+100} \cdot 100 \quad \text{.....(A.1)}$$

$$X = \frac{100.e_L}{G_{sg}.(\frac{1}{G_{sc}} + \frac{w_c}{100})} \quad \text{.....(A.2)}$$

where,

e_L = maximum void ratio of granular portion (in this study, dry sand was poured with using a funnel in a mold, that has a specified volume, at 0.3 m. above from the top of the mold until filling the mold. Then filled mold was weighed and minimum dry density of sand was calculated. This procedure was repeated until getting a decrease in the minimum dry density ($\rho_{min.dry}$).

$$(e_L = \frac{1}{\rho_{min.dry}}) \text{.....(A.3)}$$

G_{sg} = specific gravity of granular portion

w_c = water content of clay portion

G_{sc} = specific gravity of clay portion

C_{fv} = clay fraction just enough to fill the voids of the granular portion at its maximum porosity

According to conclusions chapter in this study, this change occured about 20 % kaolin content. In the following part, this limiting value (C_{fv}) was calculated provided that the soil mixture was assumed to be fully saturated;

for 20 % kaolin and 80 % sand mixture; (w_i = initial water content of the mixture, w_i = 13.6 %),

w_{clay} = initial water content of the clay part (amount of adsorbed water from granular portion is considered zero and water in the mixture was assumed to be fully in the clay portion).

$$w_{clay} = \frac{13.6}{20} \cdot 100 = 68\ \% \quad , \quad e_L = 0.71$$

$$X = \frac{100x0.71}{2.67x(\frac{1}{2.60} + \frac{68}{100})} = 24.98$$

$$C_{fv} = \frac{24.98}{24.98 + 100} \text{ x } 100 = 19.98\ \%$$

As shown, after computings this limiting clay fraction value C_{fv} is of 19.98 % and this result is in a good agreement with the conclusions in this study.